UNIVERSIDADE FEDERAL DE UBERLÂNDIA
INSTITUTO DE GENÉTICA E BIOQUÍMICA
PÓS-GRADUAÇÃO EM GENÉTICA E BIOQUÍMICA

AVALIAÇÃO DO POTENCIAL GENOTÓXICO DE NANOPARTÍCULAS DE ÓXIDO DE ZINCO E DIÓXIDO DE TITÂNIO PELO ENSAIO DO MICRONÚCLEO EM CÉLULAS V79 E TESTE DA MANCHA DA ASA EM *Drosophila melanogaster*

Aluna: Érica de Melo Reis

Orientador: Prof. Dr. Mário Antônio Spanó

Co-Orientador: Prof. Dr. Alexandre Azenha Alves de Rezende

UBERLÂNDIA - MG

2014

UNIVERSIDADE FEDERAL DE UBERLÂNDIA
INSTITUTO DE GENÉTICA E BIOQUÍMICA
PÓS-GRADUAÇÃO EM GENÉTICA E BIOQUÍMICA

AVALIAÇÃO DO POTENCIAL GENOTÓXICO DE NANOPARTÍCULAS DE ÓXIDO DE ZINCO E DIÓXIDO DE TITÂNIO PELO ENSAIO DO MICRONÚCLEO EM CÉLULAS V79 E TESTE DA MANCHA DA ASA EM *Drosophila melanogaster*

Aluna: Érica de Melo Reis

Orientador: Prof. Dr. Mário Antônio Spanó

Co-Orientador: Prof. Dr. Alexandre Azenha Alves de Rezende

Tese apresentada à Universidade Federal de Uberlândia como parte dos requisitos para obtenção do Título de Doutor em Genética e Bioquímica (Área: Genética)

UBERLÂNDIA - MG

2014

Dados Internacionais de Catalogação na Publicação (CIP)
Sistema de Bibliotecas da UFU, MG, Brasil.

R375a
2014

Reis, Érica de Melo, 1980-
Avaliação do potencial genotóxico de nanopartículas de óxido de zinco e dióxido de titânio pelo ensaio do micronúcleo em células V79 e teste da mancha da asa em *Drosophila melanogaster* / Érica de Melo Reis. - 2014.
127 f. : il.

Orientador: Mário Antônio Spanó.
Coorientador: Alexandre Azenha Alves de Rezende.
Tese (doutorado) - Universidade Federal de Uberlândia, Programa de Pós-Graduação em Genética e Bioquímica.
Inclui bibliografia.

1. Bioquímica - Teses. 2. Nanocristais - Teses. 3. Óxido de zinco - Teses. 4. Dióxido de titânio - Teses. I. Spanó, Mário Antônio. II. Rezende, Alexandre Azenha Alves de. III. Universidade Federal de Uberlândia. Programa de Pós-Graduação em Genética e Bioquímica. IV. Título.

CDU: 577.1

UNIVERSIDADE FEDERAL DE UBERLÂNDIA
INSTITUTO DE GENÉTICA E BIOQUÍMICA
PÓS-GRADUAÇÃO EM GENÉTICA E BIOQUÍMICA

AVALIAÇÃO DO POTENCIAL GENOTÓXICO DE NANOPARTÍCULAS DE ÓXIDO DE ZINCO E DIÓXIDO DE TITÂNIO PELO ENSAIO DO MICRONÚCLEO EM CÉLULAS V79 E TESTE DA MANCHA DA ASA EM *Drosophila melanogaster*

Aluna: Érica de Melo Reis

COMISSÃO EXAMINADORA

Presidente: Prof. Dr. Mário Antônio Spanó

Examinadores: Profa. Dra. Heloísa Helena Rodrigues de Andrade
Profa. Dra. Zaira da Rosa Guterres
Prof. Dr. Carlos Ueira Vieira
Prof. Dr. Boscolli Barbosa Pereira

Data da Defesa: 31/07/2014

As sugestões da Comissão Examinadora e as Normas PGGB para o formato da Tese foram contempladas

_____
Prof. Dr. Mário Antônio Spanó

AGRADECIMENTOS

A Deus e ao meu anjo protetor, por me fortalecerem espiritualmente dia após dia perante os desafios, os medos e o cansaço.

Ao Prof. Dr. Mário Antônio Spanó, por me dar a oportunidade de ser sua orientanda. Muito obrigada por tantos ensinamentos, pela confiança, dedicação, paciência e amizade.

Ao meu coorientador, Prof. Dr. Alexandre Azenha Alves de Rezende, por tudo! Foram três anos de muito aprendizado, incentivo, companheirismo e amizade, sem os quais eu jamais teria concretizado este trabalho.

À Profa. Denise Crispim Tavares, da Universidade de Franca/SP (UNIFRAN), por ter me recebido de forma tão gentil em seu laboratório; e às suas orientandas, Pollyanna Francielli de Oliveira e Heloiza Diniz Nicolella, que, com muito empenho e dedicação, contribuíram significativamente para realização deste estudo.

Ao Prof. Dr. Noélio Oliveira Dantas, do Laboratório de Novos Materiais Isolantes e Semicondutores (LNMIS), desta Universidade, pela parceria e por fornecer as nanopartículas aqui estudadas. À Dra. Anielle Christine Almeida Silva, do mesmo laboratório, pela caracterização física das nanopartículas, pelos ensinamentos e disponibilidade em ajudar.

Aos meus pais, Humberto E. Reis e Sueli Dairel de Melo Reis, pelo exemplo de perseverança e pelo apoio incondicional em todos os momentos da minha vida. E aos meus irmãos, Bruno de Melo Reis e Thaís de Melo Reis, pelo incentivo, cumplicidade e carinho.

Ao meu marido, Diego Vilela Santos, pelo exemplo de determinação e dedicação, mas, sobretudo, pelo apoio, amor e companheirismo que foram e continuam sendo fundamentais para meu crescimento pessoal e profissional.

Ao meu filho, Davi Reis Vilela Santos, presente divino, pelo sorriso gostoso logo quando acorda e pelo abraço apertado quando retorno para casa, os quais recarregam minhas baterias, infimizam os problemas e colorem meu dia.

Às minhas avós e tias, sogro e sogra, pelas orações e pelo incentivo para que eu pudesse concluir com êxito mais essa etapa da minha formação.

Aos colegas e amigos do Programa de Pós-Graduação em Genética e Bioquímica, em especial à Juliana Franco Almeida, Janaina Lobato, Márcia Moura Nunes, Fernanda Van Petten Azevedo, Washington João de Carvalho e Cássio Resende de Morais, pelos momentos de descontração, “socorros” com a informática e pela companhia durante essa jornada.

À Coordenação e aos Docentes do Programa de Pós-Graduação em Genética e Bioquímica/UFU, pela oportunidade, apoio e pelos ensinamentos que contribuíram de forma significativa para minha formação.

À Neirevalda da Silva, secretária do Programa de Pós-Graduação em Genética e Bioquímica/UFU, pela gentileza e presteza constantes nas informações e auxílios com assuntos burocráticos.

Aos amigos do Laboratório de Análises Clínicas do Hospital das Clínicas / UFU, por apoiarem meus estudos, pelas conversas amistosas e descontraídas que deixam minhas tardes mais alegres.

Ao Sr. Paulo Roberto Moderno, pelo cafezinho diário e pela ajuda técnica no Laboratório de Mutagênese/UFU.

APOIO FINANCEIRO

Este trabalho foi realizado no Laboratório de Mutagênese do Instituto de Genética e Bioquímica da Universidade Federal de Uberlândia - UFU (Uberlândia-MG), em parceria com o Laboratório de Novos Materiais Isolantes e Semicondutores (LNMIS) do Instituto de Física da UFU e com o Laboratório de Mutagênese da Universidade de Franca (Franca-SP) com apoio financeiro das seguintes Agências de Fomento e Instituições:

- Coordenação de Aperfeiçoamento de Pessoal do Ensino Superior (CAPES);

- Conselho Nacional de Desenvolvimento Científico e Tecnológico (CNPq);

- Fundação de Amparo à Pesquisa do Estado de Minas Gerais (FAPEMIG);

- Fundação de Amparo à Pesquisa do Estado de São Paulo (FAPESP);

- Universidade de Franca (UNIFRAN);

- Universidade Federal de Uberlândia (UFU).

Lista de Figuras

Página

Capítulo 1. Fundamentação Teórica

Capítulo 2. Assessment of the genotoxic potential of two zinc oxide sources (amorphous and nanoparticles) using the in vitro micronucleus test and the in vivo wing somatic test

Lista de Tabelas

Página

Capítulo 2. Assessment of the genotoxic potential of two zinc oxide sources (amorphous and nanoparticles) using the in vitro micronucleus test and the in vivo wing somatic test

Capítulo 3. Evaluation of titanium dioxide nanoparticles-induced genotoxicity by the Cytokinesis-Block Micronucleus assay and the *Drosophila* wing spot test

Resumo

A crescente exploração de nanopartículas – estruturas sintetizadas artificialmente que apresentam pelo menos uma dimensão entre 1 e 100 nm – está relacionada a vasta gama de aplicações em diferentes áreas. Devido às suas propriedades específicas, nanopartículas de óxido de zinco (NPs de ZnO) e nanopartículas de dióxido de titânio (NPs de TiO_2) têm recebido muita atenção por causa das diversas possibilidade de utilização em produtos de consumo, principalmente em protetores solares, visto à eficácia aumentada na proteção contra luz UV e por serem menos opacas que os respectivos compostos de tamanho maior. O objetivo deste estudo foi avaliar os efeitos citotóxicos, mutagênicos e recombinogênicos de NPs de ZnO (21 nm), ZnO comercial, e três tipos diferentes de NPs de TiO_2: TiO_2 anatase (5,2 nm), TiO_2 anatase (9,1 nm) e TiO_2 rutila (55,1 nm). O teste *in vivo Somatic Mutation and Recombination Test* (SMART) em asa de *Drosophila melanogaster* e o teste do Micronúcleo com Bloqueio de Citocinese (CBMN), *in vitro,* utilizando fibroblastos de pulmão de hâmster Chinês (células V79) foram os escolhidos para realizar este trabalho. Larvas de 72 ± 4 h de *D. melanogaster* obtidas por meio do cruzamento padrão (ST) ou cruzamento de alta bioativação (HB) foram tratadas com 1,5625; 3,125; 6,25 ou 12,5 mM para o teste SMART. Para os dois tipos de compostos, ZnO e TiO_2, foram observados efeitos mutagênicos apenas no cruzamento HB. Em relação ao ZnO, o comercial foi capaz de aumentar as frequências de manchas mutantes na concentração de 6,25 mM, enquanto NPs de ZnO induziram mutagenicidade na concentração mais alta. Para as NPs de TiO_2, a fase anatase de 5,2 nm foi mutagênica nas concentrações 1,5625 e 3,125 mM, e a rutila de 55,1 nm aumentou de forma significativa a frequência de manchas mutantes em todas as concentrações avaliadas, exceto com 3,125 mM. NPs de anatase TiO_2 (9,1 nm) não causaram efeitos mutagênicos em asas de *D. melanogaster* em nenhum dos cruzamentos. Os efeitos mutagênicos observados no cruzamento HB, em contraste com o cruzamento ST, no teste SMART podem ser justificados pela atividade metabólica aumentada inerente aos indivíduos HB, com aumento na produção de espécies reativas de oxigênio e, consequentemente, maior dano ao DNA. Para determinar as doses utilizadas no tratamento do teste do micronúcleo, várias concentrações

de NPs de ZnO, e dos três tipos de NPs de TiO_2, variando de 30,5 a 62.500,00 µM, foram avaliadas pelo teste colorimétrico XTT em células V79. NPs de ZnO e TiO_2 anatase de 5,2 e 9,1 nm demonstraram intensidade citotóxica similar, sendo que a partir da concentração 244,1 µM foi observada significativa redução da viabilidade celular. Por outro lado, a citotoxicidade de NPs de TiO_2 na fase de rutila (55,1 nm) começou mais tardiamente, a partir a concentração de 7.812,00 µM. Dentre as NPs avaliados, apenas ZnO (21 nm) e TiO_2 anatase (5,2 nm) na maior concentração avaliada foram capazes de induzir genotoxicidade em células V79. As fases de TiO_2 anatase (9,1 nm) e TiO_2 rutila (55,1 nm) não causaram aumento significativo de micronúcleo. Existem vários aspectos fisicoquímicos que podem influenciar nos efeitos tóxicos das NPs, o que corrobora com diferenças nos resultados citotóxicos e genotóxicos. Nas condicões experimentais deste estudo, podemos afirmar que ambos os tipos de ZnO avaliados, bem como as fases anatase e rutila das NPs de TiO_2 foram capazes de induzir mutagenicidade. Portanto, o uso desses nanomateriais deve ser cuidadosamente monitorado e os mecanismos de indução de genotoxicidade devem ser elucidados.

Palavras-chave: *Drosophila melanogaster*; micronúcleo; mutagenicidade; SMART, células V79, XTT, óxido de zinco, dióxido de titânio

Abstract

The growing exploration of nanoparticles (NPs) – engineered structures that have at least one dimension between 1 and 100 nm – has a wide range of applications in many fields. The aim of the present study was evaluate the cytotoxic, mutagenic and recombinogenic effects of: 1] Amorphous Zinc oxide (ZnO), used as cement in endodontic; 2] ZnO NPs (21 nm); 3] three different types of Titanium dioxide (TiO_2) NPs: anatase TiO_2 (5.2 nm), anatase TiO_2 (9.1 nm) and rutile TiO_2 (55.1 nm). The tests employed were the *in vivo* wing Somatic Mutation and Recombination Test (SMART) in *Drosophila melanogaster* wings and the *in vitro* Cytokinesis-Block Micronucleus (CBMN) assay using Chinese hamster lung fibroblasts (V79 culture cells). *D. melanogaster* larvae of 72 ± 4 h, obtained from standard cross (ST) or high bioactivation cross (HB) were treated with 1.5625; 3.125; 6.25 or 12.5 mM to perform wing spot test (SMART). From both crosses, were obtained marker trans-heterozygous (MH) and balancer heterozygous (BH) descendants. The analysis of MH descendants showed that, for all composites, mutagenic and recombinogenic effects were observed only in HB cross. Statistically significant increase in the frequency of mutant spots was observed in individuals treated with 6.25 mM of amorphous ZnO and 12.5 mM of ZnO NPs, mainly due to induction of small single spots. The negative results observed in correspondent BH individuals, in witch is possible the detection only of mutation and chromosomal aberration, allow us to suggest that the increase in the frequency of small single spots observed in MH descendants is mainly due to recombination between *flr3* and *mwh* loci. For TiO_2 NPs, anatase of 5.2 nm was mutagenic at concentrations 1.5625 and 3.125 mM, and rutile phase of 55.1 nm significantly increased the frequency of mutant spots at all concentrations tested, except at 3.125 mM. Anatase TiO_2 NPs (9.1 nm) did not cause mutagenic effects in wing of *D. melanogaster* neither in ST nor in HB crosses. The mutagenic effects observed in HB cross in contrast with ST cross in SMART assay can be justified possibly by the increase of metabolic activity in that cross, with an increasing production of reactive oxygen species and consequently higher DNA aggression. To determine the cell treatment for CBMN assay, several concentrations of ZnO NPs and three types of TiO_2 NPs, ranging from 30.5 to 62,500.00 µM, were tested for cytotoxic activity by XTT colorimetric assay with

V79 cells. ZnO NPs (21 nm) and anatase TiO_2 NPs (5.2 and 9.1 nm) demonstrated similar cytotoxic intensity, showing decrease of V79 cell viability since concentration 224.1 μM. On the other hand, rutile TiO_2 NPs (55.1 nm) cytotoxicity started later, at 7,812.00 μM. Among all NPs assessed, only ZnO (21 nm) and anatase TiO_2 (5.2 nm) at highest concentration were able to induce genotoxicity in V79 cells. Both, anatase TiO_2 NPs (9.1 nm) and rutile TiO_2 NPs (55.1 nm) have not caused significant micronuclei increase. There are several physicochemical parameters that can influence on toxic effects of NPs, what corroborate to differences in cytotoxic and genotoxic patterns. In the experimental conditions performed in this study, we can affirm that both kinds of ZnO, as well, both, anatase and rutile phases of TiO_2 NPs, were able to induce mutagenicity. Therefore, the use of these NPs should be closely monitored and its genotoxicity action mechanisms must be elucidated.

Key words: *Drosophila melanogaster*; micronuclei; mutagenicity; SMART, V79 cells, XTT, Zinc oxide, Titanium dioxide

Sumário

Página

Capítulo 1

Fundamentação Teórica

NANOTECNOLOGIA

A nanotecnologia pode ser entendida como a ciência que envolve a síntese, manipulação, caracterização e aplicação de compostos, estruturas ou sistemas em escalas nanométricas, denominados nanomateriais. Estes são definidos como partículas com dimensões entre 1 e 100 nm, sendo que 1 nanômetro corresponde à bilionésima parte do metro (AUFFAN *et al.*, 2009; GONZALEZ; LISON; KIRSCH-VOLDERS, 2008; RAJ *et al.*, 2012).

A redução de compostos de tamanhos convencionais a nanopartículas (NPs) confere, aos mesmos, propriedades físicas, químicas e biológicas únicas, que os tornam aplicáveis em diversas áreas. Essas propriedades derivam, em grande parte, do aumento da razão superfície/volume (NEL *et al.*, 2006). Na indústria têxtil, o emprego de NPs tem como objetivo fabricar tecidos que não amarrotem, capazes de bloquear raios ultravioleta (UV), crescimento bacteriano e, ainda, que possam repelir líquidos, tornando-os impermeáveis e à prova de manchas (MANTOVANI; ZAPPELLI, 2009; SIEGFRIED, 2007). A nanotecnologia aplicada à agricultura objetiva o aumento da produção. Utilizando nanoestruturas semicondutoras de óxidos metálicos e, por meio de fotocatálise, pode detectar e degradar agentes patogênicos e poluentes que causam prejuízo para a lavoura (BARUAH; DUTTA, 2009). Nanofilmes têm sido projetados para serem utilizados como agente antirreflexo sobre lentes de óculos, telas de computadores, telefones celulares, câmeras e outras superfícies, assim como proporcionando maior impermeabilidade à água, resistência a riscos, etc. (NANO.GOV, 2014).

A capacidade de interação entre as NPs e células as tornaram excelentes candidatas para aplicações biomédicas. Revisões recentes têm destacado o emprego de NPs como sondas de medicamentos e genes, principalmente direcionados para o tratamento oncológico, promovendo um "*drug delivery*" mais efetivo e sítio específico. Os resultados mais notáveis têm sido relacionados com melhoria na eficácia do tratamento, com maiores taxas de cura, menos efeitos colaterais, infecções e/ou dores, devido às propriedades antimicrobianas, antiinflamatórias e analgésicas inseridas nas NPs (KIM; HYEON, 2014; LEHNER *et al.*, 2013; LI; ZHANG; YAN, 2014). Além da ampla utilização terapêutica, a nanotecnologia tem contribuído para o diagnóstico por imagem e, sobretudo, para

a medicina regenerativa, por meio da utilização de nanoestruturas com propriedades bioquímicas, mecânicas e elétricas similares às dos tecidos originais, que aumentam a adesão, proliferação e até diferenciação celular, promovendo o crescimento tecidual dirigido (YANG *et al.*, 2014).

A população mundial está diariamente exposta às NPs. Na indústria alimentícia, NPs têm sido utilizadas durante o processamento dos alimentos, como por exemplo, na descontaminação de equipamentos e no processo de embalagem (KUMARI; YADAV, 2014; PETERS *et al.*, 2014). No entanto, a popularidade da nanotecnologia deve-se, principalmente, ao setor de cosméticos e produtos de cuidados pessoais. Na fabricação de protetores solares, por exemplo, o uso de ingredientes em escala nanométrica confere maior proteção contra raios UV, penetração mais profunda na pele, efeitos mais duradouros, melhor solubilidade, transparência, etc. Tais características são obtidas principalmente devido ao tamanho reduzido dos compostos (RAJ *et al.*, 2012).

Os protetores solares modernos contêm NPs de dióxido de titânio (TiO_2) e de óxido de zinco (ZnO), os quais são, respectivamente, eficientes na proteção contra raios UV-B e UV-A. A combinação dessas NPs de óxidos metálicos assegura proteção UV de amplo espectro (MONTEIRO-RIVIERE *et al.*, 2011; SMIJS; PAVEL, 2011). Trabalhos de revisão enfatizam que o emprego de TiO_2 em nanoescala devem ser utilizados como barreira física devido ao seu elevado índice de refração e acentuada capacidade de absorção de raios UV, deixando os protetores solares mais eficientes, sobretudo quando as NPs são de aproximadamente 20 nm (BANERJEE, 2011; NOHYNEK; DUFOUR, 2012; SMIJS; PAVEL, 2011).

Estima-se que cerca de 33 milhões de pessoas nos Estados Unidos da América do Norte (EUA) utilizam protetores solares diariamente e 177 milhões utilizam ocasionalmente. Devido a essa ampla difusão no uso de produtos em nano escala, muito tem sido questionado com relação à segurança no uso de cosméticos e, principalmente de protetores solares, devido aos potenciais tóxicos/genotóxicos de NPs, sobretudo de TiO_2 e ZnO (FUKUI *et al.*, 2012; KWON *et al.*, 2014; LANDSIEDEL *et al.*, 2010b; MAKUMIRE *et al.*, 2014; MONTEIRO-RIVIERE *et al.*, 2011; NEWMAN; STOTLAND; ELLIS, 2009; SMIJS; PAVEL, 2011; STROBEL *et al.*, 2014).

ÓXIDO DE ZINCO

O óxido de zinco (ZnO) é um óxido metálico, semicondutor, inorgânico, insolúvel em água, que ocorre naturalmente como mineral, sendo as formas cristalinas mais comuns *wurtzite* (hexagonal) e *zinc-blende* (tetraédrica) (**Figura 1**), sendo *wurtzite* a forma mais estável (SMIJS; PAVEL, 2011). Inicialmente, o ZnO era obtido a partir de minerais, na forma de pó branco, utilizado em diversas aplicações há milhares de anos. Atualmente, a maioria do ZnO é produzido sinteticamente. A produção mundial é de, aproximadamente, 5 toneladas por ano (KLINGSHIRN, 2007).

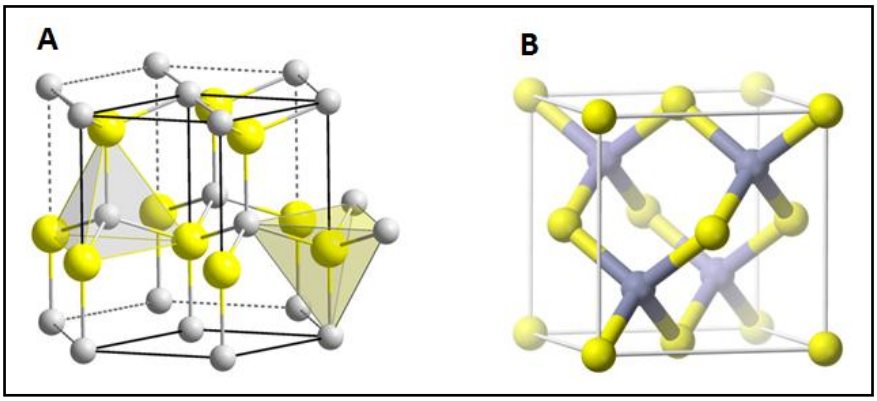

Figura 1. Estruturas cristalinas de ZnO. **A**: *wurtzite*; **B**: *zinc-blende*. As esferas cinza representam Zn e as amarelas O. FONTE: Adaptado de WIKIMEDIA.ORG (2007) e WIKIMEDIA.ORG (2008).

A síntese de ZnO pode ser realizada por diversos métodos, incluindo transporte de gás ou vapor, hidrotérmica e síntese por fusão pressurizada. Estas técnicas envolvem diferentes mecanismos de síntese, resultando em diferentes quantidades de cristais, com diversos graus de impureza e, consequentemente, diferentes propriedades ópticas e elétricas (JANOTTI; VAN DE WALLE, 2009).

Apesar de que a utilização de ZnO data de 500 anos a.C. (CRADDOCK, 1998), recentemente este óxido tem atraído muita atenção dentro da comunidade científica como o “material do futuro”. Muitos dos produtos industrializados que utilizamos no dia a dia contêm ZnO. Este componente sempre está presente em borrachas, cerâmicas, concretos, pigmentos. tintas, produtos farmacêuticos,

médicos, dentários e cosméticos, bem como em instrumentos eletrônicos, devido às suas propriedades ópticas e elétricas (JAGADISH; PEARTON, 2011; KLINGSHIRN, 2007; MOEZZI; MCDONAGH; CORTIE, 2012).

Diversos tipos de cosméticos, como por exemplo, hidratantes, batons, maquiagens, pomadas e loções possuem ZnO em sua formulação (NOHYNEK *et al.*, 2007). Uma das razões é que o ZnO auxilia na fixação do cosmético na pele, mas a principal razão, está relacionada à proteção contra luz UV de amplo espectro, principalmente UVA. ZnO já vem sendo utilizado na composição de protetores solares desde o final da década de 1990, e é considerado, dentre os diversos protetores solares regulados pela FDA/USA (Food and Drug Administration), como um dos que apresentam maior espectro de proteção contra raios UV (FDA, 2013; MOEZZI; MCDONAGH; CORTIE, 2012).

Conforme já relatado para TiO_2, há evidências de que a atenuação dos raios UV varia conforme o tamanho das partículas. O mesmo ocorre para o ZnO, sendo de 20 a 30 nm o tamanho considerado ótimo (MOEZZI; MCDONAGH; CORTIE, 2012; SINGH; NANDA, 2014; SMIJS; PAVEL, 2011). Muitos trabalhos têm avaliado o potencial de citotoxicidade e genotoxicidade de NPs de ZnO, visando contribuir para o conhecimento sobre a segurança da utilização rotineira de produtos contendo NPs (ADAMCAKOVA-DODD *et al.*, 2014; FILIPPI *et al.*, 2014; KWON *et al.*, 2014; MONTEIRO-RIVIERE *et al.*, 2011; NEWMAN; STOTLAND; ELLIS, 2009; SANTO *et al.*, 2014; SMIJS; PAVEL, 2011).

Devido à ampla aplicabilidade de ZnO na área odontológica, um estudo recente mostrou que a utilização de NPs de ZnO (21 nm), em implantes intraósseos da mandíbula, provocou discreto processo inflamatório. No entanto, houve boa tolerância, formação e remodelamento ósseo, caracterizando como biocompatíveis as NPs de ZnO utilizados no estudo (SOUSA *et al.*, 2014).

Geralmente, NPs têm maior atividade física e química do que os mesmos compostos de maior tamanho, pelo fato da área de superfície ser extremamente maior que o volume (FUKUI *et al.*, 2012). Essa maior reatividade pode, potencialmente, causar efeitos biológicos adversos, tais como toxicidade e genotoxicidade, devido à maior interação das NPs com o sistema biológico (OBERDORSTER; OBERDORSTER; OBERDORSTER, 2005; SINGH *et al.*, 2009). No entanto, resultados contraditórios têm sido descritos na literatura.

NPs de ZnO, assim como *bulk* ZnO, provocaram efeitos tóxicos em bactérias (*Vibrio fischeri*) e crustáceos (*Daphnia magna* e *Thamnocephalus platyurus*). Essa toxicidade foi associada aos íons Zn^{2+} solubilizados, o que foi comprovado por um sensor que induz a bioluminescência do íon metálico no meio intracelular (HEINLAAN *et al.*, 2008). Em cultura celular, observou-se que NPs de ZnO, de aproximadamente 45 nm, induziram redução da viabilidade celular, bem como aumento da liberação de lactato desidrogenase (LDH) e ROS. O aumento de ROS foi responsável pela ativação da via de sinalização c-Jun N-terminal kinase (JNK), comprometendo a integridade das membranas celulares e levando a apoptose dos astrócitos (WANG, J. *et al.*, 2014). Resultados semelhantes foram descritos por WANG, B. *et al.* (2014) frente à exposição de macrófagos RAW 246.7 a NPs de ZnO. Este autor associou a internalização e a dissolução intracelular das NPs com liberação de Zn^{2+} à alta toxicidade do ZnO em nanoescala. Recentemente, um estudo *in vitro* mostrou que a intensidade dos efeitos citotóxicos de NPs de ZnO de 30, 90 e 200 nm foram diretamente proporcionais ao aumento da dose e do tempo de exposição das células humanas epiteliais de adenocarcinoma (Caco-2) às NPs, além de associar o maior potencial citotóxico às partículas de menor tamanho (KANG *et al.*, 2013).

NPs de ZnO de tamanho médio de 30 nm foram observadas no interior de *Escherichia coli*, levando à indução de estresse oxidativo, com danos ao DNA e morte celular. Com base nestas observações, KUMAR *et al.* (2011) estabeleceram um mecanismo hipotético para a toxicidade celular provocada por NPs de ZnO. De acordo com esses autores, a toxicidade celular pode ser devida à geração de radical hidroxila ($OH^{\bullet}$), radical superóxido (O^{2-}), e peróxido de hidrogênio (H_2O_2) que levaram à oxidação de fosfolípidos poli-insaturados (LPO). Segundo os autores, a reação de LPO causou danos ao DNA, depleção de glutationa (GSH) e rompimento da morfologia de membranas e da cadeia de transporte de elétrons, levando à morte celular (**Figura 2**).

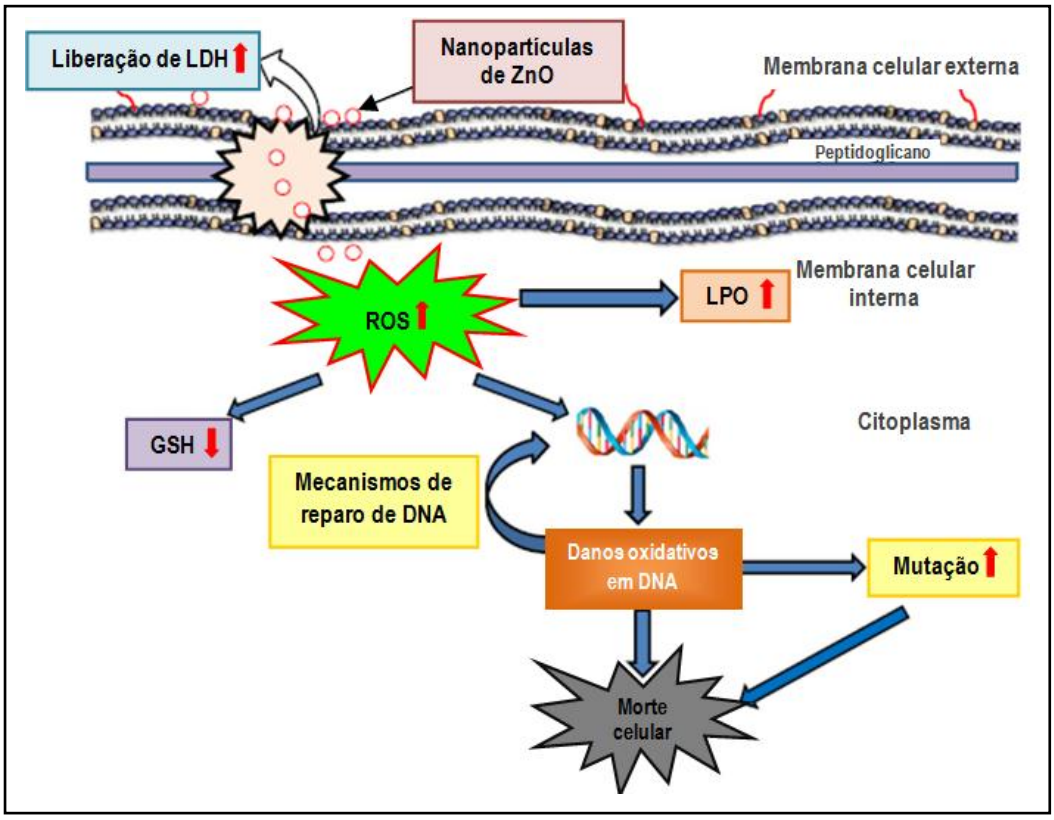

Figura 2. Possíveis mecanismos de genotoxicidade de NPs de ZnO. FONTE: Adaptado de KUMAR *et al.* (2011).

Em relação à genotoxicidade, o Teste Cometa e o Teste do Micronúcleo com bloqueio de citocinese (CBMN) têm sido bastante utilizados para avaliação de danos ao DNA mediante exposição *in vitro* ou *in vivo* às NPs de ZnO (CORRADI *et al.*, 2012; DEMIR *et al.*, 2014; GUAN *et al.*, 2012; OSMAN *et al.*, 2010; YIN *et al.*, 2010). DEMIR *et al.* (2014) encontraram resultados positivos em ambas metodologias, após o tratamento de células humanas epiteliais renais (HEK293) e fibroblastos embrionários de camundongo (NIH/3T3) com doses acima de 100 µg/mL de NPs de ZnO. Também relataram a dependência entre a concentração do composto e o tempo de exposição aos efeitos citotóxicos e danos citogenéticos em células hepatocarcinogênicas, linhagem celular HEp-2 (OSMAN *et al.*, 2010). Diante da investigação de efeitos genotóxicos de NPs de ZnO em cultura de linfócitos periféricos humanos por meio do teste de aberrações cromossômicas (AC) e do teste do micronúcleo (MN), observou-se que, além de induzir aberrações, as concentrações intermediárias de NPs de ZnO aumentaram

a frequência de células binucleadas micronucleadas de maneira dose dependente. Os autores sugerem que a ausência de efeitos tóxicos no teste do MN, conforme observado para a maior concentração testada pode ser devido ao aumento de agregação das NPs quando em altas concentrações (GUMUS *et al.*, 2014).

Quatro diferentes testes de genotoxicidade (Teste de Ames, Teste de AC *in vitro*, Teste Cometa e Teste do MN) foram realizados para avaliação de quatro tipos de NPs de ZnO (20 e 70 nm, carregadas positiva ou negativamente). Para todos os testes, *in vitro* e *in vivo*, em todas as concentrações avaliadas, nenhum efeito genotóxico foi observado. No entanto, de acordo com os autores do referido artigo, não se deve ignorar a possibilidade de genotoxicidade em doses inferiores às utilizadas neste estudo, uma vez que em altas concentrações, as NPs podem se aglomerar e deixar de exercer efeitos tóxicos (KWON *et al.*, 2014).

Devido ao fato de as NPs serem artificialmente sintetizadas e passarem por processos para aplicações específicas, suas características físico-químicas e o potencial de reatividade podem variar consideravelmente (MA; WILLIAMS; DIAMOND, 2013). Assim, diante da diversidade de propriedades das NPs, como por exemplo, tamanho da partícula, pureza, estrutura cristalina, solubilidade e modificação de superfície, e da ampla gama de linhagens celulares e organismos modelo testados, a presença de resultados heterogêneos quanto à citotoxicidade e genotoxicidade é devidamente justificada.

DIÓXIDO DE TITÂNIO

O dióxido de titânio (TiO_2) é um óxido metálico de forma cristalina, inorgânico, insolúvel em água e que ocorre naturalmente na forma de minerais. Os átomos de titânio e oxigênio podem estar organizados em três fases cristalinas fundamentais, denominadas: anatase (tetragonal), rutila (tetragonal) e brookite (ortorrômbica) (**Figura 3**). A fase rutila apresenta maior estabilidade, alta densidade, elevado índice de refração e é a mais comum. Essas características ocorrem por ser estruturalmente mais compacta que a anatase. As fases metaestáveis anatase e brookite se convertem para rutila, após aquecimento, sendo que a forma brookite é formada em ambientes ácidos (BANFIELD;

VEBLEN, 1992). A rutila, a anatase e a brookite contêm íons de titânio coordenados no centro de um octaedro formado por seis íons O^{2-}. Cada átomo de oxigênio tem três titânios vizinhos, pertencendo a três octaedros diferentes. As estruturas da rutila e da anatase diferem pela distorção nos octaedros formados pelos átomos de oxigênio. Brookite apresenta maior volume por célula comparado à anatase e rutila, com 8 grupos de TiO_2 por unidade celular, enquanto anatase e rutila apresentam 4 e 2 grupos de TiO_2 por unidade celular, respectivamente (**Figura 3**).

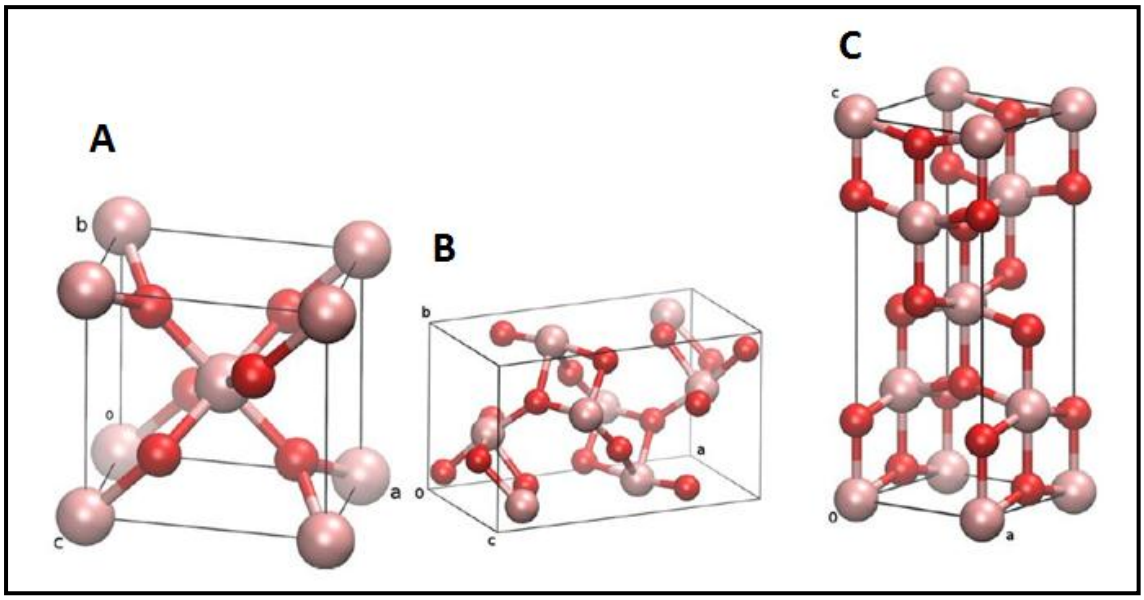

Figura 3. Estruturas unitárias de rutila (**A**); brookite (**B**) e anatase (**C**). FONTE: Adaptado de MOELLMANN *et al.* (2012)

A partir destes cristais, TiO_2 tem sido produzido comercialmente desde 1923, na forma de um pó branco, que apresenta alto índice de refração, conferindo alta opacidade e poder de cobertura. Aproximadamente 70% de todo o TiO_2 produzido é utilizado para fins de pigmentação. Pequena quantidade de TiO_2 é utilizada para outros fins, que envolvem aplicações em plásticos, papéis, produtos farmacêuticos, alimentícios, antimicrobianos, tratamento de águas residuais, etc. Devido à versatilidade deste produto, estima-se que a produção mundial de artigos/produtos que possuem TiO_2 NPs na sua composição seja em torno de 4,5 milhões de toneladas por ano (IARC, 2010; MCNULTY, 2007). (LANDSIEDEL *et al.*, 2010a). A capacidade de opacificar e branquear o meio

dispersante é controlada em função do índice de refração e do tamanho das NPs. O índice de refração é controlado em função da fase e o tamanho, pelo processo de síntese. Por exemplo, NPs de TiO_2 com fase rutila tem um efeito maior de branquear soluções do que na fase anatase ou brookite.

O procedimento mais comum para a síntese de NPs de TiO_2 utiliza a hidrólise de sais de titânio (Ti) em solução ácida (MAHSHID; ASKARI; GHAMSARI, 2007). A utilização de condensação de vapor químico ou nucleação de sol-gel podem controlar a estrutura, tamanho e forma de NPs de TiO_2 (WU *et al.*, 2005; ZHOU *et al.*, 2008).

Diversos trabalhos mostram a vasta aplicabilidade de NPs de TiO_2 (STROBEL *et al.*, 2014; WEIR *et al.*, 2012). Por apresentar potencial oxidante, associado ao baixo custo e relativa estabilidade física e química, NPs de TiO_2 são semicondutores na construção de dispositivos de diversas aplicações, como por exemplo, para aproveitar a energia solar e convertê-la em eletricidade e combustível químico (hidrogênio) e, como fotocatalisador, em que poluentes orgânicos são degradados em espécies químicas menos nocivas ao meio ambiente (BANERJEE, 2011).

WEIR *et al.* (2012) salientaram a utilização exacerbada de NPs de TiO_2 na indústria alimentícia, principalmente na cobertura de doces, balas, gomas de mascar, bem como em produtos de higiene pessoal, produtos de limpeza, entre outros. Estes autores quantificaram o montante de titânio presente em 89 alimentos, concluindo que as maiores concentrações foram encontradas em gomas de mascar.

Atualmente, são comercializadas uma série de diferentes tipos de NPs de TiO_2. Os diversos tipos de NPs diferem não somente quanto à estrutura cristalina (rutila, brookite, anatase), mas também por apresentar diferenças de tamanho, morfologia, propriedades de superfície, presença ou não de aglomerados e formação de sedimentos. Todos esses fatores têm um papel crucial na interação com o meio biológico (GITROWSKI; AL-JUBORY; HANDY, 2014; JIANG *et al.*, 2008; KARLSSON *et al.*, 2009; ZHANG *et al.*, 2013).

O aumento no número de produtos que contêm TiO_2 em nanoescala pode resultar em exposição exacerbada a esses NPs, tanto para o homem quanto para o meio ambiente.

A literatura científica apresenta elevado número de trabalhos relacionados aos efeitos adversos de NPs. Têm sido descritos efeitos inflamatórios, fibrose e até mesmo tumores, induzidos em pulmão de roedores, por exposição crônica a NPs de TiO_2 (CHEN; YAN; LI, 2014; LINDBERG *et al.*, 2012; OBERDORSTER; OBERDORSTER; OBERDORSTER, 2005; WARHEIT *et al.*, 2007; WEIR *et al.*, 2012). Além disso, vários trabalhos apresentam resultados positivos para citotoxicidade e genotoxicidade, por meio de experimentos *in vitro* e *in vivo* (CHEN *et al.*, 2014; PRASAD *et al.*, 2013; SETYAWATI *et al.*, 2013; SHUKLA *et al.*, 2013; SRIVASTAVA *et al.*, 2011; TAVARES *et al.*, 2014). CHEN *et al.* (2014) mostraram que NPs de TiO_2 (75 ± 15 nm) induziram quebra de DNA de fita dupla em células de medula óssea de ratos após administração oral, e também observaram, *in vitro*, efeitos mutagênicos em células V79, detectados pelo teste da hipoxantina-guanina fosforibosil transferase (HPRT). Efeitos genotóxicos, avaliados pelo teste CBMN, foram relatados após exposição de linfócitos humanos a NPs de TiO_2 de aproximadamente 20 nm, na forma de anatase e rutila, embora não tenha sido observado relação dose - resposta (TAVARES *et al.*, 2014). Diante das evidências em relação ao potencial carcinogênico do TiO_2 em experimentos com animais, em 2010, a Agência Internacional para Pesquisa de Câncer (IARC) reclassificou o TiO_2 como possível carcinogênico aos humanos (IARC, 2010).

Os métodos pelos quais NPs induzem efeitos citotóxicos e genotóxicos ainda não estão claramente elucidados. No entanto, trabalhos recentes têm demonstrado o aumento na produção de espécies reativas de oxigênio (ROS) frente à exposição a NPs, levando a efeitos oxidativos que podem estar diretamente relacionados ao potencial tóxico do TiO_2 em nanoescala (FU *et al.*, 2014; GUTIERREZ IGLESIAS *et al.*, 2014). As ROS oferecem uma ameaça à integridade celular por provocar dano ao DNA, lipídios, proteínas e outras macromoléculas (COOKE *et al.*, 2003). Como consequência, o estresse oxidativo causa alterações de bases do DNA e quebras de fitas simples ou duplas, que podem provocar efeitos tóxicos e/ou mutagênicos (GIRARD; BOITEUX, 1997).

Em relação às NPs de TiO_2, há evidências de que a atividade fotocatalítica, bem como a capacidade de produção de ROS é maior para a forma anatase do que para a rutila (BANERJEE, 2011; JIANG *et al.*, 2008; SMIJS; PAVEL, 2011).

Além dos efeitos oxidativos, NPs de anatase e rutila prejudicam a capacidade de reparo do DNA, por meio da inativação do reparo por excisão de bases (BER) e por excisão de nucleotídeos (NER) (JUGAN *et al.*, 2012), favorecendo o estabelecimento do dano.

A internalização de NPs de TiO_2 tanto para o citoplasma quanto para o núcleo de células de carcinoma hepatocelular humano (HepG2) foi confirmada via microscopia eletrônica de transmissão (TEM) e citometria de fluxo por SHUKLA *et al.* (2013). O referido trabalho também elenca os possíveis mecanismos de indução de toxicidade, destacando marcadores de estresse oxidativo (aumento na geração de ROS, redução dos níveis de glutationa - GSH, peroxidação lipídica - LPO) e marcadores de apoptose (redução do potencial de membrana mitocondrial - MMP, aumento da expressão de p53, caspase 3 e caspase 9, BAX, Cyto-c e Apaf-1, redução de Bcl-2), conforme demonstrado pela **Figura 4**.

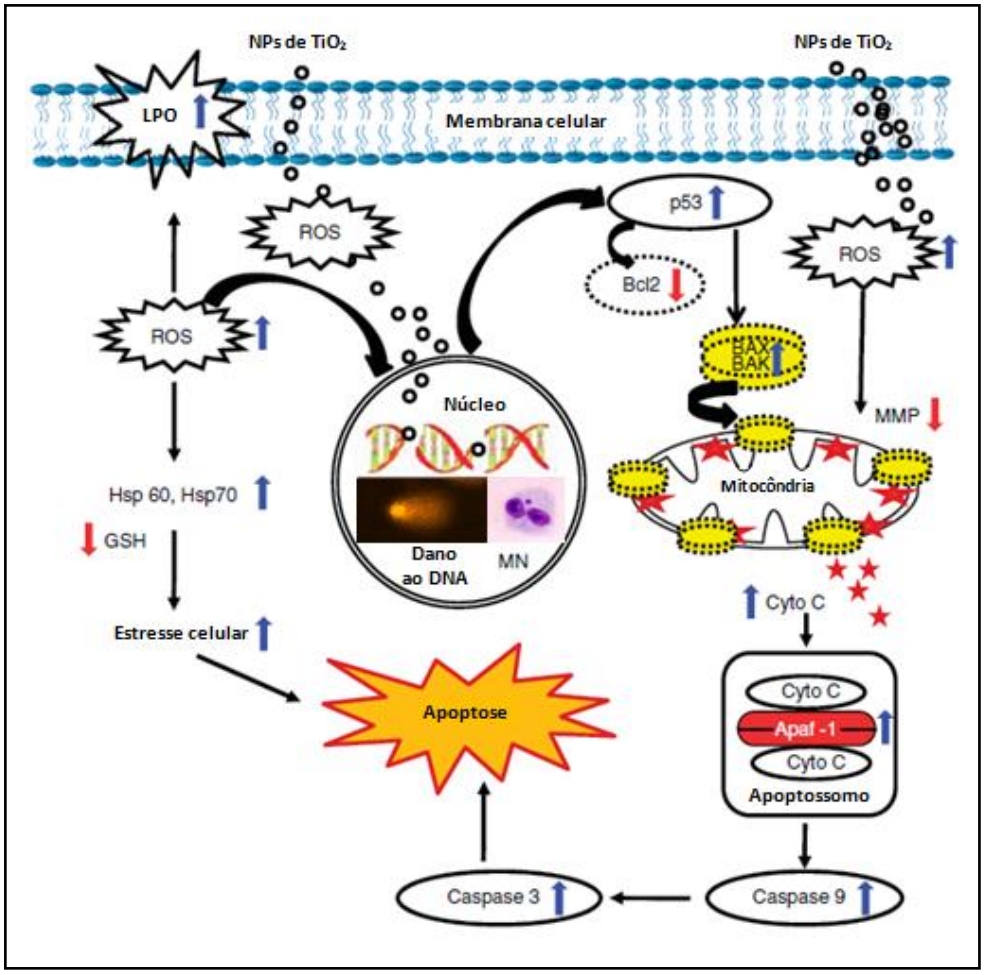

Figura 4. Representação esquemática, mostrando os possíveis mecanismos de indução de toxicidade de NPs de TiO_2 em células HepG2. FONTE: Adaptado de SHUKLA *et al.* (2013).

Por outro lado, ausência de efeitos cito e/ou genotóxicos frente à exposição às NPs de TiO_2 também é descrita em estudos *in vitro* (GUICHARD *et al.*, 2012; LANDSIEDEL *et al.*, 2010b) e *in vivo* (DEMIR *et al.*, 2013; DOBRZYNSKA *et al.*, 2014; LANDSIEDEL *et al.*, 2010b). É importante considerar que alguns trabalhos demonstraram a formação de agregados, ou aglomerados de NPs que podem aumentar em até 40 vezes o tamanho individual da partícula (STROBEL *et al.*, 2014). A presença desses agregados/aglomerados pode influenciar na interação biológica das NPs com o meio, com as células, bem como o processo de internalização e geração de efeitos cito- ou genotóxicos (BUTLER *et al.*, 2014; JANER *et al.*, 2014; LANKOFF *et al.*, 2012; PETKOVIC *et al.*, 2011).

Diante desses dados e frente ao crescente aumento da exposição humana às NPs, são necessárias mais investigações sobre a citotoxicidade, genotoxicidade e mutagênicidade das NPs de TiO_2, buscando-se estabelecer associações entre as propriedades fisicoquímicas e os efeitos tóxicos (JIANG *et al.*, 2008; LANDSIEDEL *et al.*, 2009; LI; ZHANG; YAN, 2014; STROBEL *et al.*, 2014; ZHANG *et al.*, 2013).

TESTE DO MICRONÚCLEO COM BLOQUEIO DE CITOCINESE

A ocorrência de mutação está relacionada à instabilidade cromossômica e falha no mecanismo de reparo do DNA, podendo levar à morte celular ou desenvolvimento de câncer (HERNANDEZ; BENTHEM; JOHNSON, 2013). O Teste do Micronúcleo com bloqueio de citocinese (CBMN) é um ensaio citogenético utilizado para detecção de alterações cromossômicas estruturais ou numéricas, indicado para triagem toxicológica de rotina (EL-ZEIN; VRAL; ETZEL, 2011; KIRKLAND, 2010; OECD, 2010; SCHMID, 1975).

O micronúcleo (MN) pode ser originado devido ao atraso na migração de cromossomo acêntrico ou fragmentos de cromátides, causados por reparo errôneo ou por falta de reparo na quebra do DNA. Má segregação cromossômica durante a anáfase também pode levar a formação de MN, como resultado de hipometilação de sequências repetidas na região centromérica ou pericentromérica, defeitos do cinetocoro, das fibras do fuso e dos genes envolvidos nos pontos de checagem da anáfase (FENECH *et al.*, 2011). Os fragmentos, ou cromossomos inteiros, formam um pequeno núcleo individual, denominado MN (**Figura 5**), que pode ser detectado em células interfásicas como um pequeno corpúsculo arredondado de cromatina (FENECH, 2000; FENECH, 2007; PARVATHI; RAJAGOPAL, 2014; SCHMID, 1975). O aumento na frequência de células micronucleadas é um biomarcador de efeitos genotóxicos, que pode refletir a exposição a agentes clastogênicos e aneugênicos, possibilitando dimensionar os danos citogenéticos induzidos por qualquer agente químico (RAO *et al.*, 2006).

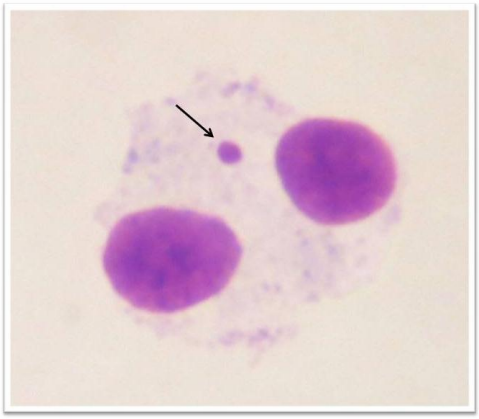

Figura 5. Fotomicrografia de célula binucleada de pulmão de hamster Chinês (V79) micronucleada. A seta indica o MN (coloração: Giemsa; analisado em microscópio óptico de luz. Aumento 1000x). FONTE: Arquivo pessoal.

O CBMN é o teste de escolha para avaliação de indução de MN em cultura de células humanas ou de mamíferos, pois avalia especificamente células que estão em processo final de uma divisão, ou seja, células ainda binucleadas (BN). A obtenção de células BN é possível por meio do bloqueio da citocinese com citocalasina-B (Cyt-B), um inibidor de polimerização da proteína actina, requerida para a formação do anel de microfilamentos que induzem a contração do citoplasma e clivagem da célula em duas células filhas (FENECH, 2000; FENECH, 2007; FENECH; MORLEY, 1985). Devido à confiabilidade e reprodutibilidade do teste, o CBMN tornou-se um dos testes citogenéticos padrão de toxicologia em células humanas e de mamíferos (FENECH, 2007).

A técnica consiste em expor uma cultura de células à substância a ser avaliada, bem como aos controles positivo e negativo. O agente alquilante metil metano sulfonato (MMS) geralmente é utilizado como controle positivo no teste do MN, uma vez que induz quebras de fita dupla do DNA (LUNDIN *et al.*, 2005), e o controle negativo é o solvente/veículo utilizado como diluente da substância teste. As células tratadas são mantidas em cultura por um período suficiente para que a substância possa atuar, causando dano cromossômico ou nas fibras do fuso que leve à formação de MN. Após o tratamento, a adição de Cyt-B é importante para demonstrar que as células analisadas passaram por uma divisão, durante ou após a exposição à substância teste. Estas células são fixadas em lâmina, coradas e

posteriormente analisadas de acordo com a presença e quantidade de MNs, por meio de microscopia óptica (OECD, 2010).

Uma das linhagens celulares comumente utilizadas para a realização do teste do MN é a linhagem V79 (fibroblastos de pulmão de hamster Chinês), pois possuem características interessantes aos ensaios de toxicologia genética, como: fácil cultivo e manutenção em laboratório e cariótipo estável. Além disso, mesmo estocadas em nitrogênio líquido, estas células não têm suas características afetadas, não comprometendo os ensaios (BRADLEY *et al.*, 1981).

Para avaliação do potencial mutagênico são realizados três ensaios independentes. Para cada tratamento são confeccionadas duas lâminas. As lâminas são analisadas em teste cego, utilizando-se microscópio óptico de luz, com objetiva de imersão (aumento final de 1000 X). Um total de, pelo menos, 1.000 células binucleadas (por tratamento) deve ser analisado, registrando-se o total de MNs. As células analisadas são distribuídas de acordo com a quantidade de MNs: 0, 1, 2 ou mais. Para quantificação da frequência de MNs, apenas células binucleadas com núcleos intactos, com tamanhos aproximadamente iguais, mesmo padrão de coloração e dentro do limite citoplasmático, com membrana nuclear intacta, e célula claramente distinguível das células adjacentes, são analisadas (FENECH, 2000).

Para avaliar a citotoxicidade e o efeito citostático da substância testada, é calculado o índice de divisão nuclear (IDN). Para tanto, são analisadas pelo menos 500 células viáveis (com citoplasma bem preservado) para cada tratamento. Para o cálculo do IDN utiliza-se a seguinte fórmula: IDN = [M1 + 2(M2) + 3(M3) + 4(M4)]/N, onde M1-M4, representam os números de células com 1, 2, 3 e 4 núcleos, respectivamente, e N o número total de células analisadas (EASTMOND; TUCKER, 1989; FENECH, 2000).

***SOMATIC MUTATION AND RECOMBINATION TEST* – SMART**

Mutação e recombinação são processos que acontecem a todo instante durante o desenvolvimento celular. A mutação, em especial, é fonte da mudança evolutiva, produzindo novos alelos espontaneamente ou por exposição a agentes físicos, químicos ou biológicos. Já a recombinação, promove o rearranjo de

alelos, agrupando-os em novas combinações. Esses processos garantem a variação genética, mas, por outro lado, também são responsáveis pelo envelhecimento e por patologias relacionadas, tais como o câncer e doenças neurodegenerativas (KENNEDY; LOEB; HERR, 2012). Para manter os processos evolutivos, os organismos biológicos dispõem de uma grande variedade de mecanismos de reparo do DNA, que promovem a replicação exata do DNA durante a divisão celular e a remoção de possíveis danos (FRIEDBERG, 2006). Entretanto, uma falha nos mecanismos de reparo possibilita a fixação da mutação.

Ensaios *in vitro* e *in vivo* são extensivamente empregados na avaliação do potencial genotóxico de nanomateriais (LANDSIEDEL *et al.*, 2009; SINGH *et al.*, 2009). A avaliação *in vivo* tem importância significativa devido a diversas interações, efeitos hormonais e enzimáticos, mecanismos de reparo do DNA, etc. No entanto, o uso de animais em pesquisas genéticas/toxicológicas é alvo de preocupações, sendo necessário o desenvolvimento de modelos animais alternativos (ARORA; RAJWADE; PAKNIKAR, 2012; SIDDIQUE *et al.*, 2005). Recentemente, a mosca da fruta, *Drosophila melanogaster*, foi destacada como modelo experimental para avaliação da toxicidade de nanomateriais.

As vantagens inerentes ao trabalho com *D. melanogaster* compreendem o tempo de geração curto, prole numerosa, baixos custos para manutenção das linhagens em laboratório, susceptibilidade para manipulação genética, facilidade de detectar alterações fenotípicas e, principalmente, homologia e conservação do genoma semelhante ao dos organismos superiores (DEMIR *et al.*, 2013; DEMIR *et al.*, 2011; GRAF *et al.*, 1996; PARVATHI; RAJAGOPAL, 2014).

As linhagens de *D. melanogaster* são cultivadas e mantidas em incubadora *Biochemical Oxigen Demand* (B.O.D.) a 25 ºC e foto período (12 h claro / 12 h escuro), dentro de frascos contendo meio de cultura à base de ágar, banana e fermento biológico. O tempo de geração do ovo ao indivíduo adulto é de aproximadamente 10 dias (Figura 5). O estágio larval é caracterizado pelo período alimentar, enquanto que durante a metamorfose de larva até adulto é o período não alimentar. Possui quatro pares de cromossomos (2n = 8), sendo três pares autossômicos e um par de cromossomos sexuais. Machos e fêmeas de *D. melanogaster* apresentam dimorfismo sexual. As fêmeas geralmente são maiores

que os machos e apresentam uma alternância típica de listas claras e escuras ao longo do abdômen. Nos machos é observada a presença de uma mancha escura na extremidade posterior do abdômen, bem como a presença de pente sexual localizado no primeiro par de patas (**Figura 6**).

Há mais de cem anos utiliza-se a *D. melanogaster* em experimentos laboratoriais. Primeiramente, essa mosca era tida como organismo modelo para estudos genéticos e contribuiu para princípios fundamentais como, por exemplo, a teoria da herança cromossômica. Dentre esses ensaios, o Teste para Detecção de Mutação e Recombinação Somática (*Somatic Mutation and Recombination Test* - SMART), também chamado de Teste da Mancha da Asa, é destacado como o padrão ouro para testes de mutagenicidade com *D. melanogaster*. Por meio deste teste, é possível avaliar perda de heterozigose (LOH) como consequência de mutação, quebra cromossômica e/ou recombinação mitótica (GRAF *et al.*, 1984; MOLLET; WURGLER, 1974; PARVATHI; RAJAGOPAL, 2014).

O SMART em células de asa de *D. melanogaster* foi desenvolvido por GRAF *et al.* (1984) e aprimorado por GRAFVAN SCHAIK (1992). Desde então, empregado na avaliação mutagênica de centenas de substâncias químicas, incluindo compostos em nanoescala (DE ANDRADE et al., 2014; DE REZENDE et al., 2013; DEMIR et al., 2013; FROLICH; WURGLER, 1990; GRAF et al., 1989; MACHADO et al., 2013; SPANO et al., 2001).

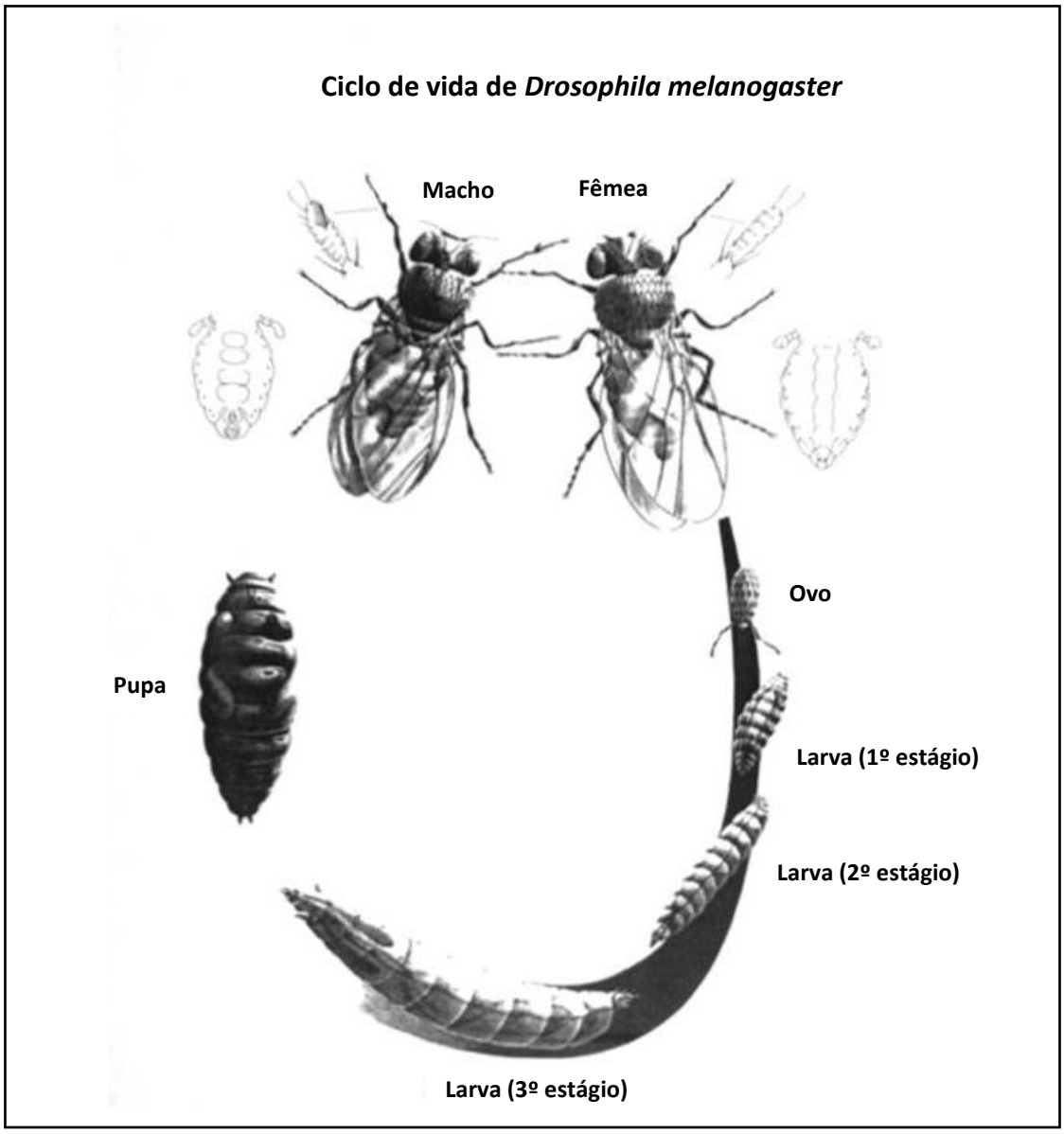

Figura 6. Esquema representativo do ciclo de vida e do dimorfismo sexual de *D. melanogaster.* FONTE: Cortesia Dr. Ulrich Graf – *Institute of Toxicology* ETH - Zurich – Suíça.

O SMART é realizado por meio de cruzamentos experimentais, utilizando três linhagens portadoras dos marcadores recessivos das células das asas: *multiple wing hairs* (*mwh*, 3-0,3) e *flare* (*flr*^{3}, 3-38,8). As linhagens utilizadas são:

1) linhagem "*multiple wing hairs*" (*mwh*) com constituição *genética y; mwh jv*. O marcador *mwh*, presente no cromossomo 3, encontra-se em posição mais distal

em relação ao centrômero (3-0,3). Quando expresso, o fenótipo do pelo selvagem da asa (**Figura 7A**) é modificado, originando pelo múltiplo (**Figura 7B**), além disso, a borda da asa é lisa.

2) linhagem "*flare-3*" (*flr*^{3}), com constituição genética *flr*^{3} / *In(3LR)TM3, ri p*^{p} *sep l(3)89Aa bx*^{34e} e *Bd*^{S} . O marcador *flr*^{3}, presente no cromossomo 3, encontra-se em posição mais proximal em relação ao centrômero (3-38,8). Quando expresso, o fenótipo do pelo da asa também é modificado, originando pelos que se assemelham a uma chama de vela (**Figura 7C**). Devido à sua letalidade em homozigose, este alelo é mantido graças à presença de um balanceador cromossômico (*TM3, Bd*^{S}). A borda da asa desses indivíduos é serrilhada, devido à presença do marcador *Bd*^{S}.

3) linhagem "ORR; flare-3" (ORR; flare-3), com constituição genética ORR; flr3 / In(3LR)TM3, ri pp sep l(3)89Aa bx34e e BdS. Os indivíduos pertencentes à essa linhagem possuem os mesmos marcadores que os da linhagem "flare-3". Entretanto, a linhagem "ORR; flare-3" é portadora de genes de expressão elevada codificadores de enzimas do complexo citocromo P450, localizados nos cromossomos 1 e 2, provenientes da linhagem "Oregon R", naturalmente resistente ao DDT (GRAF; VAN SCHAIK, 1992; GRAF et al., 1984).

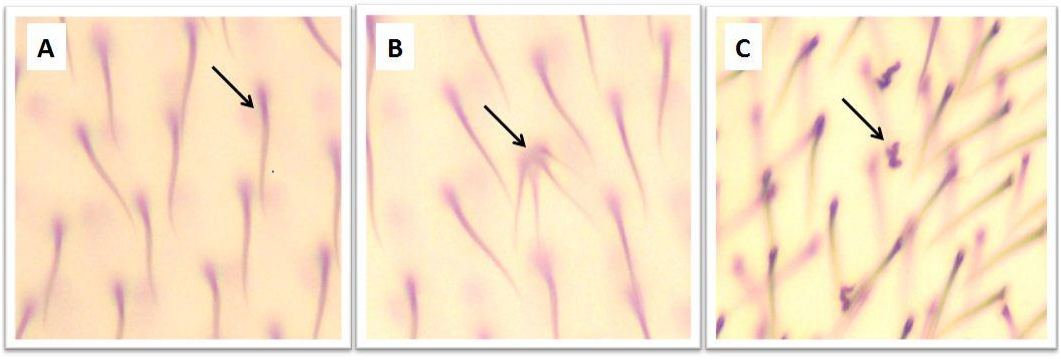

Figura 7. Fotomicrografias de diferentes fenótipos de pelos de asas de *D. melanogaster*, indicados por setas. **A**: Pelo selvagem. **B**: Pelos múltiplos (*mwh*). **C**: Pelo *flare* (*flr*^{3}). FONTE: Arquivo pessoal.

Com estas linhagens são realizados dois tipos de cruzamentos:

1) Cruzamento padrão (ST – s*tandard cross*) entre machos "*mwh*" e fêmeas virgens "*flr*^{3}". Este cruzamento é útil na detecção de agentes genotóxicos diretos (GRAF *et al.*, 1989; GRAF *et al.*, 1984).

2) Cruzamento de alta bioativação (HB - *high bioactivation cross*) entre machos "*mwh*" e fêmeas virgens "*ORR*; *flr*^{3}". Este cruzamento é útil na detecção de agentes genotóxicos indiretos, ou promutágenos, que necessitam de ativação metabólica para induzir efeitos genotóxicos (GRAF; VAN SCHAIK, 1992).

Ambos os cruzamentos produzem dois tipos de progênie: 1) Fêmeas e machos trans-heterozigotos marcados (*mwh + / + flr*^{3}) (MH), que apresentam a borda da asa lisa (**Figura 8**: **A** e **C**); e 2) Fêmeas e machos heterozigotos balanceados (*mwh + / + TM3, Bd*^{S}) (BH), que apresentam a borda da asa serrilhada (**Figura 8**: **B** e **D**).

Durante o tratamento com a substância que se deseja testar, as células dos discos imaginais das larvas de *D. melanogaster*, que darão origem às asas das moscas adultas, são expostas à substância com potencial mutagênico. A indução de LOH nas células dos discos imaginais leva à formação de clones de células mutantes (manchas). Fenotipicamente a célula mutante pode expressar pelo múltiplo e/ou pelo *flare* (GRAF *et al.*, 1984).

Indivíduos adultos resultantes da progênie MH podem expressar tanto manchas simples (*mwh* ou *flare*) quanto manchas gêmeas (*mwh* e *flare*). Manchas simples são consideradas aquelas que expressam apenas um dos genes mutantes, *flr*^{3} ou *mwh* e podem ser classificadas como simples pequenas (manchas com uma ou duas células) ou simples grandes (manchas com mais de duas células). São resultantes de LOH em qualquer um dos marcadores, por meio de mutação, aberração cromossômica, não-disjunção mitótica e recombinação, exclusivamente para manchas simples do tipo *mwh*. Enquanto, manchas gêmeas são oriundas exclusivamente de recombinação mitótica (GRAF *et al.*, 1984) (**Quadro 1**).

Na progênie BH, as manchas mutantes são sempre simples e do tipo *mwh*, resultantes de mutação, aberração cromossômica ou não-disjunção (SPANÓ; GRAF, 1998). O cromossomo balanceador (TM^3, Bd^s) apresenta múltiplas inversões, impossibilitando o desenvolvimento de células que sofreram eventos recombinogênicos (GRAF *et al.*, 1984; GUZMÁN-RINCÓN; GRAF, 1995).

Durante a análise das superfícies dorsal e ventral das asas de *D. melanogaster*, são considerados o número e o tipo de manchas encontradas, fornecendo dados quantitativos e qualitativos, que permitem o tipo e a intensidade do evento mutagênico induzido (SPANÓ; GRAF, 1998).

Quadro 1. Possíveis alterações (mutação, aberração, recombinação) responsáveis pelo aparecimento de diferentes tipos de manchas mutantes, detectadas pelo teste da mancha da asa. Adapatado de PARVATHI, RAJAGOPAL (2014).

Tipo de alteração	**Observação**	**Tipo de mancha observada**
Mutação de ponto Alteração cromossômica Recombinação mitótica	Em *flr +* ou *mwh +* Deleção de *flr +* ou *mwh +*	Manchas simples *flr*^{3} ou *mwh* (grandes ou pequenas)
Recombinação mitótica (exclusivamente)	Manchas gêmeas indicam ação recombinogênica do composto testado	Manchas gêmeas (células expressando pelos *flr*^{3} e *mwh* adjacentes)
Manchas pequenas: são expressas devido a aberrações cromossômicas, independentemente do tempo de iniciação em que as células afetadas não proliferam ou proliferam mais lentamente.	Manchas pequenas são produzidas durante o último ou penúltimo ciclo de divisão celular na fase de pupa	Manchas simples pequenas (um ou dois pelos mutantes)
Manchas grandes	Manchas grandes são produzidas mais cedo, durante o estágio larval	Manchas simples grandes (três ou mais pelos mutantes)

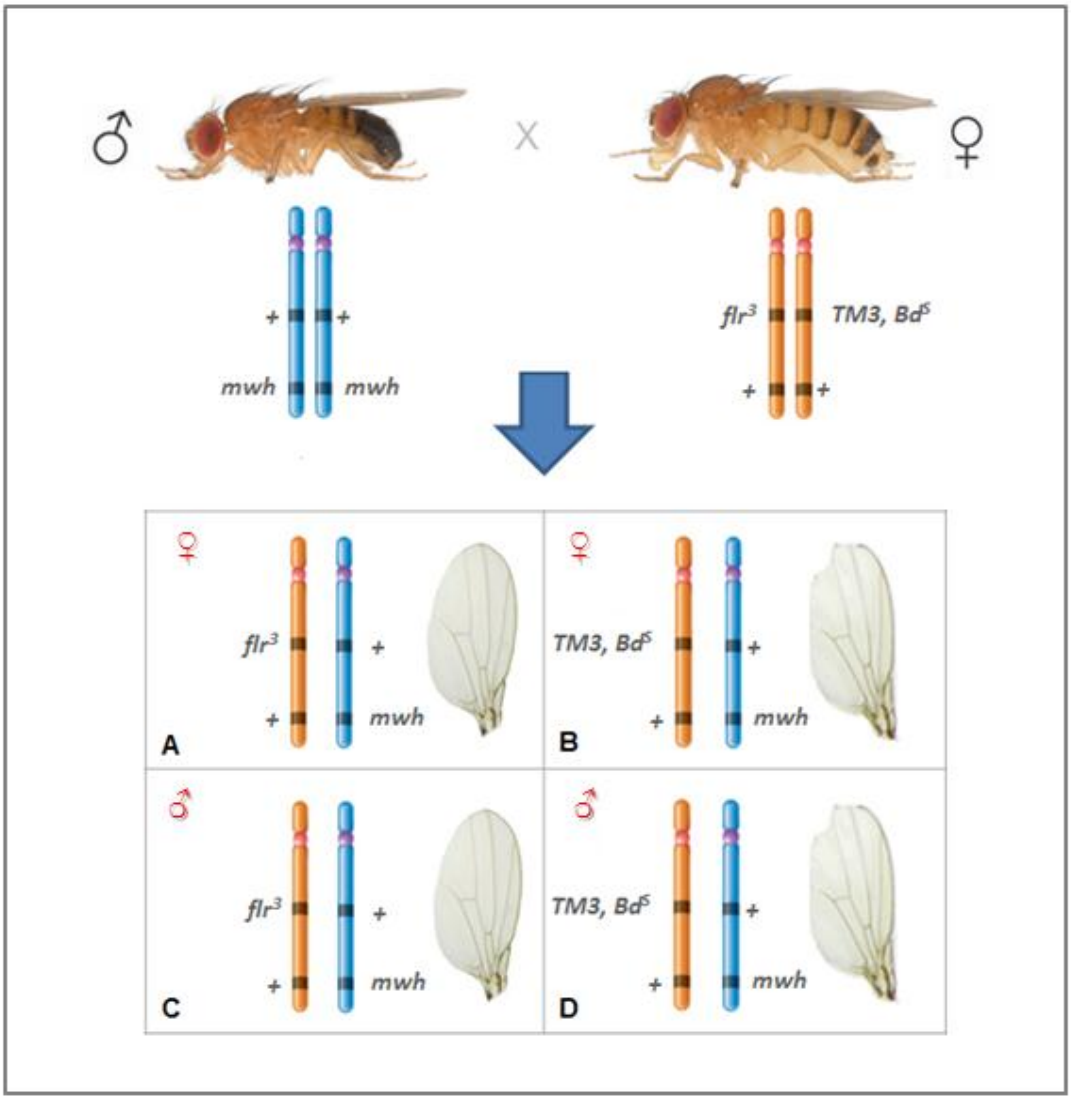

Figura 8. Esquema representativo dos Cruzamentos Padrão (ST – s*tandard cross*) e de Alta Bioativação (HB – *high bioactivation cross*), mostrando os genótipos de dois tipos de progênie. **A** e **C:** trans-heterozigotos marcados (*mwh + / + flr*^{3}) (MH), que apresentam a borda da asa lisa; **B** e **D**: heterozigotos balanceados (*mwh + / + TM3, Bd*^{S}) (BH), que apresentam a borda da asa serrilhada. FONTE: Arquivo pessoal.

REFERÊNCIAS

ADAMCAKOVA-DODD, A.; STEBOUNOVA, L. V.; KIM, J. S.; VORRINK, S. U.; AULT, A. P.; O'SHAUGHNESSY, P. T.; GRASSIAN, V. H.; THORNE, P. S. Toxicity assessment of zinc oxide nanoparticles using sub-acute and sub-chronic murine inhalation models. **Part Fibre Toxicol**, 11-15,2014.

ARORA, S.; RAJWADE, J. M.; PAKNIKAR, K. M. Nanotoxicology and in vitro studies: the need of the hour. **Toxicol Appl Pharmacol**, 258, 151-165,2012.

AUFFAN, M.; ROSE, J.; BOTTERO, J.-Y.; LOWRY, G. V.; JOLIVET, J.-P.; WIESNER, M. R. Towards a definition of inorganic nanoparticles from an environmental, health and safety perspective. **Nat Nano**, 4, 634-641,2009.

BANERJEE, A. N. The design, fabrication, and photocatalytic utility of nanostructured semiconductors: focus on TiO2-based nanostructures. **Nanotechnol Sci Appl**, 4, 35-65,2011.

BANFIELD, J. F.; VEBLEN, D. R. Conversion of perovskite to anatase and TiO2 (B): A TEM study and the use of fundamental building blocks for understanding relationships among the TiO, minerals. **American Mineralogist**, 77, 545-557,1992.

BARUAH, S.; DUTTA, J. Nanotechnology applications in pollution sensing and degradation in agriculture: a review. **Environmental Chemistry Letters**, 7, 191-204,2009.

BRADLEY, M. O.; BHUYAN, B.; FRANCIS, M. C.; LANGENBACH, R.; PETERSON, A.; HUBERMAN, E. Mutagenesis by chemical agents in V79 chinese hamster cells: a review and analysis of the literature. A report of the Gene-Tox Program. **Mutat Res**, 87, 81-142,1981.

BUTLER, K. S.; CASEY, B. J.; GARBOCAUSKAS, G. V.; DAIR, B. J.; ELESPURU, R. K. Assessment of titanium dioxide nanoparticle effects in bacteria: Association, uptake, mutagenicity, co-mutagenicity and DNA repair inhibition. **Mutat Res Genet Toxicol Environ Mutagen**, 2014.

CHEN, T.; YAN, J.; LI, Y. Genotoxicity of titanium dioxide nanoparticles. **J Food Drug Anal**, 22, 95-104,2014.

CHEN, Z.; WANG, Y.; BA, T.; LI, Y.; PU, J.; CHEN, T.; SONG, Y.; GU, Y.; QIAN, Q.; YANG, J.; JIA, G. Genotoxic evaluation of titanium dioxide nanoparticles in vivo and in vitro. **Toxicology Letters**, 226, 314-319,2014.

COOKE, M. S.; EVANS, M. D.; DIZDAROGLU, M.; LUNEC, J. Oxidative DNA damage: mechanisms, mutation, and disease. **FASEB J**, 17, 1195-1214,2003.

CORRADI, S.; GONZALEZ, L.; THOMASSEN, L. C.; BILANICOVA, D.; BIRKEDAL, R. K.; POJANA, G.; MARCOMINI, A.; JENSEN, K. A.; LEYNS, L.; KIRSCH-VOLDERS, M. Influence of serum on in situ proliferation and genotoxicity in A549 human lung cells exposed to nanomaterials. **Mutat Res**, 745, 21-27,2012.

CRADDOCK, P. T. **2000 Years of Zinc and Brass**. British Museum, 1998. ISBN 9780861591244. Disponível em: < http://books.google.com.br/books?id=3dTbAAAAMAAJ >.

DE ANDRADE, L. R.; BRITO, A. S.; MELERO, A. M.; ZANIN, H.; CERAGIOLI, H. J.; BARANAUSKAS, V.; CUNHA, K. S.; IRAZUSTA, S. P. Absence of mutagenic and recombinagenic activity of multi-walled carbon nanotubes in the Drosophila wing-spot test and Allium cepa test. **Ecotoxicol Environ Saf**, 99, 92-97,2014.

DE REZENDE, A. A.; MUNARI, C. C.; DE OLIVEIRA, P. F.; FERREIRA, N. H.; TAVARES, D. C.; ANDRADE, E. S. M. L.; REZENDE, K. C.; SPANO, M. A. A comparative study of the modulatory effects of (-)-cubebin on the mutagenicity/recombinogenicity induced by different chemical agents. **Food Chem Toxicol**, 55, 645-652,2013.

DEMIR, E.; AKCA, H.; KAYA, B.; BURGUCU, D.; TOKGUN, O.; TURNA, F.; AKSAKAL, S.; VALES, G.; CREUS, A.; MARCOS, R. Zinc oxide nanoparticles: genotoxicity, interactions with UV-light and cell-transforming potential. **J Hazard Mater**, 264, 420-429,2014.

DEMIR, E.; TURNA, F.; VALES, G.; KAYA, B.; CREUS, A.; MARCOS, R. In vivo genotoxicity assessment of titanium, zirconium and aluminium nanoparticles, and their microparticulated forms, in Drosophila. **Chemosphere**, 93, 2304-2310,2013.

DEMIR, E.; VALES, G.; KAYA, B.; CREUS, A.; MARCOS, R. Genotoxic analysis of silver nanoparticles in Drosophila. **Nanotoxicology**, 5, 417-424,2011.

DOBRZYNSKA, M. M.; GAJOWIK, A.; RADZIKOWSKA, J.; LANKOFF, A.; DUSINSKA, M.; KRUSZEWSKI, M. Genotoxicity of silver and titanium dioxide nanoparticles in bone marrow cells of rats in vivo. **Toxicology**, 315, 86-91,2014.

EASTMOND, D. A.; TUCKER, J. D. Identification of aneuploidy-inducing agents using cytokinesis-blocked human lymphocytes and an antikinetochore antibody. **Environ Mol Mutagen**, 13, 34-43,1989.

EL-ZEIN, R.; VRAL, A.; ETZEL, C. J. Cytokinesis-blocked micronucleus assay and cancer risk assessment. **Mutagenesis**, 26, 101-106,2011.

FDA. Sun Protection. 2013. Disponível em: < http://www.fda.gov/Radiation-EmittingProducts/RadiationEmitting-ProductsandProcedures/Tanning/ucm116445.htm. >. Acesso em: 27/06/2014.

FENECH, M. The in vitro micronucleus technique. **Mutat Res**, 455, 81-95,2000.

FENECH, M. Cytokinesis-block micronucleus cytome assay. **Nat Protoc**, 2, 1084-1104,2007.

FENECH, M.; KIRSCH-VOLDERS, M.; NATARAJAN, A. T.; SURRALLES, J.; CROTT, J. W.; PARRY, J.; NORPPA, H.; EASTMOND, D. A.; TUCKER, J. D.; THOMAS, P. Molecular mechanisms of micronucleus, nucleoplasmic bridge and nuclear bud formation in mammalian and human cells. **Mutagenesis**, 26, 125-132,2011.

FENECH, M.; MORLEY, A. A. Measurement of micronuclei in lymphocytes. **Mutat Res**, 147, 29-36,1985.

FILIPPI, C.; PRYDE, A.; COWAN, P.; LEE, T.; HAYES, P.; DONALDSON, K.; PLEVRIS, J.; STONE, V. Toxicology of ZnO and TiO nanoparticles on hepatocytes: Impact on metabolism and bioenergetics. **Nanotoxicology**, 2014.

FRIEDBERG, E. C. **DNA Repair And Mutagenesis**. 2nd. Amer Society for Microbiology, 2006. 1118 ISBN 9781555813192.

FROLICH, A.; WURGLER, F. E. Genotoxicity of ethyl carbamate in the Drosophila wing spot test: dependence on genotype-controlled metabolic capacity. **Mutat Res**, 244, 201-208,1990.

FU, P. P.; XIA, Q.; HWANG, H. M.; RAY, P. C.; YU, H. Mechanisms of nanotoxicity: generation of reactive oxygen species. **J Food Drug Anal**, 22, 64-75,2014.

FUKUI, H.; HORIE, M.; ENDOH, S.; KATO, H.; FUJITA, K.; NISHIO, K.; KOMABA, L. K.; MARU, J.; MIYAUHI, A.; NAKAMURA, A.; KINUGASA, S.; YOSHIDA, Y.; HAGIHARA, Y.; IWAHASHI, H. Association of zinc ion release and oxidative stress induced by intratracheal instillation of ZnO nanoparticles to rat lung. **Chem Biol Interact**, 198, 29-37,2012.

GIRARD, P. M.; BOITEUX, S. Repair of oxidized DNA bases in the yeast Saccharomyces cerevisiae. **Biochimie**, 79, 559-566,1997.

GITROWSKI, C.; AL-JUBORY, A. R.; HANDY, R. D. Uptake of different crystal structures of TiO(2) nanoparticles by Caco-2 intestinal cells. **Toxicol Lett**, 226, 264-276,2014.

GONZALEZ, L.; LISON, D.; KIRSCH-VOLDERS, M. Genotoxicity of engineered nanomaterials: A critical review. **Nanotoxicology**, 2, 252-273,2008.

GRAF, U.; FREI, H.; KAGI, A.; KATZ, A. J.; WURGLER, F. E. Thirty compounds tested in the Drosophila wing spot test. **Mutat Res**, 222, 359-373,1989.

GRAF, U.; SPANÓ, M. A.; GUZMÁN RINCÓN, J.; ABRAHAM, S. K.; ANDRADE, H. H. The wing somatic mutation and recombination test (SMART) in *Drosophila melanogaster*: an efficient tool for the detection of genotoxic activity of pure

compounds or complex mixtures as well as for studies of antigenotoxicity. **Afr Newslett on Occup Health and Safety**, 6, 9-13,1996.

GRAF, U.; VAN SCHAIK, N. Improved high bioactivation cross for the wing somatic mutation and recombination test in Drosophila melanogaster. **Mutat Res**, 271, 59-67,1992.

GRAF, U.; WÜRGLER, F. E.; KATZ, A. J.; FREI, H.; JUON, H.; HALL, C. B.; KALE, P. G. Somatic mutation and recombination test in Drosophila melanogaster. **Environ Mutagen**, 6, 153-188,1984.

GUAN, R.; KANG, T.; LU, F.; ZHANG, Z.; SHEN, H.; LIU, M. Cytotoxicity, oxidative stress, and genotoxicity in human hepatocyte and embryonic kidney cells exposed to ZnO nanoparticles. **Nanoscale Res Lett**, 7, 602,2012.

GUICHARD, Y.; SCHMIT, J.; DARNE, C.; GATE, L.; GOUTET, M.; ROUSSET, D.; RASTOIX, O.; WROBEL, R.; WITSCHGER, O.; MARTIN, A.; FIERRO, V.; BINET, S. Cytotoxicity and genotoxicity of nanosized and microsized titanium dioxide and iron oxide particles in Syrian hamster embryo cells. **Ann Occup Hyg**, 56, 631-644,2012.

GUMUS, D.; BERBER, A. A.; ADA, K.; AKSOY, H. In vitro genotoxic effects of ZnO nanomaterials in human peripheral lymphocytes. **Cytotechnology**, 66, 317-325,2014.

GUTIERREZ IGLESIAS, E.; PEREZ-ARIZTI, J. A.; MARQUEZ-RAMIREZ, S. G.; DELGADO-BUENROSTRO, N. L.; CHIRINO, Y. I.; IGLESIAS, G. G.; LOPEZ-MARURE, R. Titanium dioxide nanoparticles induce strong oxidative stress and mitochondrial damage in glial cells. **Free Radic Biol Med**, 73C, 84-94,2014.

GUZMÁN-RINCÓN, J.; GRAF, U. Drosophila melanogaster somatic mutation and recombination test as a biomonitor. In: BUTTERWORTH, F. M.;CORKUM, L. D.; GUZMÁN-RINCÓN, J. (Ed.). **Biomonitors and Biomarkers as Indicators of Environmental Change.** . New York: Plenum Press, 1995. p.169-181.

HEINLAAN, M.; IVASK, A.; BLINOVA, I.; DUBOURGUIER, H. C.; KAHRU, A. Toxicity of nanosized and bulk ZnO, CuO and TiO2 to bacteria Vibrio fischeri and crustaceans Daphnia magna and Thamnocephalus platyurus. **Chemosphere**, 71, 1308-1316,2008.

HERNANDEZ, L. G.; BENTHEM, J. V.; JOHNSON, G. E. A Mode-of-Action Approach for the Identification of Genotoxic Carcinogens. **PLoS One**, 8, e64532,2013.

IARC. **Carbon black, titanium dioxide, and talc.** . IARC Monographs on the Evaluation of Carcinogenic Risks to Humans. Lyon, France: World Health Organization - International Agency on Cancer Research 2010.

JAGADISH, C.; PEARTON, S. J. **Zinc Oxide Bulk, Thin Films and Nanostructures: Processing, Properties, and Applications**. Elsevier Science, 2011. ISBN 9780080464039. Disponível em: < http://books.google.com.br/books?id=-MUOCKEiZYQC >.

JANER, G.; MAS DEL MOLINO, E.; FERNANDEZ-ROSAS, E.; FERNANDEZ, A.; VAZQUEZ-CAMPOS, S. Cell uptake and oral absorption of titanium dioxide nanoparticles. **Toxicol Lett**, 228, 103-110,2014.

JANOTTI, A.; VAN DE WALLE, C. G. Fundamentals of zinc oxide as a semiconductor. **Reports on Progress in Physics**, 72, 126501,2009.

JIANG, J.; OBERDORSTER, G.; ELDER, A.; GELEIN, R.; MERCER, P.; BISWAS, P. Does Nanoparticle Activity Depend upon Size and Crystal Phase? **Nanotoxicology**, 2, 33-42,2008.

JUGAN, M. L.; BARILLET, S.; SIMON-DECKERS, A.; HERLIN-BOIME, N.; SAUVAIGO, S.; DOUKI, T.; CARRIERE, M. Titanium dioxide nanoparticles exhibit genotoxicity and impair DNA repair activity in A549 cells. **Nanotoxicology**, 6, 501-513,2012.

KANG, T.; GUAN, R.; CHEN, X.; SONG, Y.; JIANG, H.; ZHAO, J. In vitro toxicity of different-sized ZnO nanoparticles in Caco-2 cells. **Nanoscale Res Lett**, 8, 2013.

KARLSSON, H. L.; GUSTAFSSON, J.; CRONHOLM, P.; MOLLER, L. Size-dependent toxicity of metal oxide particles--a comparison between nano- and micrometer size. **Toxicol Lett**, 188, 112-118,2009.

KENNEDY, S. R.; LOEB, L. A.; HERR, A. J. Somatic mutations in aging, cancer and neurodegeneration. **Mech Ageing Dev**, 133, 118-126,2012.

KIM, T.; HYEON, T. Applications of inorganic nanoparticles as therapeutic agents. **Nanotechnology**, 25, 012001,2014.

KIRKLAND, D. Evaluation of different cytotoxic and cytostatic measures for the in vitro micronucleus test (MNVit): introduction to the collaborative trial. **Mutat Res**, 702, 135-138,2010.

KLINGSHIRN, C. ZnO: material, physics and applications. **Chemphyschem**, 8, 782-803,2007.

KUMAR, A.; PANDEY, A. K.; SINGH, S. S.; SHANKER, R.; DHAWAN, A. Engineered ZnO and TiO(2) nanoparticles induce oxidative stress and DNA damage leading to reduced viability of Escherichia coli. **Free Radic Biol Med**, 51, 1872-1881,2011.

KUMARI, A.; YADAV, S. K. Nanotechnology in agri-food sector. **Crit Rev Food Sci Nutr**, 54, 975-984,2014.

KWON, J. Y.; LEE, S. Y.; KOEDRITH, P.; LEE, J. Y.; KIM, K. M.; OH, J. M.; YANG, S. I.; KIM, M. K.; LEE, J. K.; JEONG, J.; MAENG, E. H.; LEE, B. J.; SEO, Y. R. Lack of genotoxic potential of ZnO nanoparticles in in vitro and in vivo tests. **Mutat Res Genet Toxicol Environ Mutagen**, 761, 1-9,2014.

LANDSIEDEL, R.; KAPP, M. D.; SCHULZ, M.; WIENCH, K.; OESCH, F. Genotoxicity investigations on nanomaterials: methods, preparation and characterization of test material, potential artifacts and limitations--many questions, some answers. **Mutat Res**, 681, 241-258,2009.

LANDSIEDEL, R.; MA-HOCK, L.; KROLL, A.; HAHN, D.; SCHNEKENBURGER, J.; WIENCH, K.; WOHLLEBEN, W. Testing metal-oxide nanomaterials for human safety. **Adv Mater**, 22, 2601-2627,2010a.

LANDSIEDEL, R.; MA-HOCK, L.; VAN RAVENZWAAY, B.; SCHULZ, M.; WIENCH, K.; CHAMP, S.; SCHULTE, S.; WOHLLEBEN, W.; OESCH, F. Gene toxicity studies on titanium dioxide and zinc oxide nanomaterials used for UV-protection in cosmetic formulations. **Nanotoxicology**, 4, 364-381,2010b.

LANKOFF, A.; SANDBERG, W. J.; WEGIEREK-CIUK, A.; LISOWSKA, H.; REFSNES, M.; SARTOWSKA, B.; SCHWARZE, P. E.; MECZYNSKA-WIELGOSZ, S.; WOJEWODZKA, M.; KRUSZEWSKI, M. The effect of agglomeration state of silver and titanium dioxide nanoparticles on cellular response of HepG2, A549 and THP-1 cells. **Toxicol Lett**, 208, 197-213,2012.

LEHNER, R.; WANG, X.; MARSCH, S.; HUNZIKER, P. Intelligent nanomaterials for medicine: carrier platforms and targeting strategies in the context of clinical application. **Nanomedicine**, 9, 742-757,2013.

LI, Y.; ZHANG, Y.; YAN, B. Nanotoxicity overview: nano-threat to susceptible populations. **Int J Mol Sci**, 15, 3671-3697,2014.

LINDBERG, H. K.; FALCK, G. C.; CATALAN, J.; KOIVISTO, A. J.; SUHONEN, S.; JARVENTAUS, H.; ROSSI, E. M.; NYKASENOJA, H.; PELTONEN, Y.; MORENO, C.; ALENIUS, H.; TUOMI, T.; SAVOLAINEN, K. M.; NORPPA, H. Genotoxicity of inhaled nanosized TiO(2) in mice. **Mutat Res**, 745, 58-64,2012.

LUNDIN, C.; NORTH, M.; ERIXON, K.; WALTERS, K.; JENSSEN, D.; GOLDMAN, A. S.; HELLEDAY, T. Methyl methanesulfonate (MMS) produces heat-labile DNA damage but no detectable in vivo DNA double-strand breaks. **Nucleic Acids Res**, 33, 3799-3811,2005.

MA, H.; WILLIAMS, P. L.; DIAMOND, S. A. Ecotoxicity of manufactured ZnO nanoparticles--a review. **Environ Pollut**, 172, 76-85,2013.

MACHADO, N. M.; LOPES, J. C.; SATURNINO, R. S.; FAGAN, E. B.; NEPOMUCENO, J. C. Lack of mutagenic effect by multi-walled functionalized

carbon nanotubes in the somatic cells of Drosophila melanogaster. **Food Chem Toxicol**, 62, 355-360,2013.

MAHSHID, S.; ASKARI, M.; GHAMSARI, M. S. Synthesis of TiO2 nanoparticles by hydrolysis and peptization of titanium isopropoxide solution. **Journal of Materials Processing Technology**, 189, 296-300,2007.

MAKUMIRE, S.; CHAKRAVADHANULA, V. S.; KOLLISCH, G.; REDEL, E.; SHONHAI, A. Immunomodulatory activity of zinc peroxide (ZnO(2)) and titanium dioxide (TiO(2)) nanoparticles and their effects on DNA and protein integrity. **Toxicol Lett**, 227, 56-64,2014.

MANTOVANI, E.; ZAPPELLI, P. ObservatoryNano Technology Sector Report on Textiles. 2009. Disponível em: < http://www.observatorynano.eu/project/document/2402/ >. Acesso em: 24/06/2014.

MCNULTY, G. S. **Production of titanium dioxide**. Proc. Conf. Seville, Spain. 2007

MOELLMANN, J.; EHRLICH, S.; TONNER, R.; GRIMME, S. A DFT-D study of structural and energetic properties of TiO2 modifications. **J Phys Condens Matter**, 24, 424206,2012.

MOEZZI, A.; MCDONAGH, A. M.; CORTIE, M. B. Zinc oxide particles: Synthesis, properties and applications. **Chemical Engineering Journal**, 185-186, 1-22,2012.

MOLLET, P.; WURGLER, F. E. Detection of Somatic Recombination and Mutation in Drosophila - Method for Testing Genetic Activity of Chemical Compounds. **Mutat Res**, 25, 421-424,1974.

MONTEIRO-RIVIERE, N. A.; WIENCH, K.; LANDSIEDEL, R.; SCHULTE, S.; INMAN, A. O.; RIVIERE, J. E. Safety evaluation of sunscreen formulations containing titanium dioxide and zinc oxide nanoparticles in UVB sunburned skin: an in vitro and in vivo study. **Toxicol Sci**, 123, 264-280,2011.

NANO.GOV. Benefits and Applications. 2014. Disponível em: < http://www.nano.gov/you/nanotechnology-benefits >. Acesso em: 23 junho.

NEL, A.; XIA, T.; MADLER, L.; LI, N. Toxic potential of materials at the nanolevel. **Science**, 311, 622-627,2006.

NEWMAN, M. D.; STOTLAND, M.; ELLIS, J. I. The safety of nanosized particles in titanium dioxide- and zinc oxide-based sunscreens. **J Am Acad Dermatol**, 61, 685-692,2009.

NOHYNEK, G. J.; DUFOUR, E. K. Nano-sized cosmetic formulations or solid nanoparticles in sunscreens: a risk to human health? **Arch Toxicol**, 86, 1063-1075,2012.

NOHYNEK, G. J.; LADEMANN, J.; RIBAUD, C.; ROBERTS, M. S. Grey goo on the skin? Nanotechnology, cosmetic and sunscreen safety. **Crit Rev Toxicol**, 37, 251-277,2007.

OBERDORSTER, G.; OBERDORSTER, E.; OBERDORSTER, J. Nanotoxicology: an emerging discipline evolving from studies of ultrafine particles. **Environ Health Perspect**, 113, 823-839,2005.

OECD. **In Vitro Mammalian Cell Micronucleus Test**. 2010.

OSMAN, I. F.; BAUMGARTNER, A.; CEMELI, E.; FLETCHER, J. N.; ANDERSON, D. Genotoxicity and cytotoxicity of zinc oxide and titanium dioxide in HEp-2 cells. **Nanomedicine**, 5, 1193–1203,2010.

PARVATHI, V. D.; RAJAGOPAL, K. Nanotoxicology testing: Potential of Drosophila in toxicity assessment of nanomaterials. **International Journal of NanoScience and Nanotechnology**, 5, 25-35,2014.

PETERS, R. J.; VAN BEMMEL, G.; HERRERA-RIVERA, Z.; HELSPER, J. P.; MARVIN, H. J.; WEIGEL, S.; TROMP, P.; OOMEN, A. G.; RIETVELD, A.; BOUWMEESTER, H. Characterisation of titanium dioxide nanoparticles in food products: Analytical methods to define nanoparticles. **J Agric Food Chem**, 2014.

PETKOVIC, J.; ZEGURA, B.; STEVANOVIC, M.; DRNOVSEK, N.; USKOKOVIC, D.; NOVAK, S.; FILIPIC, M. DNA damage and alterations in expression of DNA damage responsive genes induced by TiO2 nanoparticles in human hepatoma HepG2 cells. **Nanotoxicology**, 5, 341-353,2011.

PRASAD, R. Y.; CHASTAIN, P. D.; NIKOLAISHVILI-FEINBERG, N.; SMEESTER, L.; KAUFMANN, W. K.; FRY, R. C. Titanium dioxide nanoparticles activate the ATM-Chk2 DNA damage response in human dermal fibroblasts. **Nanotoxicology**, 7, 1111-1119,2013.

RAJ, S.; JOSE, S.; SUMOD, U. S.; SABITHA, M. Nanotechnology in cosmetics: Opportunities and challenges. **J Pharm Bioallied Sci**, 4, 186-193,2012.

RAO, B. S.; SHANBHOGE, R.; UPADHYA, D.; JAGETIA, G. C.; ADIGA, S. K.; KUMAR, P.; GURUPRASAD, K.; GAYATHRI, P. Antioxidant, anticlastogenic and radioprotective effect of Coleus aromaticus on Chinese hamster fibroblast cells (V79) exposed to gamma radiation. **Mutagenesis**, 21, 237-242,2006.

SANTO, N.; FASCIO, U.; TORRES, F.; GUAZZONI, N.; TREMOLADA, P.; BETTINETTI, R.; MANTECCA, P.; BACCHETTA, R. Toxic effects and ultrastructural damages to Daphnia magna of two differently sized ZnO nanoparticles: does size matter? **Water Res**, 53, 339-350,2014.

SCHMID, W. The micronucleus test. **Mutat Res**, 31, 9-15,1975.

SETYAWATI, M. I.; KHOO, P. K.; ENG, B. H.; XIONG, S.; ZHAO, X.; DAS, G. K.; TAN, T. T.; LOO, J. S.; LEONG, D. T.; NG, K. W. Cytotoxic and genotoxic characterization of titanium dioxide, gadolinium oxide, and poly(lactic-co-glycolic acid) nanoparticles in human fibroblasts. **J Biomed Mater Res A**, 101, 633-640,2013.

SHUKLA, R. K.; KUMAR, A.; GURBANI, D.; PANDEY, A. K.; SINGH, S.; DHAWAN, A. TiO(2) nanoparticles induce oxidative DNA damage and apoptosis in human liver cells. **Nanotoxicology**, 7, 48-60,2013.

SIDDIQUE, H. R.; CHOWDHURI, D. K.; SAXENA, D. K.; DHAWAN, A. Validation of Drosophila melanogaster as an in vivo model for genotoxicity assessment using modified alkaline Comet assay. **Mutagenesis**, 20, 285-290,2005.

SIEGFRIED, B. NanoTextiles: Functions, nanoparticles and commercial applications. 2007. Disponível em: < www.empa.ch/plugin/template/empa/*/78337/—-/NanoSafeTextiles_1.pdf >. Acesso em: 22/06/2014.

SINGH, N.; MANSHIAN, B.; JENKINS, G. J.; GRIFFITHS, S. M.; WILLIAMS, P. M.; MAFFEIS, T. G.; WRIGHT, C. J.; DOAK, S. H. NanoGenotoxicology: the DNA damaging potential of engineered nanomaterials. **Biomaterials**, 30, 3891-3914,2009.

SINGH, P.; NANDA, A. Enhanced sun protection of nano-sized metal oxide particles over conventional metal oxide particles: an in vitro comparative study. **Int J Cosmet Sci**, 36, 273-283,2014.

SMIJS, T. G.; PAVEL, S. Titanium dioxide and zinc oxide nanoparticles in sunscreens: focus on their safety and effectiveness. **Nanotechnol Sci Appl**, 4, 95-112,2011.

SOUSA, C. J.; PEREIRA, M. C.; ALMEIDA, R. J.; LOYOLA, A. M.; SILVA, A. C.; DANTAS, N. O. Synthesis and characterization of zinc oxide nanocrystals and histologic evaluation of their biocompatibility by means of intraosseous implants. **Int Endod J**, 47, 416-424,2014.

SPANO, M. A.; FREI, H.; WURGLER, F. E.; GRAF, U. Recombinagenic activity of four compounds in the standard and high bioactivation crosses of Drosophila melanogaster in the wing spot test. **Mutagenesis**, 16, 385-394,2001.

SPANÓ, M. A.; GRAF, U. Segundo Taller sobre SMART: um método para detectar las actividades mutagénica y recombinogénica em células somáticas de Drosophila en la Universidad Federal de Uberlândia **Rev Int Contam Ambient**, 14, 111-114,1998.

SRIVASTAVA, R. K.; RAHMAN, Q.; KASHYAP, M. P.; LOHANI, M.; PANT, A. B. Ameliorative effects of dimetylthiourea and N-acetylcysteine on nanoparticles induced cyto-genotoxicity in human lung cancer cells-A549. **PLoS One**, 6, e25767,2011.

STROBEL, C.; TORRANO, A. A.; HERRMANN, R.; MALISSEK, M.; BRAUCHLE, C.; RELLER, A.; TREUEL, L.; HILGER, I. Effects of the physicochemical properties of titanium dioxide nanoparticles, commonly used as sun protection agents, on microvascular endothelial cells. **J Nanopart Res**, 16, 2130,2014.

TAVARES, A. M.; LOURO, H.; ANTUNES, S.; QUARRE, S.; SIMAR, S.; DE TEMMERMAN, P. J.; VERLEYSEN, E.; MAST, J.; JENSEN, K. A.; NORPPA, H.; NESSLANY, F.; SILVA, M. J. Genotoxicity evaluation of nanosized titanium dioxide, synthetic amorphous silica and multi-walled carbon nanotubes in human lymphocytes. **Toxicol In Vitro**, 28, 60-69,2014.

WANG, B.; ZHANG, Y.; MAO, Z.; YU, D.; GAO, C. Toxicity of ZnO Nanoparticles to Macrophages Due to Cell Uptake and Intracellular Release of Zinc Ions. **Journal of Nanoscience and Nanotechnology**, 14, 5688-5696,2014.

WANG, J.; DENG, X.; ZHANG, F.; CHEN, D.; DING, W. ZnO nanoparticle-induced oxidative stress triggers apoptosis by activating JNK signaling pathway in cultured primary astrocytes. **Nanoscale Res Lett**, 9, 117,2014.

WARHEIT, D. B.; WEBB, T. R.; REED, K. L.; FRERICHS, S.; SAYES, C. M. Pulmonary toxicity study in rats with three forms of ultrafine-TiO2 particles: differential responses related to surface properties. **Toxicology**, 230, 90-104,2007.

WEIR, A.; WESTERHOFF, P.; FABRICIUS, L.; HRISTOVSKI, K.; VON GOETZ, N. Titanium dioxide nanoparticles in food and personal care products. **Environ Sci Technol**, 46, 2242-2250,2012.

WIKIMEDIA.ORG. 2007. Disponível em: < http://commons.wikimedia.org/wiki/File:Sphalerite-unit-cell-depth-fade-3D-balls.png >. Acesso em: 27/06/2014.

WIKIMEDIA.ORG. 2008. Disponível em: < http://commons.wikimedia.org/wiki/File%3AWurtzite_polyhedra.png >. Acesso em: 27/06/2014.

WU, J.; BAI, G.-R.; EASTMAN, J. A.; ZHOU, G.; VASUDEVAN, V. K. Synthesis of TiO2 Nanoparticles Using Chemical Vapor Condensation. **Mater. Res. Soc. Symp. Proc.**, 879, 2005.

YANG, H. S.; IERONIMAKIS, N.; TSUI, J. H.; KIM, H. N.; SUH, K. Y.; REYES, M.; KIM, D. H. Nanopatterned muscle cell patches for enhanced myogenesis and dystrophin expression in a mouse model of muscular dystrophy. **Biomaterials**, 35, 1478-1486,2014.

YIN, H.; CASEY, P. S.; MCCALL, M. J.; FENECH, M. Effects of surface chemistry on cytotoxicity, genotoxicity, and the generation of reactive oxygen species induced by ZnO nanoparticles. **Langmuir**, 26, 15399-15408,2010.

ZHANG, J.; SONG, W.; GUO, J.; ZHANG, J.; SUN, Z.; LI, L.; DING, F.; GAO, M. Cytotoxicity of different sized TiO2 nanoparticles in mouse macrophages. **Toxicol Ind Health**, 29, 523-533,2013.

ZHOU, X.; NI, S.; ZHANG, X.; WANG, X.; HU, X.; ZHOU, Y. Controlling Shape and Size of TiO2 Nanoparticles with Sodium Acetate. Curr. Nanosci., 4, 397-401, 2008.

Objetivos

Diante da importância do ZnO e TiO_2 nas aplicações nanotecnológicas, sua ampla utilização e riscos oferecidos pela exposição aos seres vivos, este trabalho teve como objetivos:

1. Avaliar, por meio dos cruzamentos Padrão (ST) e de Alta Bioativação (HB), do *Somatic Mutation and Recombination Test* (SMART) em asas de *Drosophila melanogaster* o potencial mutagênico e recombinogênico de ZnO comercial e na forma de NPs, bem como de três tipos diferentes de NPs de TiO_2.

2. Avaliar, por meio do teste do Micronúcleo com Bloqueio de Citocinese (CBMN) em fibroblastos de pulmão de hamster Chinês (células V79) os efeitos clastogênicos e aneugênicos induzidos por NPs de ZnO, e três tipos diferentes de NPs de dióxido de titânio (TiO_2).

Capítulo 2

Assessment of the genotoxic potential of two zinc oxide sources (amorphous and nanoparticles) using the in vitro micronucleus test and the in vivo wing somatic test

Manuscrito a ser submetido para publicação no Periódico *Food and Chemical Toxicology* – Fator de Impacto: 2.610

ASSESSMENT OF THE GENOTOXIC POTENTIAL OF TWO ZINC OXIDE SOURCES (AMORPHOUS AND NANOPARTICLES) USING THE *IN VITRO* MICRONUCLEUS TEST AND THE *IN VIVO* WING SOMATIC TEST

Érica de Melo Reis[a], Alexandre Azenha Alves de Rezende[a], Diego Vilela Santos[a], Pollyanna Francielli de Oliveria[b], Heloisa Diniz Nicolella[b], Denise Crispim Tavares[b], Anielle Christine Almeida Silva[c], Noelio Oliveira Dantas[c], and Mário Antônio Spanó[a*]

[a]Laboratório de Mutagênese, Instituto de Genética e Bioquímica, Universidade Federal de Uberlândia, Uberlândia - MG, 38400-902, Brazil

[b]Universidade de Franca, Franca - SP, 14404-600, Brazil

[c]Laboratório de Novos Materiais Isolantes e Semicondutores (LNMIS), Instituto de Física, Universidade Federal de Uberlândia, Uberlândia - MG, 38400-902, Brazil

*Correspondence to: Mário Antônio Spanó, Universidade Federal de Uberlândia, Instituto de Genética e Bioquímica, Laboratório de Mutagênese. Av. Pará 1720, Umuarama, Uberlândia – MG, 38400-902, Brazil. Tel.: +55 34 32182505.

E-mail address: maspano@ufu.br

Abstract

The aim of this study was to synthesise zinc oxide nanoparticles (ZnO NPs) of 21 nm and to evaluate their toxic, mutagenic and genotoxic potential. The cellular viability and genotoxicity were assessed using, respectively, the XTT colorimetric assay and *in vitro* Cytokinesis Block Micronucleus Assay (CBMN) in V79 cells. ZnO NPs were toxic at concentrations equal to or higher than 240.0 μM. ZnO NPs were genotoxic at 120.0 μM but were not cytotoxic. The mutagenic potential of the ZnO NPs, as well as that of an amorphous ZnO, was assayed using the Somatic Mutation and Recombination Test (SMART) of *Drosophila*. In the Standard cross, the amorphous ZnO and ZnO NPs were not mutagenic. Nevertheless, Marker Heterozygous (MH) individuals from the High bioactivation cross treated with amorphous ZnO (6.25 mM) and ZnO NPs (12.50 mM) displayed a significant increased number of mutant spots compared with the negative control. The corresponding Balancer Heterozygous wings enabled us to suggest that the increase in mutant spots found in MH individuals were generated due to mitotic recombination, rather than mutational events. The results were not dose-related and suggested that the mutagenicity of ZnO may depend on the concentration, size and/or particle shape.

Key words: *Drosophila melanogaster*; micronuclei; mutagenicity; SMART, V79 cells, XTT.

1. Introduction

Engineered zinc oxide (ZnO) nanoparticles (NPs) have gained demand in the market owing to their unique properties (such as having a high surface to volume ratio, being less toxic, biosafe and biocompatible, cheap and easy to synthesise) and has been widely used in industry (Kwon et al., 2014; Shi et al., 2014; Singh and Nanda 2014; Willander et al., 2014).

Generally, NPs have higher physical and chemical activities than their bulk counterparts because of their extremely high surface area to volume ratio (Fukui et al., 2012). Due to the increased reactivity of NPs, some adverse biological effects, such as toxicity and genotoxicity, are observed (Oberdörster et al., 2005). ZnO NPs have been shown to be toxic (Santo et al., 2014; Wang et al., 2014); embryotoxic (Bacchetta et al., 2014); and cytotoxic (Heng et al., 2010; Kang et al., 2013).

The mechanisms of toxicity of ZnO NPs are not yet fully understood at the cellular and molecular levels (Meyer et al., 2011; von Moos and Slaveykova 2014). ZnO NPs were shown to increase the intracellular level of reactive oxygen species (ROS), leakage of the plasma membrane, dysfunction of mitochondria, cell damage, genotoxicity and death (apoptosis) (Fukui et al., 2012; Sharma et al., 2012; Wang et al., 2014). Intracellular ROS level had a high correlation with the intracellular $Zn2^{+}$ level (Fukui et al., 2012). The role of the dissolved zinc ion (Zn^{2+}) and ROS in the cytotoxicity of ZnO NPs was described by Song et al. (2010). The increased intracellular ROS and tumour suppressor p53 being highly expressed in cell cultures treated with ZnO NPs are intrinsically associated with cytotoxicity and apoptosis (Meyer et al., 2011; Ng et al., 2011). On the other hand, studies have

demonstrated that ZnO NPs induce apoptosis only in human cancer cells through ROS (Zhang et al*.,* 2011) without affecting normal culture cells (Akhtar et al*.,* 2012). In this case, ZnO NPs could be evaluated for their potential in an anticancer therapy.

Because ZnO NPs are increasingly being exposed to humans, it is mandatory that the safety of this product and its biological interactions are understood. The in vitro Cytokinesis Block Micronucleus Assay (CBMN) (Fenech and Morley 1985) is one of the standard cytogenetic tools used widely as a screening *in vitro* test for structural or numerical chromosomal anomalies induced by clastogenic or aneugenic agents (‘‘spindle poisoning’’). The *in vitro* MN assay can detect chromosomal damage in the form of clastogenicity induced by ROS, one of the main mechanisms of NP genotoxicity (Pfuhler et al*.,* 2013). The CBMN has been widely accepted to screen ZnO NPs for genotoxicity in different cell lines (Osman et al*.,* 2010; Corradi et al*.,* 2012; Wahab et al*.,* 2013; Bhattacharya et al*.,* 2014; Demir et al*.,* 2014; Gümüs et al*.,* 2014).

Nevertheless, the *in vivo* evaluation shows significant importance due to a broad range of interactions, hormonal and enzymatic effects, DNA repair mechanisms, and so on. The wing Somatic Mutation And Recombination Test (SMART) in *Drosophila melanogaster* is a short-term *in vivo* assay for screening chemical mutagenic or recombinogenic activity (Graf et al*.,* 1984; Graf and van Schaik 1992). Many hundreds of chemicals have been tested using SMART, including NPs (Demir et al*.,* 2011; Demir et al*.,* 2013; Vales et al*.,* 2013; de Andrade et al*.,* 2014).

The aim of this work was to synthesise and characterise ZnO nanoparticles (ZnO NPs), as well as assess their toxic/genotoxic properties using the *in vitro*

CBMN in Chinese hamster lung fibroblasts (V79 cells) and to assess their mutagenicity/recombinogenicity regarding their bulk counterparts (an amorphous ZnO), in *D. melanogaster* wing SMART.

2. Materials and methods

2.1. Chemicals

Amorphous ZnO (CAS 1314-13-2) was obtained from SS White Artigos Dentários Ltda., Rio de Janeiro, RJ, Brazil. The ZnO NPs used in this study were synthesised and characterised at Instituto de Física, Universidade Federal de Uberlândia, Uberlândia, Brazil. HAM-F10, DMEM, streptomycin (CAS 3810-74-0), penicillin (CAS 113-98-4), Hepes (CAS 7365-45-8), dimethyl sulphoxide (DMSO; CAS 67-68-5), methyl methanesulphonate (MMS; CAS 66-27-3), and cytochalasin-B (CAS 14930-96-2) were purchased from Sigma-Aldrich. Ethyl carbamate (Urethane - URE; CAS: 51-79-6) was from Fluka AG (Buchs, Switzerland), and foetal bovine serum was from Nutricell (Campinas, SP, Brazil). As an alternative *Drosophila* instant medium, instant mashed potato flakes (Yoki® Alimentos S. A., São Bernardo do Campo, SP, Brazil) were used. The solutions were always prepared immediately before use with ultrapure water obtained from a MilliQ system (Millipore; Vimodrome, Milan, Italy).

2.2. Synthesis and Characterisation of ZnO NPs

ZnO NPs (average size of 21 nm) were synthesised by coprecipitation (Dantas et al*.,* 2008a; Dantas et al*.,* 2008b; Sousa et al*.,* 2014). The reaction was complete after four hours and yielded a ZnO precipitate that was collected, centrifuged and washed five times, first with distilled water and then absolute ethanol. Next, the precipitate was dried in a vacuum at 60ºC for 24 hours. This yielded a white, probably mostly amorphous, powder that was characteristic of ZnO. Finally, the white powder was heated for 2 hours at 500ºC to facilitate

crystallisation and the production of ZnO NPs. X-ray diffractograms (XRD) were taken using an XRD-6000 (Shimadzu) and monochromatic Cu-Ka1 (λ = 1.54056 Å) radiation. The XRDs were used to confirm the formation of ZnO NP and to determine their crystal structure and average size. The micro-Raman spectrum was obtained using the line 780-nm spectrometer from Ocean Optics. All characterisations were performed at room temperature.

2.3. *In vitro* Assays

2.3.1. Cell Line and Culture Conditions

Chinese hamster lung fibroblasts (V79 cells) were maintained as monolayers in plastic culture flasks (25 cm^2) in HAM-F10 and DMEM (1:1) medium supplemented with 10% foetal bovine serum, antibiotics (0.01 mg/mL streptomycin; 0.005 mg/mL penicillin), and 2.38 mg/mL Hepes at 36.5ºC in a BOD-type incubator. The average cell cycle time was 12 h under these conditions, and the experiments were carried out using V79 cells between the 6^{th} and 12^{th} culture passage after thawing. The protocols used in this study were performed in triplicate.

2.3.2. XTT Colorimetric Assay

The cytotoxic activity was evaluated using the in vitro colorimetric assay - XTT kit (Roche Diagnostics) according to the manufacturer's instructions. For the experiments, 1 x 10^4 cells were seeded into microplates containing 96 wells. Each well received a maximum of 100 µL of culture medium (DMEM + HAM F10 1:1) supplemented with 10% fetal bovine serum containing different concentrations of

ZnO NPs (21 nm). The concentrations tested ranged from 30.0 to 61,440.0 µM. Negative (no treatment) and positive (dimethylsulfoxide - DMSO 25%) controls were included in the microplates. After incubation with the compound for 24 h at 36.5 °C, the culture medium was removed and cells were washed with 100 µL of PBS to remove the compound and exposed to 100 µL of HAM-F10 medium red-free culture phenol. Then, 25 µL of XTT were added to each well. The microplates were incubated at 36.5 °C for 17h. The absorbance of the samples was determined by means of a multi-plate reader (ELISA -Asys - UVM 340 / MicroWIN 2000) at a wavelength of 450 nm and a reference length of 620 nm. The amount of formed soluble product (formazan) was proportional to the number of viable cells. The negative control group was designated as 100% and the results were expressed as a percentage of the negative control. The experiments were performed in triplicate.

2.3.3. Cytokinesis Block Micronucleus Assay (CBMN)

The V79 cells (500,000) were seeded into tissue culture flasks, incubated for 25 h in 5 mL of complete HAM-F10/DMEM medium and washed with PBS (pH 7.4). After the incubation, the cultures were rinsed with PBS, and then submitted to one of the following treatments: negative control (no treatment); ZnO NPs (21 nm) at concentrations of 30.0, 60.0 or 120.0 µM; positive control (MMS, 400 µM). All of the experiments were performed in triplicate. After the treatment period, the cells were washed with PBS, culture medium supplemented with foetal bovine serum containing 3 µg/mL of cytochalasin-B was added, and the cells were incubated for 17 h. Next, the cells were rinsed with 5 mL of PBS, trypsinised using 0.025% trypsin-EDTA and centrifuged for 5 min at 900 rpm. The pellet was hypotonised in

sodium citrate 1% at 37ºC and then homogenised using a Pasteur pipette. This cell suspension was centrifuged again, the supernatant was discarded, and the pellet was resuspended in methanol:acetic acid (3:1) and homogenised again with a Pasteur pipette. Fixed cells were then transferred to slides and stained with 5% Giemsa.

The analysis established by Fenech (2000) was performed as follows: 1,000 cells were counted by culturing using 3,000 binucleated cells per treatment. The nuclear division index (NDI) was determined for 500 cells analysed per repetition, for a total of 1,500 cells per treatment group using the same slides used in the micronucleus assay. Cells with well-preserved cytoplasm containing 1–4 nuclei were scored, and the NDI was calculated using the following formula (Eastmond and Tucker 1989):

$$NDI = \frac{[M1 + 2(M2) + 3(M3) + 4(M4)]}{N}$$

where M1–M4 is the number of cells with 1, 2, 3 and 4 nuclei, respectively, and N is the total number of viable cells.

2.3.4. Statistical Analysis

The data were analysed statistically by analysis of variance for completely randomised experiments, with the calculation of F statistics and respective *P* values. For cases in which $P < 0.05$, the treatment means were compared by the Tukey test, and the minimum significant difference was calculated for 0.05.

2.4. *In Vivo* Assay

2.4.1. *D. melanogaster* Strains and Crosses

Three *D. melanogaster* strains with the genetic markers multiple wing hairs (*mwh*, 3-0.3) and flare-3 (flr^3, 3-38.9) were used: (1) multiple wing hairs (*mwh/mwh*); (2) flare-3 (flr^3*/In(3LR)TM3, ri* p^p *sep l(3)89Aa bx34*^{e} *and* Bd^S); and (3) ORR; flare-3 (*ORR/ORR;* flr^3*/In(3LR)TM3, ri* p^p *sep l(3)89Aa bx34*^{e} *and* Bd^S). The ORR strain has chromosomes 1 and 2 from a DDT-resistant Oregon R(R) line, which are responsible for a high constitutive level of cytochrome P450 enzymes (Graf and van Schaik 1992) . These strains were maintained in glass vials filled with a maintenance medium (i.e., banana, sucrose, yeast and methylparaben) under light/dark cycles (12 h:12 h), at 25 ± 1º C and approximately 60% humidity in a BOD-type chamber (Model: SL224, SOLAB – Equipamentos para Laboratórios Ltda., São Paulo, SP, Brazil).

Two crosses were carried out to produce the experimental larval progeny: (1) Standard (ST) cross: *mwh/mwh* males crossed with flr^3*/In(3LR)TM3, ri* p^p *sep l(3)89Aa bx34*^{e} *and* Bd^S virgin females (Graf et al*.,* 1984; Graf et al*.,* 1989); (2) High bioactivation (HB) cross: *mwh/mwh* males crossed with *ORR/ORR;* flr^3*/In(3LR)TM3, ri* p^p *sep l(3)89Aa bx34*^{e} *and* Bd^S virgin females (Graf and van Schaik 1992). The two crosses produce two types of flies: marker trans-heterozygous (MH) flies (*mwh* +/+ flr^3) and balancer-heterozygous (BH) flies (*mwh*+/+*TM3*, Bd^S). The former has normal wings, while the latter can be distinguished phenotypically by its serrated wings.

2.4.2. Somatic Mutation and Recombination Test – SMART

From the ST and HB crosses, eggs were collected for 8 h in culture bottles with 4% w/v agar-agar base, topped with a thick layer of live baker's yeast supplemented with sucrose. Larvae of 72 ± 4 h were transferred to glass vials to chronic feeding (approximately 48 h). Four sets of vials for each cross were prepared with 1.5 g of mashed potato flakes and 5 mL of a solution containing amorphous ZnO (1.5625, 3.125, 6.25 or 12.5 mM) or ZnO NPs (1.5625, 3.125, 6.25 or 12.5 mM). Negative (ultrapure water) and positive (URE 10 mM) controls were included in both experiments. The larvae were counted before the distribution in two series of these vials. The number of hatched flies was used to calculate the survival rates upon exposure. Larvae were allowed to feed on the above medium for the remainder of their development, pupate and hatch as adult flies. All of the experiments were conducted at 25 ± 1 °C and approximately 60% humidity.

The hatched flies were stored in 70% (v/v) ethanol. The wings of MH flies were removed and mounted on glass slides with Faure's solution (30 g of gum Arabic, 20 ml of glycerol, 50 g of chloral hydrate, and 50 mL of water) and analysed for the size and frequency of spots under a compound microscope at 400 × magnification.

2.4.3. Statistical Analysis

The experimental data were evaluated according to the multiple-decision procedure (Frei and Würgler 1988; Frei and Würgler 1995). The frequencies of each type of mutant clone per fly were compared with the concurrent negative control series using the conditional binomial test (Kastenbaum and Bowman

1970), which is used to decide whether a result is positive, inconclusive or negative. Chi-squared test was performed for statistical comparisons of the survival rate ratios for independent samples. Each statistical test was evaluated at the 5% significance level.

3. Results

3.1. ZnO NPs Characterisation

Zinc oxide nanoparticles were characterised by X-ray diffractograms (XRD) (Fig. 1a) that shows the typical Bragg diffraction peaks of hexagonal ZnO crystals (JCPDS: 36-1451) (Dantas et al*.,* 2008b). The absence of impurity peaks reinforces evidence that these ZnO NPs are of high purity. The average size of the ZnO NPs obtained was approximately 21 nm as determined by the Debye–Scherrer formula (Guinier 1994). The bands observed in the micro-Raman spectrum (Fig. 1b) are Raman-active modes, found to be approximately 334, 382, 410, 439, 516, 541 and 586 cm^{-1}, characteristic of ZnO NPs (Damen et al*.,* 1966; Dantas et al*.,* 2008a). Therefore, these results confirm the formation of ZnO NPs and absence of other types of nanostructures in the sample.

3.2. XTT Colorimetric Assay

The percentages of cell viability as measured by the XTT colorimetric assay obtained in V79 cells treated with ZnO NPs are shown in Fig. 2. The treatments with concentrations up to 240 μM showed statistically significant differences compared with the negative control.

3.3. Micronucleus Assay

The mean of the micronuclei frequency and NDI obtained after the treatment with different concentrations of ZnO NPs and the respective controls are shown in Table 1. The treatment with ZnO NPs demonstrated a statistically significant increase in the frequency of micronuclei at the highest concentration tested (120 μM), showing a genotoxic effect. In relation to NDI, no statistically significant difference was observed for any of the treatment groups compared with the negative control group, demonstrating the absence of cytotoxicity with various treatments under the experimental conditions used (Table 1).

3.4. SMART

Amorphous ZnO and ZnO NP concentrations were chosen based on a dose-response test, for which the survival rates of flies are given in Fig. 3. The highest concentration (12.5 mM) of ZnO NPs was found to be toxic in the ST and HB crosses. A significant decrease in survival rates relative to the negative control group (ultrapure water) was observed. This concentration was not found to be toxic for amorphous ZnO. At concentrations equal to or below 6.25 mM, ZnO and ZnO NPs were not toxic. Thus, we found it particularly important to evaluate the mutagenic or recombinogenic effects of ZnO NPs in somatic cells of *D. melanogaster*. Although 12.5 mM ZnO NPs significantly decreases the survival rates in both crosses, this concentration was also tested in SMART.

Third instar larvae of *D. melanogaster* obtained from both (ST and HB) crosses were fed chronically (approximately 48 h) with amorphous ZnO (1.5625, 3.125, 6.25 or 12.5 mM) or ZnO NPs (1.5625, 3.125, 6.25 or 12.5 mM). Each

treatment was performed in duplicate. The data were pooled after verifying that there were no significant differences between repetitions.

The results of the ST cross of the SMART assays using *D. melanogaster* are depicted in Table 2. In the MH (*mwh*/*flr*^{3}) individuals, amorphous ZnO and ZnO NPs showed no genotoxicity at the doses used. URE treatment induced positive results for all spot categories compared with the negative control.

Analysis of the HB cross by the SMART assay is presented in Table 3. In the MH individuals from the HB cross, URE statistically increased all of the spot categories compared with those of the negative control. The administration of 6.25 mM amorphous ZnO and 12.50 mM ZnO NPs also significantly increased the number of wing spots compared with those of the negative control.

The wings of the BH (*mwh/TM3*) flies resulting from these same treatments (URE, 6.25 mM amorphous ZnO, and 12.50 mM ZnO NPs) were also mounted and scored. This procedure enabled us to quantify the contribution of mutagenic and recombinogenic events to the final genotoxicity observed (Graf et al*.,* 1992). In BH individuals from the HB cross, only URE (10 mM) significantly increased the mutant spot frequency compared with that of the negative control. We verified that the induction of spots by URE was mainly due to somatic point mutations or chromosome aberrations rather than mitotic recombination. The total mutant spots observed for both treatments (amorphous ZnO and ZnO NPs) in the BH individuals were similar to those found for the negative control.

By comparing the number of observed mutant spots in the MH flies of each treatment group from ST and HB crosses, it can be concluded that induction of mutant spots by amorphous ZnO and ZnO NPs was not dose related.

4. Discussion

Engineered ZnO NPs are widely used in many amorphous products and research; however, their possible impact on human health is not yet well understood, and their potential genotoxicity/mutagenicity remains controversial (Adamcakova-Dodd et al*.,* 2014; Kwon et al*.,* 2014).

The biological effects of NPs depend on their physicochemical properties (Kwon et al*.,* 2014). Here, the X-ray diffractogram and micro-Raman spectrum confirmed that the synthesis methodology employed produced pure, homogeneous and uncontaminated ZnO NPs, in hexagonal wurtzite (Wz) structures, with an average size of 21 nm. This methodology has been widely used and provides the best control over properties such as dimension, structure, purity and stability that are fundamental in biological assays (Song et al*.,* 2010; Sousa et al*.,* 2014).

The CBMN allows the detection of both aneugen and clastogen agents, shows simplicity of scoring, is predictive of cancer and is widely applicable in different cell types (Kirsch-Volders et al*.,* 2011). Here, the concentrations of ZnO NPs (30.0, 60.0 and 120.0 μM) used in the CBMN were chosen based on the results observed in the XTT colorimetric assay. Thus, in the CBMN no cytotoxic concentrations were used. According to our results (Fig. 2 and Table 1), ZnO NPs were cytotoxic at concentrations equal to or higher than 240.0 μM and genotoxic (clastogenic or aneugenic) only at 120.0 μM.

Similar results to those found in this study for cytotoxicity analyses and MN induction due to ZnO NP exposure have been described by different authors in different cell lines. Dose-dependent effects on cytotoxicity and an increase in DNA

and cytogenetic damage were observed in the HEp-2 cell line, with increasing ZnO NP concentrations. Although ZnO NPs (50 and 100 µg/mL) induced a significant increase in MNs, lower concentrations (<50 µg/mL) did not induce significant alterations in MN induction (Osman et al*.,* 2010). When investigated in cultured human peripheral lymphocytes, ZnO NPs significantly increased the MN frequency at concentrations of 10 and 15 g/mL compared with that in the control. However, lower concentrations (<10 g/mL) did not induce significant alterations in the MN frequency (Gümüs et al*.,* 2014). ZnO NPs and its bulky forms evaluated in human embryonic kidney (HEK293) and mouse embryonic fibroblast (NIH/3T3) cells were able to increase significantly the number of MNs at doses up 100 µg/mL (Demir et al*.,* 2014). Similar results were also observed in A549 human lung epithelial carcinoma cells treated in 10% serum with ZnO NPs at 50 µg/mL. In 0% serum, the concentrations tested led to high toxicity. These observations demonstrated the protective effect of serum (Corradi et al*.,* 2012). When used as an inducer of cell death, ZnO NPs in the Wz phase were more effective in malignant human T98G gliomas, moderately in KB epithermoids and less toxic in HEK normal non-malignant kidney cells. The results demonstrated that treatment with ZnO NPs sensitise T98G cells by increasing both the mitotic (linked to cytogenetic damage) and interphase (apoptosis) death. ZnO NPs functioned as genotoxic drugs by inducing MN formation, indicating that these structures may interfere with the rejoining of DNA strand breaks (Wahab et al*.,* 2013).

The *Drosophila* SMART is an efficient tool that can detect the loss of heterozygosity (LOH), as a consequence of gene mutation, chromosome breaks/rearrangement or chromosome loss, and the corresponding expression of suitable recessive markers, multiple wing hairs (*mwh*) and flare-3 (*flr*^{3}), which can

lead to the formation of mutant clones in treated larvae, which are expressed as mutant spots on the wings of adult flies (Demir et al*.,* 2013). The importance of *Drosophila* as an effective *in vivo* model system and the advantages it offers over other animal models and *in vitro* systems, as well as its potential in the toxicity assessment of NPs, have been demonstrated (Deepa Parvathi and Rajagopal 2014).

Three types of spots can be observed on the wings of the MH genotype: small single spots (1 or 2 cells); large single spots (3 or more cells), both resulting from deletions, point mutations, specific chromosome aberrations, or from recombination between the two marker genes; and twin spots, consisting of adjacent cells with mwh and flr-3 hairs, produced by mitotic recombination between the proximal marker flr^3 and the centromere of chromosome 3. By contrast, in the BH genotype, only mutational events lead to spot formation because recombinational events are suppressed due to multiple inverted TM3 balancer chromosomes (Graf et al*.,* 1984; Spanó et al*.,* 2001). Therefore, it is evident that the *mwh* clones are always smaller in the BH wings than in the corresponding MH wings (Spanó et al*.,* 2001). Thus, as a rule, the wings of BH flies are scored only if positive results are found in the wings of MH flies. To determine the fraction of recombinational events responsible for induced wing spots, both types of wings of the surviving flies are analysed (Graf et al*.,* 1992). An appropriate determination of the fraction of recombinational events should be based on the frequency of *mwh* clones of single and twin spots induced in MH and BH wing primordia (Graf et al*.,* 1992; Frei and Würgler 1995).

Four different concentrations (ranging from 1.56 to 12.50 mM) of amorphous ZnO and ZnO NPs were assayed for mutagenicity and/or

recombinogenicity using two crosses (ST and HB) of the wing SMART in *D. melanogaster*. Amorphous ZnO and ZnO NPs did not modify the frequency of spontaneous mutant spots in the ST cross. The absence of positive effects in MH wings of the ST cross, and that in the corresponding BH wings, were not scored.

In the HB cross, the frequencies of mutant spots observed in individuals treated with both substances were slightly higher than those observed in the ST cross, results that may be attributed to the increased metabolic transformation capacity of this genotype. Our results showed that, among HB individuals, only the higher concentration (12.5 mM) of ZnO NPs could induce mutagenic effects, while the amorphous ZnO treatment increased mutant spots only at 6.25 mM. These results suggest that ZnO mutagenicity can also be related to particle size and shape. As ZnO NPs used here had a uniform feature with an average size of 21 nm, it could enter the cell homogeneously and cause mutagenicity at higher concentrations. On the other hand, as the amorphous ZnO comprises a mixture of structures of different shapes and sizes, its mutagenicity could be variable, according to the size and shape of the crystals and its ability to enter the cell. Consequently, mutagenic effects related to the dose could not be expected. Additionally, particles agglomerates/aggregates can also decrease NPs genotoxic effects. Prior studies demonstrated that when ZnO NPs were investigated in cultured human peripheral lymphocytes, using chromosome aberrations assays (CA), no dose dependence was observed in the frequencies of CA/cell. Some reports have shown that, paradoxically, high doses of ZnO NPs lead to fewer abnormalities. The authors suggested that this could be due to an increased aggregation of ZnO NPs at high concentrations in the lymphocyte culture. Therefore, the addition of increasing concentrations/doses of ZnO NPs to

lymphocyte cultures may not be paralleled by an equivalent increase in the genotoxic effects of this nanomaterial (Gümüs et al*.,* 2014).

Owing to their small size and large specific surface area, NPs exhibit unique physicochemical properties that may differ dramatically from their bulk counterparts (Yin et al*.,* 2010). Prior studies have shown that, in *Daphnia magna*, two different sizes of ZnO NPs caused qualitatively similar effects, but the smaller was quantitatively more toxic (Santo et al*.,* 2014).

Nevertheless, according to one group (Song et al*.,* 2010), due to conflicting results observed in the literature, it can be concluded that the impact of particle size on the toxicity of ZnO needs further studies.

In the HB cross, treatments with amorphous ZnO (6.25 mM) and ZnO NPs (12.5 mM) were found to significantly increase the frequency of mutant spots in MH individuals, mainly by increasing small single spots. The corresponding BH wings were also analysed aiming to calculate the contribution of mutagenic and recombinogenic effects on the total mutant spots in MH individuals. However, for both amorphous ZnO (6.25 mM) and ZnO NPs (12.5 mM), the frequencies of total mutant spots were not statistically significant. According to this data, we can propose that the increase in mutant spots found in MH individuals was generated due to mitotic recombination rather than mutational events.

Due to the extremely small size of the NPs, there is a concern that they may interact directly with macromolecules such as DNA. When the genotoxicity of ZnO NPs was assessed in the human epidermal cell line A431, a reduction in cell viability as a function of both NP concentrations, as well as exposure time, was observed. ZnO NPs were also found to induce oxidative stress in cells induced by depletion of glutathione (59% and 51%), catalase (64% and 55%) and superoxide

dismutase (72% and 75%). The data demonstrate that ZnO NPs, even at low concentrations, possess a genotoxic potential in human epidermal cells that may be mediated through lipid peroxidation and oxidative stress (Sharma et al*.,* 2009).

Results have shown that ZnO cytotoxicity was much greater than non-metal nanoparticles. Those findings were significantly in accordance with intracellular oxidative stress levels measured by glutathione depletion, malondialdehyde production, superoxide dismutase inhibition and ROS generation. The results indicated that oxidative stress might be a key route in inducing the cytotoxicity of NPs (Yang et al*.,* 2009). The ZnO NPs have induced the elevation of intracellular Zn^{2+} concentration, leading to the over generation of intracellular ROS, leakage of plasma membrane, dysfunction of mitochondria and cell death. The dissolved Zn^{2+} played the main role in the toxic effect of ZnO particles (Song et al*.,* 2010; Wang et al*.,* 2014). The effects of ZnO NPs on the growth, reproduction and accumulation of zinc in *Daphnia magna* have demonstrated that the toxicological effects of ZnO NPs at the chronic level can be largely attributed to the dissolved fraction rather than the NPs or initially formed aggregates (Adam et al*.,* 2014).

5. Conclusions

According to our results, ZnO NPs were toxic at concentrations equal to or higher than 240.0 μM and genotoxic (clastogenic or aneugenic) at 120.0 μM. Amorphous ZnO and ZnO NPs were metabolically activated by cytochrome P450 enzymes and induced mainly recombinogenicity depending on the concentration, size and/or particle shape. Due to the biological activities of these compounds and increased human exposure, further evaluation of their genotoxic/recombinogenic potentials is warranted.

ACKNOWLEDGEMENTS

This work was supported by Conselho Nacional de Desenvolvimento Científico e Tecnológico (CNPq), Fundação de Amparo à Pesquisa do Estado de Minas Gerais (FAPEMIG), Fundação de Amparo à Pesquisa do Estado de São Paulo (FAPESP), Universidade de Franca (UNIFRAN) and Universidade Federal de Uberlândia (UFU).

CONFLICT OF INTEREST

The authors did not report any conflict of interest.

REFERENCES

Adam N, Schmitt C, Galceran J, Companys E, Vakurov A, Wallace R, Knapen D, Blust R. 2014. The chronic toxicity of ZnO nanoparticles and $ZnCl_2$ to *Daphnia magna* and the use of different methods to assess nanoparticle aggregation and dissolution. **Nanotoxicology** 8:709-717.

Adamcakova-Dodd A, Stebounova LV, Kim JS, Vorrink SU, Ault AP, O'Shaughnessy PT, Grassian VH, Thorne PS. 2014. Toxicity assessment of zinc oxide nanoparticles using sub-acute and sub-chronic murine inhalation models. **Part Fibre Toxicol** 11:15.

Akhtar MJ, Ahamed M, Kumar S, Khan MAM, Ahmad J, Alrokayan SA. 2012. Zinc oxide nanoparticles selectively induce apoptosis in human cancer cells through reactive oxygen species. **Int J Nanomed** 7:845-857.

Bacchetta R, Moschini E, Santo N, Fascio U, Del Giacco L, Freddi S, Camatini M, Mantecca P. 2014. Evidence and uptake routes for zinc oxide nanoparticles through the gastrointestinal barrier in *Xenopus laevis*. **Nanotoxicology** 8:728-744.

Bhattacharya D, Santra CR, Ghosh AN, Karmakar P. 2014. Differential toxicity of rod and spherical zinc oxide nanoparticles on human peripheral blood mononuclear cells. **J Biomed Nanotechnol** 10:707-716.

Corradi S, Gonzalez L, Thomassen LCJ, Bilaničová D, Birkedal RK, Pojana G, Marcomini A, Jensen KA, Leyns L, Kirsch-Volders M. 2012. Influence of serum on *in situ* proliferation and genotoxicity in A549 human lung cells exposed to nanomaterials. **Mutat Res** 745:21-27.

Damen TC, Porto SPS, Tell B. 1966. Raman effect in zinc oxide. **Phys Rev** 142:570-574.

Dantas NO, Damigo L, Qu F, Cunha JFR, Silva RS, Miranda KL, Vilela EC, Sartoratto PPC, Morais PC. 2008a. Raman investigation of ZnO and $Zn_{1-x}Mn_xO$ nanocrystals synthesized by precipitation method. **J Non-Cryst Solids** 354:4827-4829.

Dantas NO, Damigo L, Qu F, Silva RS, Sartoratto PPC, Miranda KL, Vilela EC, Pelegrini F, Morais PC. 2008b. Structural and magnetic properties of ZnO and $Zn_{1-x}Mn_xO$ nanocrystals. **J Non-Cryst Solids** 354:4727-4729.

de Andrade LR, Brito AS, Melero AMGS, Zanin H, Ceragioli HJ, Baranauskas V, Cunha KS, Irazusta SP. 2014. Absence of mutagenic and recombinagenic activity of multi-walled carbon nanotubes in the *Drosophila* wing-spot test and *Allium cepa* test. **Ecotox Environ Safe** 99:92-97.

Deepa Parvathi V, Rajagopal K. 2014. Nanotoxicology testing: Potential of *Drosophila* in toxicity assessment of nanomaterials. **Int J NanoSci Nanotechnol** 5:25-35.

Demir E, Akça H, Kaya B, Burgucu D, Tokgün O, Turna F, Aksakal S, Vales G, Creus A, Marcos R. 2014. Zinc oxide nanoparticles: Genotoxicity, interactions with UV-light and cell-transforming potential. **J Hazard Mater** 264:420-429.

Demir E, Turna F, Vales G, Kaya B, Creus A, Marcos R. 2013. *In vivo* genotoxicity assessment of titanium, zirconium and aluminium nanoparticles, and their microparticulated forms, in *Drosophila*. **Chemosphere** 93:2304-2310.

Demir E, Vales G, Kaya B, Creus A, Marcos R. 2011. Genotoxic analysis of silver nanoparticles in *Drosophila*. **Nanotoxicology** 5:417-424.

Eastmond DA, Tucker JD. 1989. Identification of aneuploidy-inducing agents using cytokinesis-blocked human lymphocytes and an antikinetochore antibody. **Environ Mol Mutagen** 13:34-43.

Fenech M, Morley AA. 1985. Measurement of micronuclei in lymphocytes. **Mutat Res** 147:29-36.

Fenech M. 2000. The *in vitro* micronucleus technique. Mutat Res 455:81-95.
Frei H, Würgler FE. 1988. Statistical methods to decide whether mutagenicity test data from *Drosophila* assays indicate a positive, negative, or inconclusive result. **Mutat Res** 203:297-308.

Frei H, Würgler FE. 1995. Optimal experimental design and sample size for the statistical evaluation of data from somatic mutation and recombination tests (SMART) in *Drosophila*. **Mutat Res** 334:247-258.

Fukui H, Horie M, Endoh S, Kato H, Fujita K, Nishio K, Komaba LK, Maru J, Miyauhi A, Nakamura A, Kinugasa S, Yoshida Y, Hagihara Y, Iwahashi H. 2012. Association of zinc ion release and oxidative stress induced by intratracheal instillation of ZnO nanoparticles to rat lung. **Chem-Biol** Interact 198:29-37.

Graf U, Frei H, Kägi A, Katz AJ, Würgler FE. 1989. Thirty compounds tested in the *Drosophila* wing spot test. **Mutat Res** 222:359-373.

Graf U, Heo O-S, Ramirez OO. 1992. The genotoxicity of chromium(VI) oxide in the wing spot test of *Drosophila melanogaster* is over 90% due to mitotic recombination. **Mutat Res** 266:197-203.

Graf U, van Schaik N. 1992. Improved high bioactivation cross for the wing somatic mutation and recombination test in *Drosophila melanogaster*. **Mutat Res** 271:59-67.

Graf U, Würgler FE, Katz AJ, Frei H, Juon H, Hall CB, Kale PG. 1984. Somatic mutation and recombination test in *Drosophila melanogaster*. **Environ Mutagen** 6:153-188.

Guinier A. (1994). X-ray Diffraction in Crystals, Imperfect Crystals, and Amorphous Bodies. New York, United States: Courier Dover Publications.

Gümüs D, Berber AA, Ada K, Aksoy H. 2014. In vitro genotoxic effects of ZnO nanomaterials in human peripheral lymphocytes. **Cytotechnology** 66:317-325.

Heng BC, Zhao X, Xiong S, Ng KW, Boey FYC, Loo JSC. 2010. Toxicity of zinc oxide (ZnO) nanoparticles on human bronchial epithelial cells (BEAS-2B) is accentuated by oxidative stress. **Food Chem Toxicol** 48: 1762–1766.

Kang T, Guan R, Chen X, Song Y, Jiang H, Zhao J. 2013. In vitro toxicity of different-sized ZnO nanoparticles in Caco-2 cells. **Nanoscale Res** Lett 8:496.

Kastenbaum MA, Bowman KO. 1970. Tables for determining the statistical significance of mutation frequencies. **Mutat Res** 9:527-549.

Kirsch-Volders M, Plas G, Elhajouji A, Lukamowicz M, Gonzalez L, Loock KV, Decordier I. 2011.

The in vitro MN assay in 2011: origin and fate, biological significance, protocols, high throughput methodologies and toxicological relevance. **Arch Toxicol** 85:873-899.

Kwon JY, Lee SY, Koedrith P, Lee JY, Kim K-M, Oh J-M, Yang SI, Kim M-K, Lee JK, Jeong J, Maeng EH, Lee BJ, Seo YR. 2014. Lack of genotoxic potential of ZnO nanoparticles in *in vitro* and *in vivo* tests. **Mutat Res** 761:1-9.

Meyer K, Rajanahalli P, Ahamed M, Rowe JJ, Hong Y. 2011. ZnO nanoparticles induce apoptosis in human dermal fibroblasts via p53 and p38 pathways. **Toxicol In Vitro** 25:1721-1726.

Ng KW, Khoo SP, Heng BC, Setyawati MI, Tan EC, Zhao X, Xiong S, Fang W, Leong DT, Loo JS. 2011. The role of the tumor suppressor p53 pathway in the cellular DNA damage response to zinc oxide nanoparticles. **Biomaterials** 32:8218-8225.

Oberdörster G, Oberdörster E, Oberdörster J. 2005. Nanotoxicology: An emerging discipline evolving from studies of ultrafine particles. **Environ Health Persp** 113:823-839.

Osman IF, Baumgartner A, Cemeli E, Fletcher JN, Anderson D. 2010. Genotoxicity and cytotoxicity of zinc oxide and titanium dioxide in HEp-2 cells. **Nanomedicine** 5:1193-1203.

Pfuhler S, Elespuru R, Aardema MJ, Doak SH, Donner EM, Honma M, Kirsch-Volders M, Landsiedel R, Manjanatha M, Singer T, Kim JH. 2013. Genotoxicity of nanomaterials: refining strategies and tests for hazard identification. **Environ Mol Mutagen** 54:229-239.

Santo N, Fascio U, Torres F, Guazzoni N, Tremolada P, Bettinetti R, Mantecca P, Bacchetta R. 2014. Toxic effects and ultrastructural damages to *Daphnia magna* of two differently sized ZnO nanoparticles: Does size matter? **Water Res** 53:339-350.

Sharma V, Anderson D, Dhawan A. 2012. Zinc oxide nanoparticles induce oxidative DNA damage and ROS-triggered mitochondria mediated apoptosis in human liver cells (HepG2). **Apoptosis** 17:852-870.

Sharma V, Shukla RK, Saxena N, Parmar D, Das M, Dhawan A. 2009. DNA damaging potential of zinc oxide nanoparticles in human epidermal cells. **Toxicol Lett** 185:211-218.

Shi H, Liu X, Zhang Y. 2014. Fabrication of novel antimicrobial poly(vinyl chloride) plastic for automobile interior applications. *Iran Polym* J 23:297-305.
Singh P, Nanda A. 2014. Enhanced sun protection of nano-sized metal oxide particles over conventional metal oxide particles: An in vitro comparative study. **Int J Cosmetic Sci** 36: 273–283.

Song W, Zhang J, Guo J, Zhang J, Ding F, Li L, Sun Z. 2010. Role of the dissolved zinc ion and reactive oxygen species in cytotoxicity of ZnO nanoparticles. **Toxicol Lett** 199:389-397.

Sousa CJA, Pereira MC, Almeida RJ, Loyola AM, Silva ACA, Dantas NO. 2014. Synthesis and characterization of zinc oxide nanocrystals and histologic evaluation of their biocompatibility by means of intraosseous implants. **Int Endod J** 47:416-424.

Spanó MA, Frei H, Würgler FE, Graf U. 2001. Recombinagenic activity of four compounds in the standard and high bioactivation crosses of *Drosophila melanogaster* in the wing spot test. **Mutagenesis** 16:385-394.

Vales G, Demir E, Kaya B, Creus A, Marcos R. 2013. Genotoxicity of cobalt nanoparticles and ions in *Drosophila*. **Nanotoxicology** 7:462-468.

von Moos N, Slaveykova VI. 2014. Oxidative stress induced by inorganic nanoparticles in bacteria and aquatic microalgae - state of the art and knowledge gaps. **Nanotoxicology** 8:605-630.

Wahab R, Kaushik NK, Kaushik N, Choi EH, Umar A, Dwivedi S, Musarrat J, Al-Khedhairy AA. 2013. ZnO nanoparticles induces cell death in malignant human T98G gliomas, KB and non-malignant HEK cells. **J Biomed Nanotechnol** 9:1181-1189.

Wang B, Zhang Y, Mao Z, Yu D, Gao C. 2014. Toxicity of ZnO nanoparticles to macrophages due to cell uptake and intracellular release of zinc ions. **J Nanosci Nanotechno** 14:5688-5696.

Willander M, Khun K, Ibupoto ZH. 2014. ZnO based potentiometric and amperometric nanosensors. **J Nanosci Nanotechno** 14:6497-6508.

Yang H, Liu C, Yang D, Zhang H, Xi Z. 2009. Comparative study of cytotoxicity, oxidative stress and genotoxicity induced by four typical nanomaterials: the role of particle size, shape and composition. **J Appl Toxicol** 29:69-78.

Yin H, Casey PS, McCall MJ, Fenech M. 2010. Effects of surface chemistry on cytotoxicity, genotoxicity, and the generation of reactive oxygen species induced by ZnO nanoparticles. **Langmuir** 26:15399-15408.

Zhang H, Chen B, Jiang H, Wang C, Wang H, Wang X. 2011. A strategy for ZnO nanorod mediated multi-mode cancer treatment. **Biomaterials** 32:1906-1914.

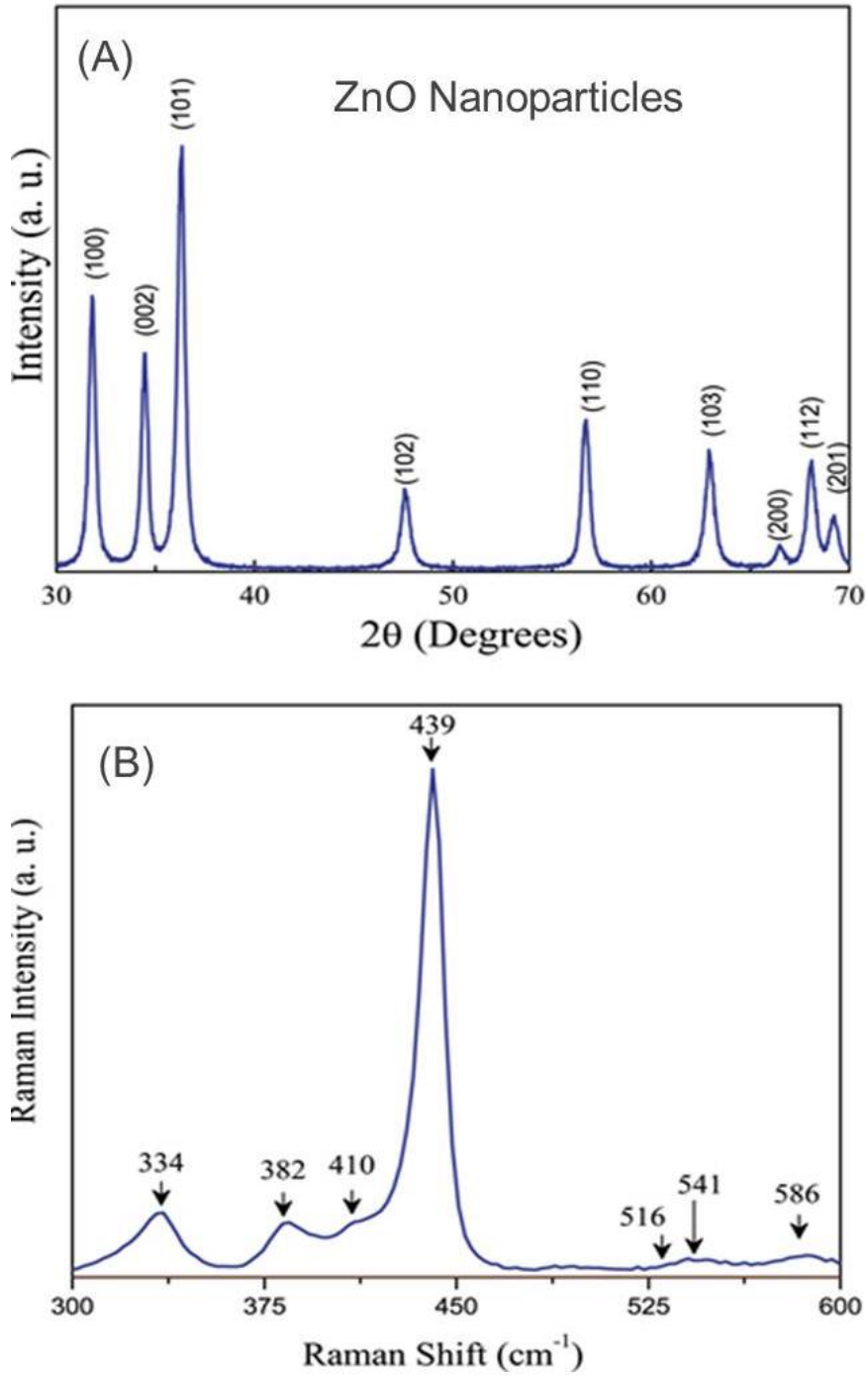

Fig. 1. (A) X-ray diffractogram and (B) micro-Raman spectrum of the ZnO NPs.

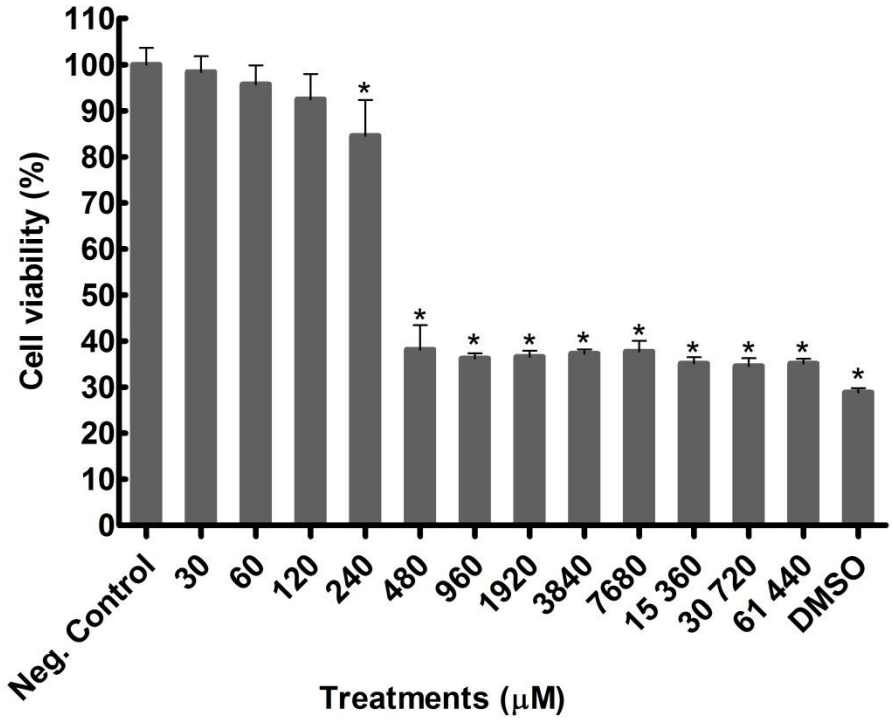

Fig. 2. Cell viability observed in V79 cells treated with different concentrations of ZnO NPs and respective controls. *Significantly different from the control group ($P < 0.05$).

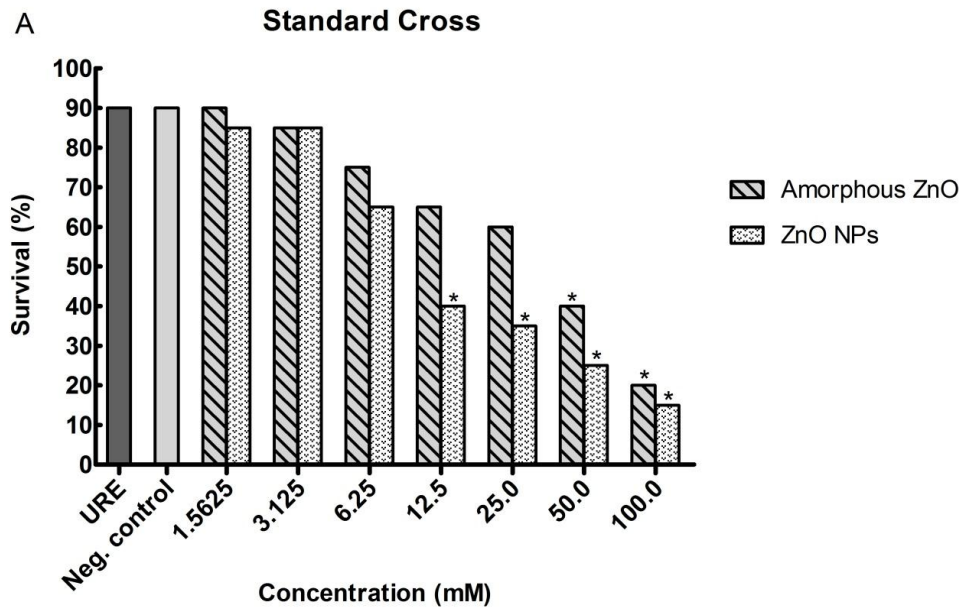
A
Standard Cross
Survival (%)
100
90
80
70
60
50
40
30
20
10
0
URE
Neg. control
1.5625
3.125
6.25
12.5
25.0
50.0
100.0
Concentration (mM)
Amorphous ZnO
ZnO NPs

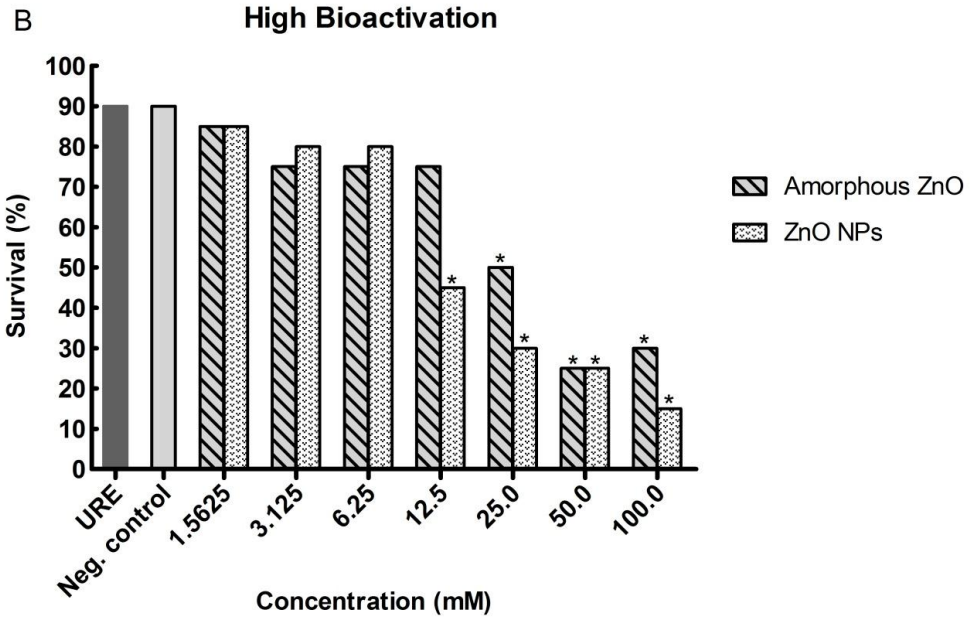
B
High Bioactivation
Survival (%)
100
90
80
70
60
50
40
30
20
10
0
URE
Neg. control
1.5625
3.125
6.25
12.5
25.0
50.0
100.0
Concentration (mM)
Amorphous ZnO
ZnO NPs

Fig. 3. Survival rates upon exposure to different concentrations (1.5625, 3.125, 6.25 or 12.5, 25.0, 50.0, 100.0 mM) of amorphous ZnO, ZnO NPs, and positive control urethane (10.0 mM) relative to control group (ultrapure water) in the wing Somatic Mutation and Recombination Test in *D. melanogaster*. A: Standard cross; B: High bioactivation cross. Statistical comparisons of survival rates were made by using Chi-square test for ratios for independent samples. *Significantly different from the control group ($P < 0.05$).

Table 1

Frequency of micronuclei (MNs) and the nuclear division index (NDI) observed in V79 cells treated with different concentrations of zinc oxide nanoparticles (ZnO NPs) and the respective controls.

Treatments (μM)	MNs[†] Mean ± SD	NDI[‡] Mean ± SD
Negative control	7.00 ± 1.00	1.78 ± 0.03
MMS	45.00 ± 3.61[*]	1.78 ± 0.03
ZnO NPs		
30.0	10.67 ± 0.58	1.85 ± 0.05
60.0	10.67 ± 0.58	1.84 ± 0.03
120.0	11.67 ± 0.58[*]	1.88 ± 0.06

Positive control: MMS – metil metanosulfonate (44 μg/mL).

[†] 3,000 Binucleated cells were analyzed per treatment group.

[‡] 1,500 cells were analyzed per treatment group.

[*] Significantly different from negative control group ($P < 0.05$).

Table 2

Sumary of results obtained with the Somatic Mutation and Recombination Test (SMART) in the marker-heterozygous (MH) progeny of the Standard (ST) cross after chronic treatment of larvae with amorphous ZnO, ZnO nanoparticles (ZnO NPs), and Urethane.

Genotypes and treatments (mM)	Spots per fly (number of spots); statistical diagnoses[†]				Spots with *mwh* clone[§]	Frequency of clone formation per 10^5cells[¶]	
	Nº of flies	Small single spots (1-2 cells)[‡]	Large single spots (> 2 cells)[‡]	Twin	Total spots	Observed	Control corrected
mwh/flr³							
Ultrapure water	50	0.36(18)	0.02(01)	0.10(05)	0.48(24)	22	0.90	
Urethane 10	50	1.76(88) +	0.30(15) +	0.18(09) +	2.24(112) +	111	4.55	3.65
Amorphous ZnO							
1.56	50	0.26(13) -	0.10(05) i	0.04(02) -	0.40(20) -	20	0.82	-0.08
3.12	*50*	0.36(18) -	0.10(05) i	0.02(01) -	0.48(24) -	24	0.98	0.08
6.25	50	0.42(21) i	0.08(04) i	0.04(02) -	0.54(27) -	25	1.02	0.12
12.50	50	0.30(15) -	0.00(00) i	0.06(03) i	0.36(18) -	18	0.74	-0.16
ZnO NPs							
1.56	50	0.54(27) i	0.08(04) i	0.04(02) i	0.66(33) i	33	1.35	0.45
3.12	50	0.38(19) -	0.12(06) i	0.02(01) -	0.52(26) -	25	1.02	0.12
6.25	50	0.38(19) -	0.12(06) i	0.02(01) -	0.52(26) -	25	1.02	0.12
12.50	50	0.36(18) -	0.08(04) i	0.08(04) -	0.52(26) -	23	0.94	0.04

[†] Statistical diagnoses according to Frei and Würgler (1988; 1995): *U*-test, two-sided; probability levels: -, negative; +, positive; i, inconclusive; P ≤ 0.05 vs. negative control;
[‡] Including rare *flr³* single spots.
[§] Considering *mwh* clones from *mwh* single and twin spots.
[¶] Frequency of clone formation: clones/flies/48,800 cells (without size correction).

Table 3

Summary of results obtained with the Somatic Mutation and Recombination Test (SMART) in the marker-heterozygous (MH) and balancer trans-heterozygous (BH) progeny of the High Bioactivation (HB) cross after chronic treatment of larvae with amorphous ZnO, ZnO nanoparticles (ZnO NPs), and Urethane.

Genotypes and treatments (mM)	Number of flies	Spots per fly (number of spots) statistical diagnosis[†]				Spots with mwh clone[§]	Frequency of clone formation per10^5 cells[¶]	
		Small single spots (1-2 cells)[‡]	Large single spots (>2 cells)[‡]	Twin spots	Total spots		Observed	Control Corrected
mwh/flr³								
Ultrapure water	60	0.45 (27)	0.07 (04)	0.05 (03)	0.57 (34)	34	1.16	
Urethane 10	60	9.90 (594) +	1.22 (73) +	0.58 (35) +	11.70 (702) +	688	23.50	22.34
Amorphous ZnO								
1.56	50	0.62 (31) i	0.04 (02) i	0.04 (02) i	0.70 (35) -	35	1.43	0.27
3.12	50	0.32 (16) -	0.06 (03) i	0.08 (04) i	0.46 (23) -	22	0.90	-0.26
6.25	50	0.78 (39) +	0.12 (06) i	0.08 (04) i	0.98 (49) +	47	1.93	0.77
12.50	50	0.58 (29) i	0.06 (03) i	0.04 (02) i	0.68 (34) -	34	1.39	0.23
ZnO NPs								
1.56	60	0.57 (34) -	0.10 (06) i	0.03 (02) i	0.70 (42) -	38	1.30	0.14
3.12	60	0.58 (35) i	0.08 (05) i	0.07 (04) i	0.73 (44) -	42	1.43	0.27
6.25	60	0.52 (31) -	0.17 (10) i	0.08 (05) i	0.77 (46) i	46	1.57	0.41
12.50	60	0.80 (48) +	0.05 (03) i	0.02 (01) i	0.87 (52) +	50	1.71	0.55
mwh/TM3								
Ultrapure water	60	0.50 (30)	0.02 (01)	0.00 (00)	0.52 (31)	31	1.06	
Urethane 10	60	6.22 (373) +	0.18 (11) +	0.00 (00) i	06.40 (384) +	384	13.11	12.05
Amorphous ZnO								
6.25	50	0.58 (29) -	0.04 (02) i	0.00 (00) i	0.62 (31) -	31	1.27	0.21
ZnO NPs								
12.50	60	0.42 (25) -	0.00 (00) i	0.00 (00) i	0.42 (25) -	25	0.85	-0.21

Marker-trans-heterozygous flies (*mwh/flr*^{3}) and balancer-heterozygous flies (*mwh/TM3*) were evaluated.
† Statistical diagnoses according to Frei and Würgler (1988; 1995): *U*-test, two-sided; probability levels: -, negative; +, positive; i, inconclusive;
P ≤ 0.05 vs. negative control;
‡ Including rare *flr*^{3} single spots.
§ Considering *mwh* clones from *mwh* single and twin spots.
¶ Frequency of clone formation: clones/flies/48,800 cells (without size correction).

Capítulo 3

Evaluation of titanium dioxide nanoparticles-induced genotoxicity by the cytokinesis-block micronucleus assay and the Drosophila wing spot test

Manuscrito a ser submetido para publicação no Periódico *Environmental and Molecular Mutagenesis* – Fator de Impacto: 2.553

EVALUATION OF TITANIUM DIOXIDE NANOPARTICLES-INDUCED GENOTOXICITY BY THE CYTOKINESIS-BLOCK MICRONUCLEUS ASSAY AND THE DROSOPHILA WING SPOT TEST

Érica de Melo Reis[1], Alexandre Azenha Alves de Rezende[1], Pollyanna Francielli de Oliveria[2], Heloisa Diniz Nicolella[2], Denise Crispim Tavares[2], Anielle Christine Almeida Silva[3], Noelio Oliveira Dantas[3], and Mário Antônio Spanó[1*]

[1] Laboratório de Mutagênese, Instituto de Genética e Bioquímica, Universidade Federal de Uberlândia, Uberlândia, MG 38400-902, Brazil

[2] Universidade de Franca, Franca, SP 14404-600, Brazil

[3] Laboratório de Novos Materiais Isolantes e Semicondutores (LNMIS), Instituto de Física, Universidade Federal de Uberlândia, Uberlândia, MG 38400-902, Brazil

* Corresponding author address: Mário Antônio Spanó, Universidade Federal de Uberlândia, Instituto de Genética e Bioquímica, Laboratório de Mutagênese. Av. Pará 1720, Umuarama, Uberlândia (MG) 38400-902, Brazil. Tel.: +55 34 32182505.
E-mail address: maspano@ufu.br

ABSTRACT

Titanium dioxide nanoparticles (TiO_2 NPs) have been widely used in pharmaceuticals and cosmetics. TiO_2 NPs can occur at different crystalline structures, as anatase, rutile or brookite. This study evaluated genotoxic effects of anatase TiO_2 NPs of 5.2 and 9.1 nm, and a predominantly rutile TiO_2 NPs of 55.1 nm through *in vitro* Micronucleus (MN) assay, using Chinese hamster lung fibroblasts (V79 cells), and *in vivo* Somatic Mutation and Recombination Test (SMART), on wings of *Drosophila.* MN assay was performed with nontoxic concentrations: 30.5; 61.0 or 122.0 µM of anatase TiO_2 (5.2 and 9.1 nm), and 976.0; 1,953.0 or 3,906.0 µM of rutile TiO_2 (55.1 nm). Only anatase (5.2 nm) at highest concentration was able to induce genotoxicity in V79 cells. In the *in vivo* test, *Drosophila melanogaster* larvae obtained from standard (ST) or high bioactivation (HB) crosses were treated with 1.5625; 3.125; 6.25 or 12.5 mM of TiO_2 NPs (anatase 5.2 and 9.1; rutile 55.1 nm). In ST cross, no mutagenic effects were observed. However, in HB cross, TiO_2 NPs (5.2 nm) was mutagenic at concentrations 1.5625 and 3.125 mM, while 55.1 nm increased mutant spots at all concentrations tested, except at 3.125 mM. Among anatase TiO_2 NPs, only the smallest size induced mutagenic effects *in vitro* and *in vivo.* For rutile TiO_2 NPs, no clastogenic/aneugenic effects were observed in MN assay, however, they were mutagenic for *Drosophila*. Therefore, both anatase and rutile TiO_2 NPs were able to induce mutagenicity. Further research is necessary to clarify TiO_2 NPs genotoxic/mutagenic potential.

Key words: *In vitro, in vivo*, mutagenicity, nanotoxicology, titania, titanium(IV) oxide.

INTRODUCTION

Titanium dioxide (TiO_2), titanium (IV) oxide or titania, is the naturally occurring oxide of titanium (Di Carlo et al. 2014; Grabowska et al. 2014). TiO_2 nanoparticles (NPs) are the most prevalent NPs in day-to-day use. Four naturally occurring TiO_2 exist as: rutile, anatase, brookite and titanium dioxide (B) (Banfield and Veblen 1992). Nowadays they are present in electronics, inks, food colorings, coatings for drugs and vitamins and several kinds of personal care products, as toothpastes, sunscreens, soaps and shampoos (Yu and Li 2011; Weir et al. 2012; Chen et al. 2014).

One of the major applications of TiO_2 NPs is their use as effective physical absorbers of UV rays in sun protection agents (Strobel et al. 2014). At a nanoscale, TiO_2 is more efficient in filtering UV light when compared with the microscale counterparts (Smijs and Pavel 2011). Furthermore, its use makes sunscreens more transparent, without opaqueness feature and with better tactile sensation (Newman et al. 2009).

The main feature of nanoscale products and the reason that makes them widely applicable is their reduced size. However, with the size decreasing, there is an increase in their surface area to mass ratio, which makes them extremely more reactive than the conventional formulation of the same product. Previous studies have shown TiO_2 NPs can cause several adverse effects, such as inflammation, pulmonary damage, fibrosis and lung tumors to rodents. Besides, due to harmful interactions of NPs with biological systems and the environment, they are raising concerns about their toxic/genotoxic potential (Foth et al. 2012; Lindberg et al. 2012; Weir et al. 2012; Chen et al. 2014). Other parameters that can influence the toxic/genotoxic potential of TiO_2 NPs are the crystalline structure and chemical concentration (Jiang et al. 2008; Fu et al. 2014).

Besides, TiO_2 was classified by the International Agency for Research on Cancer (IARC) as possibly carcinogenic to humans (IARC 2010). Due to these data and the increasing risk of human exposure to NPs, investigations on the genotoxicity and mutagenicity aiming understanding the safety of TiO_2 NPs are necessary to establish associations between its physicochemical properties and toxic effects (Jiang

et al. 2008; Landsiedel et al. 2009; Zhang et al. 2013; Shi et al. 2014; Strobel et al. 2014). Based on the importance of TiO_2 NPs and the suggestion that size could be related with toxicity and mutagenicity, we tested the hypothesis.

TiO_2 NPs can be internalized to the cytoplasm and into to the cell nucleus as demonstrated by Shukla et al. (2013), in human hepatocellular carcinoma cells (HepG2) using flow cytometry and transmission electron microscopy (TEM). That study also listed the possible mechanisms of induction of toxicity, highlighting markers of oxidative stress (increased generation of reactive oxygen species - ROS, reduced glutathione levels and lipid peroxidation) and apoptosis markers (reduction of mitochondrial membrane potential, increased expression of p53, BAX, Cyto-c, Apaf-1, caspase-9 and caspase-3 and decreased the level of Bcl-2).

Micronuclei (MN) are derived from chromosomal fragments and whole chromosomes that were retained in anaphase (Fenech 2007). The MN can be evaluated by the cytokinesis-block micronucleus (CBMN) assay, which blocks the cell cycle using a cytokinesis block referred as cytochalasin B that produces binucleated cells, allowing a more accurate score of MN and excluding the dividing cells from non dividing cells to enhance the reliability by reducing the incidence of false positive data (Deepa Parvathi and Rajagopal 2014). The Micronucleus test (MNT) has been used to evaluate clastogenic and aneugenic effects of different compounds, including nanoscale TiO_2 (Dobrzynska et al. 2014; Tavares et al. 2014).

The relevancy of *Drosophila* in toxicity assessment of nanomaterials was reviewed recently by Deepa Parvathi and Rajagopal (2014). Among the mentioned assays, the wing Somatic Mutation and Recombination Test (SMART), considered one of the gold standard for mutagenicity, have the ability to assess loss of heterozygosity (LOH) as a consequence of gene mutation, chromosome breaks/rearrangement or chromosome loss of suitable gene markers that have detectable phenotypes when expressed on the wings (Graf et al. 1984).

Therefore, the aim of the present study was to evaluate the genotoxic and mutagenic potentials of TiO_2 NPs using, respectively, the *in vitro* CBMN assay on Chinese hamster lung fibroblast cells (V79) and the *in vivo* wing SMART assay in *Drosophila melanogaster*.

MATERIAL AND METHODS

Chemicals

The three types of TiO_2 nanoparticles (NPs) used in this study were designated as following: anatase TiO_2 NPs of 5.2 nm (A5.2 TiO_2); anatase TiO_2 NPs of 9.1 nm (A9.1 TiO_2) and a mixture of rutile (64%) / brokite (35%) / anatase (1%) TiO_2 NPs of 55.1 nm (R55.1 TiO_2). All TiO_2 NPs were provided, synthetized and characterized at Laboratório de Novos Materiais Isolantes e Semicondutores (LNMIS), Instituto de Física, Universidade Federal de Uberlândia, Uberlândia, Brazil. HAM-F10; DMEM; streptomycin (CAS 3810-74-0); penicillin (CAS 113-98-4); Hepes (CAS 7365-45-8); dimethyl sulfoxide (DMSO; CAS 67-68-5); methyl methanesulfonate (MMS; CAS 66-27-3); cytochalasin-B (CAS 14930-96-2), HNO_3, $Ti(OCH(CH_3)_2)_4$ and NaOH were purchased from Sigma-Aldrich. Ethyl carbamate (Urethane - URE; CAS: 51-79-6) was from Fluka AG, (Buchs, Switzerland); and fetal bovine serum from Nutricell (Campinas, SP, Brazil). As an alternative *Drosophila* instant medium, the instant mashed potato flakes (Yoki®Alimentos S. A., São Bernardo do Campo, SP, Brazil) were used. The solutions were always prepared immediately before use with ultrapure water obtained from a MilliQ system (Millipore, Vimodrome, Milan, Italy).

Synthesis and Characterization of TiO_2 NPs

The TiO_2 NPs were synthesized in aqueous solution at room temperature. The process of synthesis consists of the following steps: (i) prepared at room temperature, a solution containing 300 mL of ultrapure water and 90 mL of nitric acid (HNO_3, 70%, Sigma Aldrich), under magnetic stirring for 20 minutes; (ii) was added 60 mL of titanium isopropoxide ($Ti(OCH(CH_3)_2)_4$, 97%). The pH of this solution was adjusted to 5.6 using a solution of 4M sodium hydroxide (NaOH, 98%) and subsequently was added 400 mL of ultrapure water, keeping under magnetic stirring for 30 minutes. The resulting solution was left to stand for the process of precipitation of TiO_2 NPs. The precipitate was monodisperse in utrapure water under magnetic stirring, and centrifuged at 6,000 rpm for 10 minutes. This procedure was repeated several times to obtain the solution to pH 7.0. Finally, the resulting precipitate was purified from this

solution was subjected to the following successive thermal treatments in ambient atmosphere: (i) 100 °C / 12 hr, (ii) 500 °C / 1 hr and (iii) 800 °C / 1hr.

The X-ray diffraction (XRD) were recorded with a DRX-6000 (Shimadzu), using monochromatic radiation Cu-K$_{\square 1}$ (λ = 1.54056 Å) to confirm the formation of TiO_2 NPs as well as the crystal structure, size and average mass fraction of rutile phase. The size of the NPs was estimated based on the Debye-Scherrer equation (Guinier 1963). In the XRD patterns of the samples treated at 100 ^{o}C / 24 hr and 500 ^{o}C / 1 hr was used the (101) Bragg diffraction peak of anatase phase located around 2θ = 25.4^{o} and in samples treated at 800 ^{o}C / 1 hr used the peak (110) of rutile phase located around 2θ = 27.8^{o}. The mass fraction of rutile phase was calculated using the following equation (Yu et al. 2003; Koo et al. 2006):

$$W_R = \frac{A_R}{K_A A_A + A_R + K_B A_B},$$

where A_B is the integrated intensity of the peak (121) of brookite phase, K_A and K_B are two coefficients with values of 0886 and 2721, respectively. The micro-Raman spectra were obtained using as excitation source the 780 nm line of Ocean Optics spectrometer. All characterizations were performed at room temperature.

In vitro assays

Cell line and culture conditions

Chinese hamster lung fibroblasts (V79 cells) were kindly provided by the Laboratory of Mutagenesis, State University of Londrina (UEL), Paraná, Brazil. The cells were maintained as monolayers in plastic culture flasks (25 cm^2) in HAM-F10 and DMEM (1:1) medium supplemented with 10% fetal bovine serum, antibiotics (0.01 mg/mL streptomycin; 0.005 mg/mL penicillin), and 2.38 mg/mL Hepes at 36.5 ºC in a BOD type incubator. The average cell cycle time was 12 h under these conditions and the experiments were carried out using V79 cells between the 6th and the 12th culture passage after thawing. The protocols used in this study were performed in triplicate.

XTT colorimetric assay

The cytotoxic activity was evaluated using the in vitro colorimetric assay - XTT kit (Roche Diagnostics) according to the manufacturer's instructions. For the experiments, 1 x 10^4 cells were seeded into microplates containing 96 wells. Each well received a maximum of 100 µL of culture medium (DMEM + HAM F10 1:1) supplemented with 10% fetal bovine serum containing different concentrations of TiO_2 NPs (A5.2, A9.1 or R55.1). The concentrations tested ranged from 30.5 to 62,500.0 µM. Negative (no treatment) and positive (dimethylsulfoxide - DMSO 25%) controls were included in the microplates. After incubation with the compound for 24 h at 36.5 °C, the culture medium was removed and cells were washed with 100 µL of PBS to remove the compound and exposed to 100 µL of HAM-F10 medium red-free culture phenol. Then, 25 µL of XTT were added to each well. The microplates were incubated at 36.5 °C for 17h. The absorbance of the samples was determined by means of a multi-plate reader (ELISA -Asys - UVM 340 / MicroWIN 2000) at a wavelength of 450 nm and a reference length of 620 nm. The amount of formed soluble product (formazan) was proportional to the number of viable cells. The negative control group was designated as 100% and the results were expressed as a percentage of the negative control. The experiments were performed in triplicate.

Cytokinesis-block micronucleus (CBMN) assay

The V79 cells (500,000) were seeded into tissue-culture flasks and incubated for 25 hr in complete 5 mL HAM-F10/DMEM medium and washed with PBS (pH 7.4). After the incubation, the cultures were rinsed with PBS, and then submitted to one of the following treatments: negative control (without treatment); A5.2 or A9.1 TiO_2 at concentrations of 30.5, 61.0 or 122.0 µM; R55.1 TiO_2 at 976.5, 1,953.0 or 3,906.0 µM; positive control (MMS) at 400 µM. All the experiments were performed in triplicate. After the treatment period, the cells were washed with PBS and a culture medium supplemented with fetal bovine serum containing 3 µg/mL of cytochalasin-B was added and the cells were incubated for 17 hr. Then, the cells were rinsed with 5 mL PBS, trypsinized using 0.025% trypsin-EDTA and centrifuged for 5 min at 900 rpm.

The pellet was hypotonized in sodium citrate 1% at 37 ºC and then homogenized with a Pasteur pipette. This cell suspension was centrifuged again and the supernatant was discarded and the pellet was resuspended in methanol:acetic acid (3:1) and homogenized again with a Pasteur pipette. After fixation, the cells were stained in a Giemsa solution 5%.

The analysis was established by Fenech (2000): 1,000 cells were counted by culturing in a total of 3,000 binucleated cells per treatment. The nuclear division index (NDI) was determined for 500 cells analyzed per repetition, for a total of 1,500 cells per treatment group using the same slides used on the micronucleus assay. Cells with well-preserved cytoplasm containing 1 - 4 nuclei were scored and the NDI was calculated using the following formula (Eastmond and Tucker 1989):

$$NDI = \frac{[M1 + 2(M2) + 3(M3) + 4(M4)]}{N}$$

Where *M1-M4* is the number of cells with 1, 2, 3 and 4 nuclei, respectively, and *N* is the total number of viable cells.

Statistical analysis - CBMN

The data were analyzed statistically by analysis of variance for completely randomized experiments, with calculation of F statistics and respective *P* values. In cases in which $P < 0.05$, treatment means were compared by the Tukey test and the minimum significant difference was calculated for 0.05.

In vivo assay

D. melanogaster strains and crosses

Three *D. melanogaster* strains with the genetic markers multiple wing hairs (*mwh*, 3-0.3) and flare-3 (flr^3, 3-38.9) were kindly provided by the Physiology and Animal Husbandry Institute of Animal Sciences (University of Zurich, Schwerzenbach, Switzerland): (1) multiple wing hairs (*mwh/mwh*); (2) flare-3 (flr^3*/In(3LR)TM3, ri* p^p*sep l(3)89Aa bx34*^{e} *and* Bd^S); and (3) ORR; flare-3 (*ORR/ORR;* flr^3*/In(3LR)TM3, ri* p^p*sep*

l(3)89Aa bx34^{e} and Bd^{S}). The ORR strain has chromosomes 1 and 2 from a DDT-resistant Oregon R(R) line, which are responsible for a high constitutive level of cytochromes P450 (Graf and van Schaik 1992). These strains were maintained in glass vials filled with a maintenance medium (i.e., banana, sucrose, yeast and methylparaben) under light/dark cycles (12 hr:12 hr), at 25 ± 1º C and approximately 60% humidity in a BOD-type chamber (Model: SL224, SOLAB – Equipamentos para Laboratórios Ltda., São Paulo, SP, Brazil).

Two crosses were carried out to produce the experimental larval progeny: (1) Standard (ST) cross, *mwh/mwh* males crossed with *flr^{3}/In(3LR)TM3, ri p^{p}sep l(3)89Aa bx34^{e} and Bd^{S}* virgins females (Graf et al., 1984; 1989); (2) High bioactivation (HB) cross, *mwh/mwh* males crossed with *ORR/ORR; flr^{3}/In(3LR)TM3, ri p^{p}sep l(3)89Aa bx34^{e} and Bd^{S}* virgins female (Graf and van Schaik 1992). The two crosses produce two types of flies. Marker trans-heterozygous (MH) flies (*mwh*+/+ *flr^{3}*) and balancer-heterozygous (BH) flies (*mwh*+/+*TM3*, *Bd^{S}*). The first one has normal wings while the latter can be distinguished phenotypically by its serrated wings.

Somatic Mutation and Recombination Test – SMART

From the ST and HB crosses eggs were collected for 8 hr in culture bottles with 4% w/v agar-agar base, topped with a thick layer of live baker's yeast supplemented with sucrose. Larvae of 72 ± 4 hr were transferred to glass vials to a chronic feeding (approximately 48 hr). Four sets of vials for each cross were prepared with 1.5 g of mashed potato flakes and 5 mL of a solution containing TiO_2 NPs (A5.2, A9.1 or R55.1) at concentrations 1.5625, 3.125, 6.25, 12.5, 25.0, 50.0 and 100.0 mM. Negative (ultrapure water) and positive (URE 10mM) controls were included in this experiment. The larvae were counted before the distribution in two series of these vials to calculate the survival rates upon exposure. Larvae were allowed to feed on the above medium for the remainder of their development, to pupate and to hatch as adult flies. All experiments were conducted at 25 ± 1 °C and approximately 60% humidity.

The hatched flies were stored in 70% (v/v) ethanol. The wings of MH flies were removed and mounted in glass slides with Faure's solution (gum Arabic 30 g, glycerol

20 mL, chloral hydrate 50 g, water 50 mL) and analyzed for size and frequency of spots under a compound microscope at 400 x magnification.

Three types of spots can be observed on the wings of MH flies: (i) Small single spots (*mwh* or *flr*^{3}), consisting of one or two mutant hairs, resulting from deletions, point mutations, specific chromosome aberrations, or from recombination between the two marker genes; (ii) Large single spots (*mwh* or *flr*^{3}), consisting of three or more hairs; and (iii) Twin spots (*mwh* and *flr*^{3}*),* consisting of adjacent *mwh* and *flr*^{3} hairs, produced by mitotic recombination between the proximal marker *flr*^{3} and the centromere of chromosome 3. Only *mwh* single spots can be recovered on the wings of BH flies. They are all due to mutational events because recombinational events are suppressed due to multiply inverted *TM3* balancer chromosome (Graf et al. 1984; Guzmán-Rincón and Graf 1995). For each analyzed wing the three kinds of spots were recorded for further statistical analysis.

Statistical analysis - SMART

The experimental data were evaluated according to the multiple-decision procedure (Frei and Wurgler 1988; Frei and Wurgler 1995). The frequencies of each type of mutant clone per fly were compared with the concurrent negative control series using the conditional binomial test (Kastenbaum and Bowman 1970), used to decide whether a result is positive, inconclusive or negative. Chi-square test was performed for statistical comparisons of survival rates for independent samples. Each statistical test was evaluated at the 5% significance level.

RESULTS

Nanoparticles characterization

Figure 1A shows the X-ray diffraction (XRD) patterns of TiO_2 NPs subjected to thermal treatment at 100 ^oC / 24 hr, 500 ^oC / 1 hr, e 800 ^oC / 1 hr. In the XRD patterns of all samples are represented diffraction patterns characteristic of the TiO_2 NPs anatase (JCPDS: 1:21-1272), rutile (JCPDS: 1:21-1276) and brookite (JCPDS: 29-1360) phases, respectively, by the symbols (*), (**) and (***). It is observed in the XRD pattern of TiO_2 NPs subjected to thermal treatment of 100 ^oC / 24 hr that all these NPs are crystalline and have only anatase phase. The increase in temperature of thermal treatment of 100 ^oC to 500 ^oC, did not alter the crystalline NP phase. With the increase in heat treatment temperature to 800 ^oC / 1hr is observed the conversion of anatase to rutile phase. This is justified by the increase in temperature enhancing the transformation of anatase, which is thermodynamically metastable, to the rutile phase that is more stable (Gaynor et al. 1997; Wu et al. 2002). Moreover, it was also noted in the diffractograms the presence of brookite phase, which occur due to the synthesis procedure used (Pottier et al. 2001; Abbas et al. 2011).

Table I shows the mean size and the mass fraction of rutile of TiO_2 NPs with thermal treatment at 100 ^oC / 24 hr, 500 ^oC / 1 hr and 800 ^oC/ 1hr. It is observed that the increase in thermal treatment temperature favors the growth of TiO_2 NPs and the reduction of mass fraction of rutile. This reduction occurs due to the phase transformation from anatase to brookite, as shown in the diffractograms of Figure 1A.

Figure 1B shows the micro-Raman spectra of TiO_2 NPs undergoing thermal treatments 100 ^oC / 24 hr, 500 ^oC / 1 hr and 800 ^oC / 1 hr. All spectra were normalized to the peak of greater intensity to facilitate the visualization of active modes of anatase, brookite and rutile phases presents in the TiO_2 NPs. It was verified that the TiO_2 NPs with thermal treatment at 100 ^oC / 24 hr exhibited characteristic bands of vibrations of anatase phase (Ohsaka 1980; Zhang et al. 2000). Raman bands are shifted to higher wave numbers, which occurs due to decrease in size of the NPs, in accordance with the size values obtained based on the results of XRD (see Table I) (Choi et al. 2005). The Raman band around 144 cm^{-1} was not visualized because the

detector of the Raman system used only detects in the range of 150 to 1000 cm^{-1}, observing the descent of the band. In the micro-Raman spectrum of the samples, thermal treatment at 500 ^{o}C / 1 hr are also observed the modes of anatase phase. The increase in annealing temperature to 800 ^{o}C / 1 hr favored the formation of rutile and brookite, both observed in Raman spectrum as in the XRD diffractogram (Fig. 1B). The three types of TiO_2 NPs used in this study were designated as anatase TiO_2 NPs of 5.2 nm (A5.2 TiO_2); anatase TiO_2 NPs of 9.1 nm (A9.1 TiO_2) and a mixture of rutile (64%) / brookite (35%) / anatase (1%) TiO_2 NPs of 55.1 nm (R55.1 TiO_2).

XTT colorimetric assay

The cytotoxicity of TiO_2 NPs (A5.2, A9.1 or R55.1) were assessed by XTT colorimetric assay in V79 cells at concentrations ranging from 30.5 to 62,500.0 μM. Figure 2 shows the cell viability percentage of each treatment. The results demonstrated that treatments with A5.2 and A9.1 TiO_2 showed significant difference from negative control at concentrations higher than 122 μM (Fig. 2A and 2B, respectively), and with R55.1 TiO_2, concentrations superior than 3.906 μM were considered statistically cytotoxic (Fig. 2C).

Micronucleus assay

Micronucleus (MN) frequency in V79 cells treated with 30, 60 or 120 μM of A5.2 or A9.1 TiO_2, and 976.5, 1,953.0 or 3,906.0 μM of R55.1 TiO_2, and nuclear division index (NDI) are showed in Table II. The results demonstrated that A5.2 TiO_2 significantly increased the frequency of MN at higher concentration (120 μM), showing a genotoxic effect. No significant differences in MN induction were observed in the groups treated with 30 and 60 μM of A5.2 TiO_2 when compared to negative control ($p > 0.05$). The results also demonstrated lack of genotoxic effects for A9.1 and R55.1 TiO_2, at all concentrations tested (Table II).

Table II also displays the means nuclear division index (NDI) and the respective standard deviation (SD) obtained for all treated groups. No significant differences were observed between the total induced MN in any treatment group as

compared to the negative control, demonstrating the absence of cytotoxicity of the different treatments under our experimental conditions.

Somatic Mutation and Recombination Test – SMART

Third instar larvae of *D. melanogaster* obtained from ST and HB crosses were fed chronically with three different types of TiO_2 NPs: A5.2, A9.1 or R55.1, at concentrations ranging from 1.5625 to 100.0 mM. The survival rates are showed in Figure 3. All concentrations tested were not toxic when compared to the negative control group. The assessment for size and frequency of spots were performed with wings of flies treated with the four smallest concentrations tested (1.5625; 3.125; 6.25 or 12.5 mM).

The results of the wing spot test for mutagenic evaluation of TiO_2 NPs (A5.2, A9.1 or R55.1) are summarized in Tables III-V, for ST and HB crosses. As expected, the reference mutagen (URE) induced positive results for all spot categories in both crosses (ST and HB) compared to the negative control.

From ST cross, the results showed that TiO_2 NPs (A5.2, A9.1 or R55.1), at concentrations 1.5625; 3.125; 6.25 or 12.5 mM, did not induce significant increase in the frequency of mutant spots. Among HB individuals, A9.1 TiO_2 presented no genotoxic effect of all categories of mutant spots recorded (Table IV). On the other hand, A5.2 and R55.1 TiO_2 were able to induce mutagenic activity, but regardless dose increasing.

DISCUSSION

Studies about TiO_2 have revealed that the use of these NPs have the two sides of the same coin. While TiO_2 NPs have been widely employed in industry, researchers worldwide have raised concerns about their potential genotoxic effects, which may be related to crystalline structure, size, concentration or time exposure.

Aiming to contribute to the knowledge regarding TiO_2 NPs potential genotoxicity, the present study evaluated, *in vitro* and *in vivo*, three well physically characterized NPs: anatase TiO_2 of 5.2 and 9.1 nm (A5.2 TiO_2 and A9.1 TiO_2); and a mixed phase nanocrystal 64% rutile/ 35% brookite/ 1% anatase TiO_2 of 55.1 nm (R55.1 TiO_2), characterized by the X-ray diffraction and micro-Raman spectroscopy. The relevance of a well characterization of testing material has been highlighted by several authors as an elemental part of toxicity studies (Arora et al. 2012; Nystrom and Fadeel 2012; Chen et al. 2014).

The present investigation evaluated the cytotoxic potential of anatase TiO_2 NPs through XTT colorimetric assay with V79 cells. The results showed that both sizes of anatase TiO_2 NPs (5.2 and 9.1 nm) were similarly able to decrease cell viability in a dose-dependent manner. The observed results are in good agreement with those observed in A549 human lung carcinoma cells (CCL-185) (Jugan et al. 2012), and mouse macrophage (Ana-1) (Zhang et al. 2013). The Cytotoxic activity of metal oxide particles is often associated with an increase in intracellular reactive oxygen species (ROS) (Nel et al. 2006).

The Cytokinesis Block Micronucleus (CBMN) assay with Chinese hamster lung fibroblasts (V79 cells) was performed with the no cytotoxic TiO_2 NPs concentrations, previously determined by XTT assay. The results showed that among anatase TiO_2 NPs assessed, only A5.2, at highest concentration, was able to induce MN formation. Therefore, for these experimental conditions, we could suppose that genotoxic effects of anatase phase are dependent of crystal size. Publications with anatase TiO_2 NPs of different sizes have demonstrated a conflict in outcomes. Differences in genotoxicity without relationship with dose or size of anatase TiO_2 NPs was shown by Tavares et al. (2014). On the other hand, according to the experimental conditions,

TiO_2 NPs genotoxicity can be highly dependent upon size and shape. For example, TiO_2 anatase NPs (10-20 nm) have been shown to induce chromosomal damage through increased MN frequency, whilst in the same study such genotoxicity was not induced by 200 nm anatase (Gurr et al. 2005). Genotoxic effects of 30-70 nm anatase TiO_2 NPs were able to induce MN formation in HepG2 cells besides revealed a significant concentration-dependent increase in oxidative DNA damage, probably caused by the registered intracellular elevation of ROS (Shukla et al. 2013). Nevertheless, although demonstrate high cytotoxic activity, Guichard et al. (2012) found no significant MN formation after exposed Syrian hamster embryo cells to 14 nm anatase TiO_2 NPs treatment.

In a recent review, Arora et al. (2012) have raised the relevance of *in vivo* studies on nanotoxicolgy based on *in vitro* validated results despite of current concerns about the use of animals in research, making *in vivo* work more difficult. Currently, it has been seen a global effort to reduce the use of animals in toxicological/genetic research, particularly in regard to the development of alternative *in vivo* models (Siddique et al. 2005). One of these alternative models, either highlighted by Deepa Parvathi and Rajagopal (2014), is the fruit fly *D. melanogaster*. The ease of screening phenotypes and their susceptibility for genetic manipulation identifies *Drosophila* as an ideal model for mutagenicity and toxicological screening, corroborating with Demir et al. (2013), who considered that this *in vivo* eukaryotic model offer many advantages with respect to the *in vitro* and others *in vivo* studies using whole mammal organisms.

The Somatic Mutation and Recombination Test (SMART) is extremely sensitive and determines chemical mutagenicity assessing the loss of heterozygosity (LOH) of cellular markers. This LOH produces single spots (small and large) by point mutation, deletion or non-disjunction and twin spots, which are produced exclusively by mitotic recombination (Graf et al. 1984). For this purpose, two crosses are typically used: the standard (ST) cross and a high bioactivation (HB) cross. The latter is characterized by improved sensitivity to promutagens and procarcinogens owing to high level of constitutively expressed cytochromes P450 (Frölich and Würgler 1989; Graf et al. 1989; Graf and van Schaik 1992).

In the SMART assay of this present investigation, none mutagenic effects were observed for individuals originated from ST cross. The smallest anatase TiO_2 NPs tested (5.2 nm) were able to induced mutagenic effects on wings of HB cross, as well MNs formations as previously reported in this study. Although all concentrations of A5.2 TiO_2 induced mutagenic spots, only the effects of the two lowest concentrations were statistically significant. The inconclusive or negative results for total spots observed in the two highest concentrations of A5.2 TiO_2 can be justified by two manners. The increase in NPs concentrations can indicate cell death due to mutagenic effects, without individual death, and consequently absence of mutant spots in the wings analyzed, or, as observed in other studies, the increase in the NPs concentrations can lead to agglomeration or aggregation formation. It is important to considerer that NPs agglomerates or aggregates can become roughly 40 times larger than the individual NPs (Strobel et al. 2014). NPs agglomerates/aggregates could influence biological interaction, as cellular binding/uptake, cytotoxic and genotoxic effects (Falck et al. 2009; Petkovic et al. 2011; Lankoff et al. 2012; Butler et al. 2014; Janer et al. 2014). The highest size of TiO_2 NPs (9.2 nm), of the same anatase crystalline phase, was not mutagenic at all concentrations tested. This finding suggests that mutagenic effects of anatase TiO_2 NPs are size dependent, even that the size difference between these NPs is of only 4 nm. Others studies have been shown that NPs size does not matter in genotoxic effects (Karlsson et al. 2009; Zhang et al. 2013). The unique SMART assay, performed with TiO_2 NPs published before the present one showed no mutagenic effects for anatase NPs at 2.3 nm in ST cross, corroborating our results (Demir et al. 2013). However, this mentioned work did not evaluate HB cross, contrasting with data presented in our study, which showed positive results, probably due to increased metabolism.

Besides the size evaluation, crystalline phase of TiO_2 NPs can be considered an important parameter to be evaluated in cytotoxic and genotoxic investigations; but for this purpose, the NPs sizes among different crystalline structures must be maintained. Here, we evaluated the effects of a mixed phase of TiO_2 NPs with 55.1 nm in which the rutile phase is predominant (64%). As observed in the present study, R55.1 TiO_2 NPs were able to induce cytotoxic effects in V79 cells, but no genotoxic

effects were seen in CBMN assay. Although the sizes of anatase TiO_2 NPs and rutile TiO_2 NPs employed in this study were different, we observed higher cytotoxic potential for anatase than for rutile NPs. Some studies have shown that rutile is the most stable phase of TiO_2 NPs (Haines and Leger 1993; Smijs and Pavel 2011), and it was responsible to induce cytotoxic effects only in high concentrations. Besides that, recent reviews have emphasized the higher photoactivity of anatase NPs when compared with rutile ones (Banerjee 2011; Smijs and Pavel 2011). Jiang et al. (2008) showed that the ability of different crystal phases of TiO_2 NPs to generate ROS was higher for anatase and then for rutile samples. However, in the present study, we cannot state if the lowest cytotoxic effect observed for rutile NPs is due to its higher size (55.1 nm) or due to its crystalline structure.

Negative results on genotoxic effects after rutile TiO_2 exposure have been reported. No significant MN formation was detected in Syrian hamster embryo cells exposed to 62 nm size TiO_2 NPs (Guichard et al. 2012). Similarly, Landsiedel et al. (2010) demonstrated no genotoxicity *in vitro* (Ames' Salmonella gene mutation test and V79 micronucleus chromosome mutation test) or *in vivo* (mouse bone marrow MN test and Comet DNA damage assay in lung cells from rats exposed by inhalation) using rutile TiO_2 NPs (10 – 50 nm). Otherwise, Falck et al. (2009) showed positive cytotoxic effect and DNA damage associated to nanosized rutile TiO_2, but none significant increase in MN induction in cultured human bronchial epithelial BEAS 2B cells.

The occurrence of mutagenic effects can be associated to cell defective ability to repair DNA damage. Anatase and rutile TiO_2 NPs (< 20 nm) was showed to induce inactivation of both nucleotide excision repair (NER) and base excision repair (BER) abilities of A549 cells (Jugan et al. 2012).

Here, the NPs containing 64% of rutile phase TiO_2 (R55.1 TiO_2) was assessed for the first time by *in vivo* SMART assay. Our results showed significant mutagenic effects at all concentration tested, except at 3.125 mM. Mutagenic effects assayed by SMART in this present study were found only in HB cross. Therefore, we can suggest that the high intrinsic metabolic activity associated with HB individuals (Graf and van Schaik 1992), coupled with oxidative stress triggered by TiO_2 NPs (Gurr et al. 2005;

Jugan et al. 2012) and with the impair ability of cells to repair DNA lesions (Jugan et al. 2012) could be seen as the responsible for the appearance of mutant spot in *D. melanogaster* wings.

Our results for XTT colorimetric assay, *in vitro* Micronucleus test and *in vivo* SMART assay had revealed either absence or presence of mutagenic effects dependent of TiO_2 NPs size and independent of TiO_2 crystalline structure. However, to ensure which feature is majority on cytotoxic and genotoxic induction, others relevant parameters have to be analyzed, as agglomerate/aggregate formation, hydrodynamic size, zeta potential, time of NPs exposition for culture cells. Besides that, these conflicts in outcomes exist and will go on, due to the heterogeneity of samples types being tested and the biological models that are being challenged.

The differences observed in cytotoxic and genotoxicity for closely related NPs highlights the importance of investigating the toxic potential of each one individually, instead of assuming a common mechanism and equal genotoxic effects for a set of similar NPs (Tavares et al. 2014). Furthermore, the major relevance of this diversity of data storm is the possibility of raise information aiming corroborate the literature, whereas nanotechnology is an emerging field and needs knowledge to safety people and environment. Besides that, according to Arora et al. (2012), experimental results can also corroborate with nanomaterials synthesis on predictive toxicology that will help to remove toxicity by design parameters.

CONCLUSIONS

In conclusion, our study demonstrated that anatase TiO_2 NPs at smallest size were able to induce mutagenic effects *in vitro* and *in vivo*, and the higher anatase NPs did not caused DNA damage, despite only 4 nm of difference for the first one. For rutile TiO_2 NPs, no clastogenic/aneugenic effect were observed in MN assay, however, the increase on mutagenic spots was significant. In these experimental conditions, we can affirm that both anatase and rutile TiO_2 NPs were able to induce mutagenicity. Therefore, the use of these nanomaterials should be closely monitored and its genotoxicity action mechanisms must be elucidated.

CONFLICT OF INTEREST STATEMENT

The authors declare that there are no conflicts of interest.

ACKNOWLEDGEMENTS

This work was supported by Conselho Nacional de Desenvolvimento Científico e Tecnológico (CNPq), Fundação de Amparo à Pesquisa do Estado de Minas Gerais (FAPEMIG), Fundação de Amparo à Pesquisa do Estado de São Paulo (FAPESP), Universidade de Franca (UNIFRAN) and Universidade Federal de Uberlândia (UFU).

AUTHOR CONTRIBUTIONS

A.C.A.Silva and N.O.Dantas were responsible for synthesis and characterization of TiO_2 NPs. The generation of the data reported here was done by E.M. Reis, P.F.Oliveria and H.D.Nicolella. A.A.A.Rezende, D.C.Tavares and M.A.Spanó contributed to the conceptualization of the project, analyzed the data and prepared the manuscript draft, including figures and tables. All authors approved the final manuscript.

REFERENCES

Abbas Z, Holmberg JP, Hellstrom AK, Hagstrom M, Bergenholtz J, Hassellov M, Ahlberg E. 2011. Synthesis, characterization and particle size distribution of TiO2 colloidal nanoparticles. **Colloids and Surfaces a-Physicochemical and Engineering Aspects** 384(1-3):254-261.

Arora S, Rajwade JM, Paknikar KM. 2012. Nanotoxicology and in vitro studies: the need of the hour. **Toxicol Appl Pharmacol** 258(2):151-165.

Banerjee AN. 2011. The design, fabrication, and photocatalytic utility of nanostructured semiconductors: focus on TiO2-based nanostructures. **Nanotechnol Sci Appl** 4:35-65.

Banfield JF, Veblen DR. 1992. Conversion of perovskite to anatase and TiO2 (B): A TEM study and the use of fundamental building blocks for understanding relationships among the TiO, minerals. **American Mineralogist** 77:545-557.

Butler KS, Casey BJ, Garbocauskas GV, Dair BJ, Elespuru RK. 2014. Assessment of titanium dioxide nanoparticle effects in bacteria: Association, uptake, mutagenicity, co-mutagenicity and DNA repair inhibition. **Mutat Res Genet Toxicol Environ Mutagen.**

Chen T, Yan J, Li Y. 2014. Genotoxicity of titanium dioxide nanoparticles. **J Food Drug Anal** 22(1):95-104.

Choi HC, Jung YM, Kim SB. 2005. Size effects in the Raman spectra of TiO2 nanoparticles. **Vibrational Spectroscopy** 37(1):33-38.

Deepa Parvathi V, Rajagopal K. 2014. Nanotoxicology testing: Potential of Drosophila in toxicity assessment of nanomaterials. **International Journal of NanoScience and Nanotechnology** 5(1):25-35.

Demir E, Turna F, Vales G, Kaya B, Creus A, Marcos R. 2013. In vivo genotoxicity assessment of titanium, zirconium and aluminium nanoparticles, and their microparticulated forms, in Drosophila. **Chemosphere** 93(10):2304-2310.

Di Carlo G, Calogero G, Brucale M, Caschera D, de Caro T, Di Marco G, Ingo GM. 2014. Insights into meso-structured photoanodes based on titanium oxide thin film with high dye adsorption ability. **Journal of Alloys and Compounds** 609:116-124.

Dobrzynska MM, Gajowik A, Radzikowska J, Lankoff A, Dusinska M, Kruszewski M. 2014. Genotoxicity of silver and titanium dioxide nanoparticles in bone marrow cells of rats in vivo. **Toxicology** 315:86-91.

Eastmond DA, Tucker JD. 1989. Identification of aneuploidy-inducing agents using cytokinesis-blocked human lymphocytes and an antikinetochore antibody. **Environ Mol Mutagen** 13(1):34-43.

Falck GC, Lindberg HK, Suhonen S, Vippola M, Vanhala E, Catalan J, Savolainen K, Norppa H. 2009. Genotoxic effects of nanosized and fine TiO2. **Hum Exp Toxicol** 28(6-7):339-352.

Fenech M. 2000. The in vitro micronucleus technique. Mutat Res 455(1-2):81-95.
Fenech M. 2007. Cytokinesis-block micronucleus cytome assay. **Nat Protoc** 2(5):1084-1104.

Foth H, Stewart JD, Gebel T, Bolt HM. 2012. Safety of nanomaterials. **Arch Toxicol** 86(7):983-984.

Frei H, Wurgler FE. 1988. Statistical methods to decide whether mutagenicity test data from Drosophila assays indicate a positive, negative, or inconclusive result. **Mutat Res** 203(4):297-308.

Frei H, Wurgler FE. 1995. Optimal experimental design and sample size for the statistical evaluation of data from somatic mutation and recombination tests (SMART) in Drosophila. **Mutat Res** 334(2):247-258.

Frölich A, Würgler FE. 1989. New tester strains with improved bioactivation capacity for the Drosophila wing-spot test. **Mutat Res** 216(3):179-187.

Fu PP, Xia Q, Hwang HM, Ray PC, Yu H. 2014. Mechanisms of nanotoxicity: generation of reactive oxygen species. **J Food Drug Anal** 22(1):64-75.

Gaynor AG, Gonzalez RJ, Davis RM, Zallen R. 1997. Characterization of nanophase titania particles synthesized using in situ steric stabilization. **Journal of Materials Research** 12(7):1755-1765.

Grabowska E, Diak M, Marchelek M, Zaleska A. 2014. Decahedral TiO2 with exposed facets: Synthesis, properties, photoactivity and applications. **Applied Catalysis B-Environmental** 156:213-235.

Graf U, Frei H, Kagi A, Katz AJ, Wurgler FE. 1989. Thirty compounds tested in the Drosophila wing spot test. **Mutat Res** 222(4):359-373.

Graf U, van Schaik N. 1992. Improved high bioactivation cross for the wing somatic mutation and recombination test in Drosophila melanogaster. **Mutat Res** 271(1):59-67.

Graf U, Würgler FE, Katz AJ, Frei H, Juon H, Hall CB, Kale PG. 1984. Somatic mutation and recombination test in *Drosophila melanogaster*. **Environ Mutagen** 6(2):153-188.

Guichard Y, Schmit J, Darne C, Gate L, Goutet M, Rousset D, Rastoix O, Wrobel R, Witschger O, Martin A, Fierro V, Binet S. 2012. Cytotoxicity and genotoxicity of nanosized and microsized titanium dioxide and iron oxide particles in Syrian hamster embryo cells. **Ann Occup Hyg** 56(5):631-644.

Guinier A. 1963. X-ray diffraction in crystals, imperfect crystals, and amorphous bodies. San Francisco: W.H. Freeman.

Gurr JR, Wang AS, Chen CH, Jan KY. 2005. Ultrafine titanium dioxide particles in the absence of photoactivation can induce oxidative damage to human bronchial epithelial cells. **Toxicology** 213(1-2):66-73.

Guzmán-Rincón J, Graf U. 1995. *Drosophila melanogaster* somatic mutation and recombination test as a biomonitor. In: Butterworth FM, Corkum LD, Guzmán-Rincón J, editors. Biomonitors and Biomarkers as Indicators of Environmental Change New York: Plenum Press. p 169-181.

Haines J, Leger JM. 1993. X-ray diffraction study of TiO2 up to 49 GPa. **Physica B** 192:233 - 237.

IARC. 2010. Carbon black, titanium dioxide, and talc. . IARC Monographs on the Evaluation of Carcinogenic Risks to Humans. Lyon, France: World Health Organization - International Agency on Cancer Research.

Janer G, Mas Del Molino E, Fernandez-Rosas E, Fernandez A, Vazquez-Campos S. 2014. Cell uptake and oral absorption of titanium dioxide nanoparticles. **Toxicol Lett** 228(2):103-110.

Jiang J, Oberdorster G, Elder A, Gelein R, Mercer P, Biswas P. 2008. Does Nanoparticle Activity Depend upon Size and Crystal Phase? **Nanotoxicology** 2(1):33-42.

Jugan ML, Barillet S, Simon-Deckers A, Herlin-Boime N, Sauvaigo S, Douki T, Carriere M. 2012. Titanium dioxide nanoparticles exhibit genotoxicity and impair DNA repair activity in A549 cells. **Nanotoxicology** 6(5):501-513.

Karlsson HL, Gustafsson J, Cronholm P, Moller L. 2009. Size-dependent toxicity of metal oxide particles--a comparison between nano- and micrometer size. **Toxicol Lett** 188(2):112-118.

Kastenbaum MA, Bowman KO. 1970. Tables for determining the statistical significance of mutation frequencies. **Mutat Res** 9(5):527-549.

Koo B, Park J, Kim Y, Choi SH, Sung YE, Hyeon T. 2006. Simultaneous phase- and size-controlled synthesis of TiO2 nanorods via non-hydrolytic sol-gel reaction of syringe pump delivered precursors. **Journal of Physical Chemistry B** 110(48):24318-24323.

Landsiedel R, Kapp MD, Schulz M, Wiench K, Oesch F. 2009. Genotoxicity investigations on nanomaterials: methods, preparation and characterization of test material, potential artifacts and limitations--many questions, some answers. **Mutat Res** 681(2-3):241-258.

Landsiedel R, Ma-Hock L, Van Ravenzwaay B, Schulz M, Wiench K, Champ S, Schulte S, Wohlleben W, Oesch F. 2010. Gene toxicity studies on titanium dioxide and zinc oxide nanomaterials used for UV-protection in cosmetic formulations. **Nanotoxicology** 4:364-381.

Lankoff A, Sandberg WJ, Wegierek-Ciuk A, Lisowska H, Refsnes M, Sartowska B, Schwarze PE, Meczynska-Wielgosz S, Wojewodzka M, Kruszewski M. 2012. The effect of agglomeration state of silver and titanium dioxide nanoparticles on cellular response of HepG2, A549 and THP-1 cells. **Toxicol Lett** 208(3):197-213.

Lindberg HK, Falck GC, Catalan J, Koivisto AJ, Suhonen S, Jarventaus H, Rossi EM, Nykasenoja H, Peltonen Y, Moreno C, Alenius H, Tuomi T, Savolainen KM, Norppa H. 2012. Genotoxicity of inhaled nanosized TiO(2) in mice. **Mutat Res** 745(1-2):58-64.

Nel A, Xia T, Madler L, Li N. 2006. Toxic potential of materials at the nanolevel. **Science** 311(5761):622-627.

Newman MD, Stotland M, Ellis JI. 2009. The safety of nanosized particles in titanium dioxide- and zinc oxide-based sunscreens. **J Am Acad Dermatol** 61(4):685-692.

Nystrom AM, Fadeel B. 2012. Safety assessment of nanomaterials: implications for nanomedicine. **J Control Release** 161(2):403-408.

Ohsaka T. 1980. Temperature-Dependence of the Raman-Spectrum in Anatase TiO2. **Journal of the Physical Society of Japan** 48(5):1661-1668.

Petkovic J, Zegura B, Stevanovic M, Drnovsek N, Uskokovic D, Novak S, Filipic M. 2011. DNA damage and alterations in expression of DNA damage responsive genes induced by TiO2 nanoparticles in human hepatoma HepG2 cells. **Nanotoxicology** 5(3):341-353.

Pottier A, Chaneac C, Tronc E, Mazerolles L, Jolivet J-P. 2001. Synthesis of brookite TiO nanoparticles by thermolysis of TiCl in strongly acidic aqueous media. **Journal of Materials Chemistry** 11(4):1116-1121.

Shi H, Liu XQ, Zhang YF. 2014. Fabrication of novel antimicrobial poly(vinyl chloride) plastic for automobile interior applications. Iranian Polymer Journal 23(4):297-305.
Shukla RK, Kumar A, Gurbani D, Pandey AK, Singh S, Dhawan A. 2013. TiO(2) nanoparticles induce oxidative DNA damage and apoptosis in human liver cells. **Nanotoxicology** 7(1):48-60.

Siddique HR, Chowdhuri DK, Saxena DK, Dhawan A. 2005. Validation of Drosophila melanogaster as an in vivo model for genotoxicity assessment using modified alkaline Comet assay. **Mutagenesis** 20(4):285-290.

Smijs TG, Pavel S. 2011. Titanium dioxide and zinc oxide nanoparticles in sunscreens: focus on their safety and effectiveness. **Nanotechnol Sci Appl** 4:95-112.

Strobel C, Torrano AA, Herrmann R, Malissek M, Brauchle C, Reller A, Treuel L, Hilger I. 2014. Effects of the physicochemical properties of titanium dioxide nanoparticles, commonly used as sun protection agents, on microvascular endothelial cells. **J Nanopart Res** 16:2130.

Tavares AM, Louro H, Antunes S, Quarre S, Simar S, De Temmerman PJ, Verleysen E, Mast J, Jensen KA, Norppa H, Nesslany F, Silva MJ. 2014. Genotoxicity evaluation of nanosized titanium dioxide, synthetic amorphous silica and multi-walled carbon nanotubes in human lymphocytes. **Toxicol In Vitro** 28(1):60-69.

Weir A, Westerhoff P, Fabricius L, Hristovski K, von Goetz N. 2012. Titanium dioxide nanoparticles in food and personal care products. **Environ Sci Technol** 46(4):2242-2250.

Wu M, Lin G, Chen D, Wang G, He D, Feng S, Xu R. 2002. Sol-Hydrothermal Synthesis and Hydrothermally Structural Evolution of Nanocrystal Titanium Dioxide. **Chemistry of Materials** 14(5):1974-1980.

Yu J, Yu JC, Leung MKP, Ho W, Cheng B, Zhao X, Zhao J. 2003. Effects of acidic and basic hydrolysis catalysts on the photocatalytic activity and microstructures of bimodal mesoporous titania. **Journal of Catalysis** 217(1):69-78.

Yu JX, Li TH. 2011. Distinct biological effects of different nanoparticles commonly used in cosmetics and medicine coatings. **Cell Biosci** 1(1):19.

Zhang J, Song W, Guo J, Zhang J, Sun Z, Li L, Ding F, Gao M. 2013. Cytotoxicity of different sized TiO2 nanoparticles in mouse macrophages. **Toxicol Ind Health** 29(6):523-533.

Zhang WF, He YL, Zhang MS, Yin Z, Chen Q. 2000. Raman scattering study on anatase TiO2 nanocrystals. **Journal of Physics D-Applied Physics** 33(8):912-916.

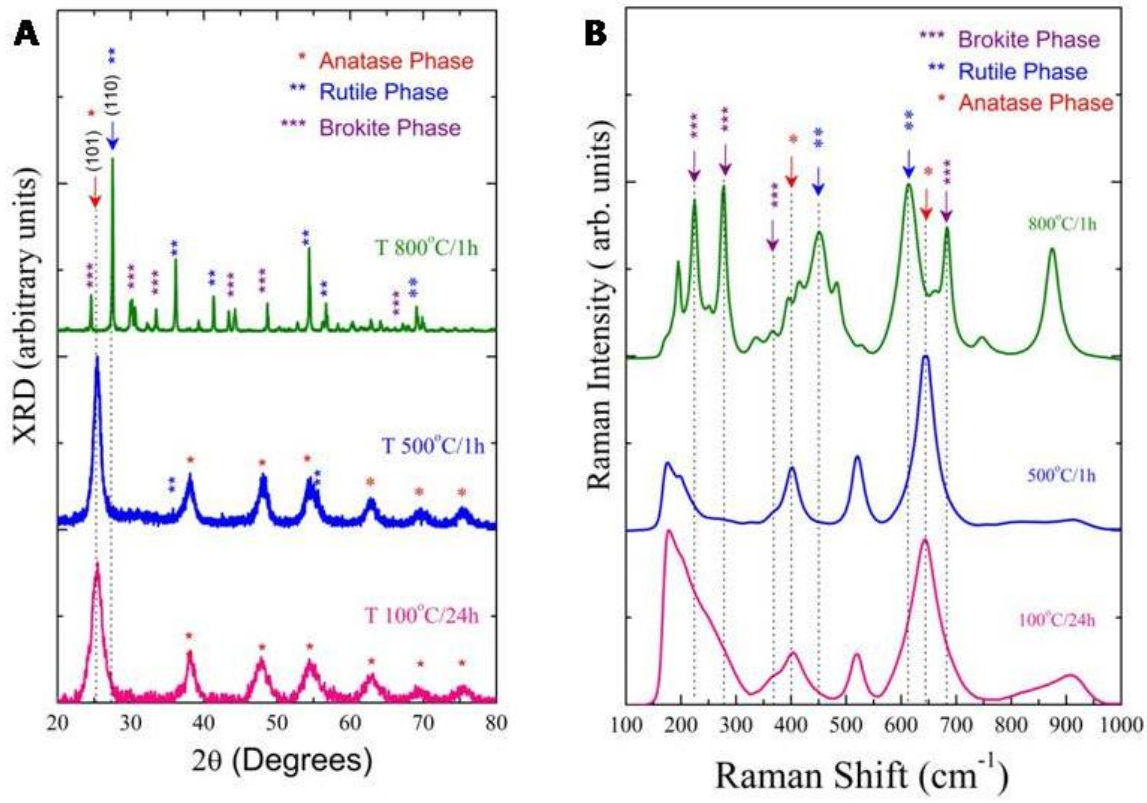

Fig. 1. A: X-ray diffraction patterns; **B**: Micro Raman spectra of TiO_2 NPs with thermal treatment at 100 ^{o}C / 24 hr, 500 ^{o}C / 1 hr and 800 ^{o}C / 1 hr.

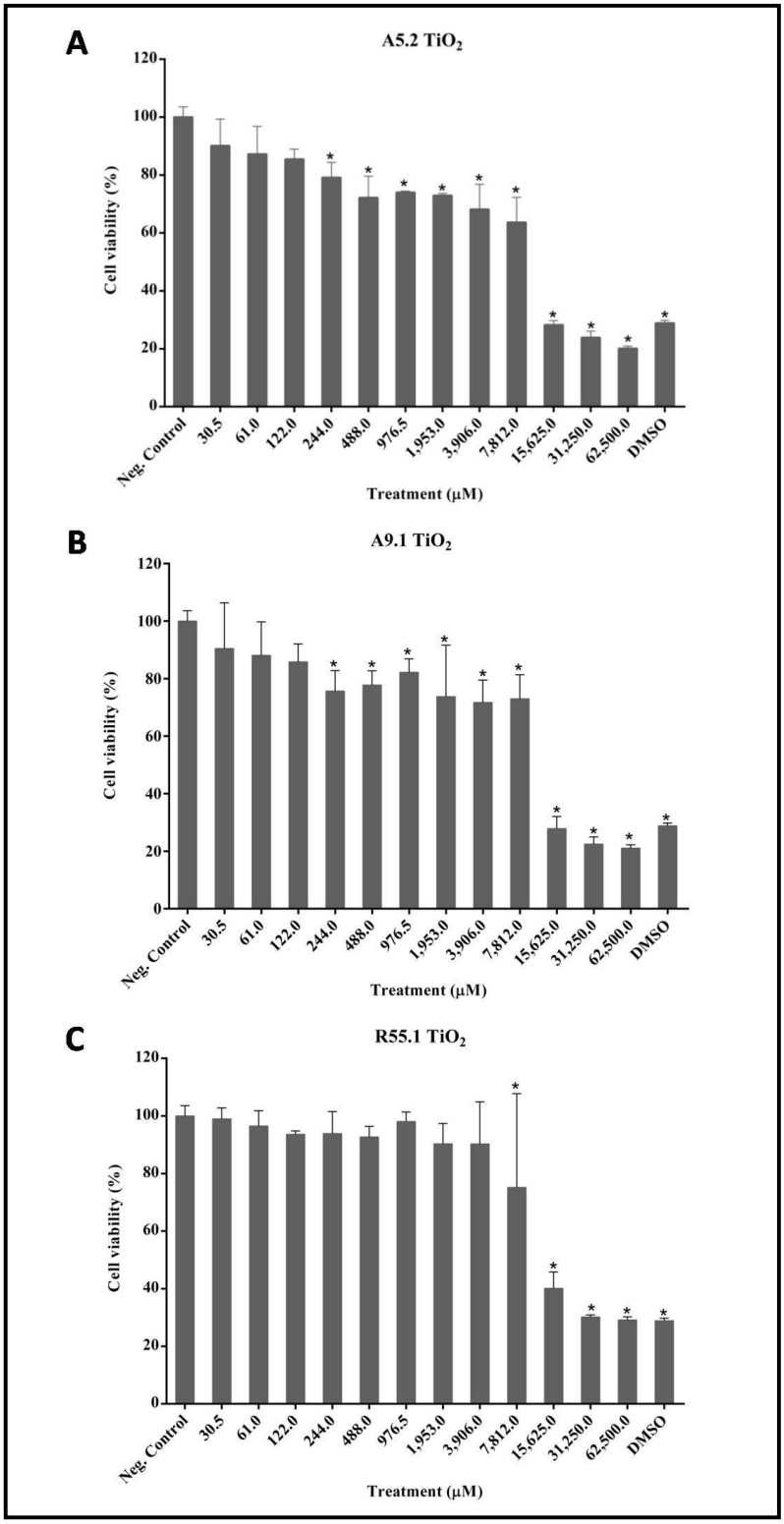
A
A5.2 TiO2
Cell viability (%)
120
100
80
60
40
20
0
Neg. Control
30.5
61.0
122.0
244.0
488.0
976.5
1,953.0
3,906.0
7,812.0
15,625.0
31,250.0
62,500.0
DMSO
Treatment (µM)
B
A9.1 TiO2
Cell viability (%)
Treatment (µM)
C
R55.1 TiO2
Cell viability (%)
Treatment (µM)

Fig. 2. Effects of TiO_2 NPs on the viability of V79 cells. **A**: A5.2 TiO_2; **B**: A9.1 TiO_2; **C**: R55.1 TiO_2 at concentrations 30.5 to 62,500.0 μM, negative and positive (DMSO 25%) controls.
* Significantly different of negative control ($p < 0.05$).

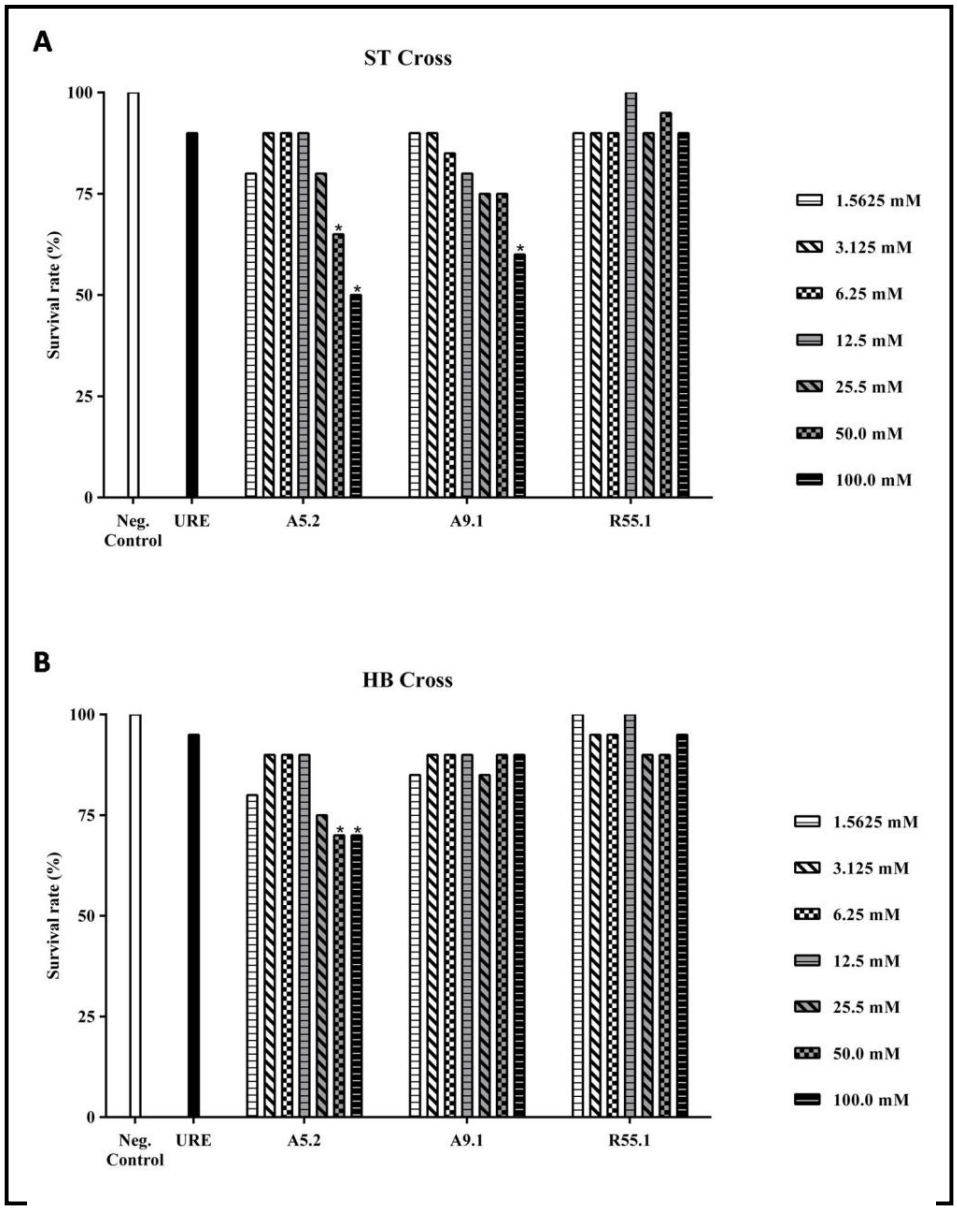

Fig. 3. Survival rates upon exposure to different concentrations of TiO_2 NPs. **A**: A5.2 TiO_2; **B**: A9.1 TiO_2; **C**: R55.1 TiO_2, relative to negative control in the wing Somatic Mutation and Recombination Test in *D. melanogaster*. * Significantly different of negative control ($p < 0.05$).

TABLE I. Average sizes and the mass fraction of rutile TiO_2 NPs of thermal treatment at 100 °C / 24 hr, 500 °C / 1 hr and 800 °C / 1 hr

Thermal treatment	NPs average size (nm)	NPs phase	Mass fraction of rutile
100°C/24hr	5.2	Anatase	-
500°C/ 1hr	9.1	Anatase	-
800°C/ 1hr	55.1	Anatase/Brookite /Rutile	0.64

TABLE II. Frequency of micronuclei (MN) and nuclear division index (NDI) observed in V79 cells treated with different concentrations of TiO_2 NPs (A5.2, A9.1 or R55.1) and respective controls

Treatments (μM)	Frequency of MNs [a]	NDI [b]
	Mean ± SD	Mean ± SD
Negative control	7.00 ± 1.00	1.78 ± 0,03
MMS	45.00 ± 3.61 [c]	1.78 ± 0,03
A5.2TiO_2		
30	6.67 ± 1.15	1,78 ± 0.03
60	12.00 ± 1.00	1.77 ± 0.02
120	14.67 ± 2.08 [c]	1.81 ± 0.02
A9.1 TiO_2		
30	11.33 ± 2.31	1.76 ± 0.03
60	8.33 ± 1.15	1.80 ± 0.05
120	10.00 ± 2.00	1.78 ± 0.01
R55.1TiO_2		
976.5	5.33 ± 1.53	1.79 ± 0.01
1,956.0	7.67 ± 1.15	1.80 ± 0.05
3,906.0	12.33 ± 2.52	1.79 ± 0.03

MMS – Methyl methanesulfonate (400 μM).

[a] 3,000 binucleated cells were analyzed per treatment group.

[b] 1,500 cells were analyzed per treatment group.

[c] Significantly different from control group ($P < 0.05$).

TABLE III. Summary of results obtained with the *Drosophila* wing spot test (SMART) in the marker-heterozygous (MH) progeny of the standard (ST) and high bioactivation (HB) crosses after chronic treatment of larvae with A5.2 TiO_2 NPs

Genotype, cross and treatment (mM)	Number of flies	Spots per fly (number of spots) statistical diagnosis[a]				Spots with *mwh* clone[c]	Frequency of clone formation/10^5 cells per cell division[d]	
		Small single spots (1-2 cells)[b]	Large single spots (>2 cells)[b]	Twin spots	Total spots		Observed	Control Corrected
ST cross								
Negative control	40	0.50 (20)	0.00 (00)	0.00 (00)	0.50 (20)	20	1.02	
URE	40	2.05 (82) +	0.30 (12) +	0.25 (10) +	2.60 (104) +	102	5.23	4.20
A5.2 TiO_2								
1.5625	40	0.38 (15) -	0.08 (03) i	0.03 (01) i	0.48 (19) -	19	0.97	-0.05
3.125	40	0.38 (15) -	0.15 (06) +	0.05 (02) i	0.58 (23) -	23	1.18	0.15
6.25	40	0.33 (13) -	0.05 (02) i	0.05 (02) i	0.43 (17) -	17	0.87	-0.15
12.5	40	0.53 (21) -	0.08 (03) i	0.00 (00) i	0.60 (24) i	23	1.18	0.15
HB cross								
Negative control	40	0.45 (18)	0.08 (03)	0.05 (02)	0.58 (23)	23	1.18	
URE	40	15.50 (620) +	2.20 (88) +	0.80 (32) +	18.50 (740) +	720	36.89	35.71
A5.2 TiO_2								
1.5625	40	0.88 (35) +	0.03 (01) i	0.05 (02) i	0.95 (38) +	37	1.90	0.72
3.125	40	1.05 (42) +	0.10 (04) i	0.05 (02) i	1.20 (48) +	47	2.41	1.23
6.25	40	0.55 (22) i	0.15 (06) i	0.08 (03) i	0.78 (31) i	29	1.49	0.31
12.5	40	0.65 (26) i	0.00 (00) -	0.00 (00) i	0.65 (26) -	25	1.28	0.10

Marquer trans-heterozygous flies (*mwh/flr*^{3}) were evaluated.
[a] Statistical diagnoses according to Frei and Würgler (1988; 1995). *U*-test, two sided; probability levels: -, negative; +, positive; i, inconclusive; P ≤0.05 vs. untreated control;
[b] Including rare *flr*^{3} single spots.
[c] Considering *mwh* clones from *mwh* single and twin spots.
[d] Frequency of clone formation: clones/flies/48,800 cells (without size correction).

TABLE IV. Summary of results obtained with the *Drosophila* wing spot test (SMART) in the marker-heterozygous (MH) progeny of the standard (ST) and high bioactivation (HB) crosses after chronic treatment of larvae with A9.1 TiO_2 NPs

Genotype, cross and treatment (mM)	Number of flies	Spots per fly (number of spots) statistical diagnosis[a]				Spots with *mwh* clone[c]	Frequency of clone formation/10^5 cells per cell division[d]	
		Small single spots (1-2 cells)[b]	Large single spots (>2 cells)[b]	Twin spots	Total spots		Observed	Control Corrected
ST cross								
Neg. control	40	0.50 (20)	0.00 (00)	0.00 (00)	0.50 (20)	20	1.02	
URE	40	2.05 (82) +	0.30 (12) +	0.25 (10) +	2.60 (104) +	102	5.23	4.20
A9.1 TiO_2								
1.5625	40	0.53 (21) -	0.08 (03) i	0.05 (02) i	0.65 (26) i	25	1.28	0.26
3.125	40	0.33 (13) -	0.05 (02) i	0.00 (00) i	0.38 (15) -	14	0.72	- 0.31
6.25	40	0.50 (20) -	0.05 (02) i	0.00 (00) i	0.55 (22) -	21	1.08	0.05
12.5	40	0.45 (18) -	0.03 (01) i	0.03 (01) i	0.50 (20) -	20	1.02	0.00
HB cross								
Neg. control	40	0.45 (18)	0.08 (03)	0.05 (02)	0.58 (23)	23	1.18	
URE	40	15.50 (620) +	2.20 (88) +	0.80 (32) +	18.50 (740) +	720	36.89	35.71
A9.1 TiO_2								
1.5625	40	0.65 (26) i	0.10 (04) i	0.05 (02) i	0.80 (32) i	31	1.59	0.41
3.125	40	0.50 (20) i	0.00 (00) -	0.03 (01) i	0.53 (21) -	20	1.02	- 0.15
6.25	40	0.50 (20) i	0.00 (00) -	0.03 (01) i	0.53 (21) -	20	1.02	- 0.15
12.5	40	0.58 (23) i	0.05 (02) i	0.05 (02) i	0.68 (27) -	27	1.38	0.20

Marquer trans-heterozygous flies (*mwh/flr*^{3}) were evaluated.
[a] Statistical diagnoses according to Frei and Würgler (1988; 1995). *U*-test, two sided; probability levels: -, negative; +, positive; i, inconclusive; P ≤0.05 vs. untreated control;
[b] Including rare *flr*^{3} single spots.
[c] Considering *mwh* clones from *mwh* single and twin spots.
[d] Frequency of clone formation: clones/flies/48,800 cells (without size correction).

Table V. Summary of results obtained with the *Drosophila* wing spot test (SMART) in the marker-heterozygous (MH) progeny of the standard (ST) and high bioactivation crosses (HB) after chronic treatment of larvae with R55.1 TiO_2 NPs

Genotype, cross and treatment (mM)	Number of flies	Spots per fly (number of spots) statistical diagnosis[a]				Spots with *mwh* clone[c]	Frequency of clone formation/10^5 cells per cell division[d]	
		Small single spots (1-2 cells)[b]	Large single spots (>2 cells)[b]	Twin spots	Total spots		Observed	Control Corrected
ST cross								
Neg. control	40	0.50 (20)	0.00 (00)	0.00 (00)	0.50 (20)	20	1.02	
URE	40	2.05 (82) +	0.30 (12) +	0.25 (10) +	2.60 (104) +	102	5.23	4.20
R55.1 TiO_2								
1.5625	40	0.38 (15) -	0.10 (04) i	0.00 (00) i	0.48 (19) -	17	0.87	-0.15
3.125	40	0.53 (21) -	0.10 (04) i	0.03 (01) i	0.65 (26) i	26	1.33	0.31
6.25	40	0.43 (17) -	0.00 (00) i	0.03 (01) i	0.45 (18) -	16	0.82	-0.20
12.5	40	0.48 (19) -	0.08 (03) i	0.10 (04) i	0.65 (26) i	26	1.33	0.31
HB cross								
Neg. control	40	0.45 (18)	0.08 (03)	0.05 (02)	0.58 (23)	23	1.18	
URE	40	15.50 (620) +	2.20 (88) +	0.80 (32) +	18.50 (740) +	720	36.89	35.71
R55.1 TiO_2								
1.5625	40	0.78 (31) +	0.18 (07) i	0.00 (00) i	0.95 (38) +	38	1.95	0.77
3.125	40	0.68 (27) i	0.13 (05) i	0.08 (03) i	0.88 (35) i	30	1.54	0.36
6.25	40	1.23 (49) +	0.05 (02) i	0.00 (00) i	1.28 (51) +	50	2.56	1.38
12.5	40	0.92 (37) +	0.05 (02) i	0.02 (01) i	1.00 (40) +	40	2.05	0.87

Marquer trans-heterozygous flies (*mwh/flr*^{3}) were evaluated.
[a] Statistical diagnoses according to Frei and Würgler (1988; 1995). *U*-test, two sided; probability levels: -, negative; +, positive; i, inconclusive; P ≤0.05 vs. untreated control;
[b] Including rare *flr*^{3} single spots.
[c] Considering *mwh* clones from *mwh* single and twin spots.
[d] Frequency of clone formation: clones/flies/48,800 cells (without size correction).